

DIRECT ARYLATION POLYMERIZATION OF 2'-OCTYL-3,4-ETHYLENEDIOXYTHIOPHENE
FOR DONOR-ACCEPTOR CONJUGATED COPOLYMER SYNTHESIS



A Thesis Submitted in Partial Fulfillment of the Requirements
for the Degree of Master of Science in Chemistry
Department of Chemistry
Faculty of Science
Chulalongkorn University
Academic Year 2018
Copyright of Chulalongkorn University

แอริลเลขชั้นพอลิเมอไรเซชันโดยตรงของ 2'-ออกทิล-3,4-เอทิลีนไดออกซีไทโอพีนเพื่อการสังเคราะห์ได
เนอร์-แอกเซฟเทอร์คอนจูเกตโคพอลิเมอร์



วิทยานิพนธ์นี้เป็นส่วนหนึ่งของการศึกษาตามหลักสูตรปริญญาวิทยาศาสตรมหาบัณฑิต
สาขาวิชาเคมี ภาควิชาเคมี
คณะวิทยาศาสตร์ จุฬาลงกรณ์มหาวิทยาลัย
ปีการศึกษา 2561
ลิขสิทธิ์ของจุฬาลงกรณ์มหาวิทยาลัย

ธณัช ดิยะสกุลชัย : แอริลเลชันพอลิเมอไรเซชันโดยตรงของ 2'-ออกทิล-3,4-เอทิลีนไดออกซีไทโอฟินเพื่อการสังเคราะห์โคเนออร์-แอกเซพเทอร์คอนจูเกตโคพอลิเมอร์. (DIRECT ARYLATION POLYMERIZATION OF 2'-OCTYL-3,4-ETHYLENEDIOXYTHIOPHENE FOR DONOR-ACCEPTOR CONJUGATED COPOLYMER SYNTHESIS) อ.ที่ปรึกษาหลัก : ผศ. ดร.ยงศักดิ์ ศรีธนาอนันต์

ปฏิกิริยาแอริลเลชันพอลิเมอไรเซชันโดยตรงเป็นปฏิกิริยาคู่ควบชนิดใหม่ที่เร่งปฏิกิริยาด้วยสารประกอบแพลเลเดียมสำหรับใช้ในการสังเคราะห์คอนจูเกตพอลิเมอร์ ปฏิกิริยานี้สามารถสร้างพันธะคาร์บอน-คาร์บอนระหว่างสารประกอบแอริลและไดโบรโมแอริล โดยที่ไม่จำเป็นต้องผ่านสารตัวกลางจำพวกสารโลหะอินทรีย์ ในงานวิจัยนี้ผู้วิจัยได้ทำการสังเคราะห์โคเนออร์-แอกเซพเทอร์คอนจูเกตโคพอลิเมอร์ชนิดใหม่ที่มีโครงสร้างส่วนของโคเนออร์เป็น 2'-ออกทิล-3,4-เอทิลีนไดออกซีไทโอฟินจับคู่กับ 3,5-ไดโบรโม-1,2,4-ไตรอะโซล 4,7-ไดโบรโม-2,1,3-เบนโซไทอะไดอะโซล 4,7-ไดโบรโม-5,6-ไดฟลูออโร-2,1,3-เบนโซไทอะไดอะโซล 4,7-ไดโบรโม-1,2,3-เบนโซไตรอะโซล 4,7-ไดโบรโม-2-ออกทิล-1,2,3-เบนโซไตรอะโซล 1,4-ไดโบรโม-2,5-(เทิร์ท-บิวทิลไธเมทิลไซเลนนิลออกซี)เบนซีน 5,7-ไดโบรโมไทโอน[3,4-ปี]ไพราซีน และ 5,7-ไดโบรโม-2,3-ไดฟีนิลไทโอน[3,4-ปี]ไพราซีน ได้พอลิเมอร์ พี1-6 และ พี8-10 ตามลำดับในปริมาณต่างๆ กันในช่วง 16-88% พอลิเมอร์พี7 เตรียมได้จากปฏิกิริยาการกำจัดหมู่ปกป้องแล้วตามด้วยปฏิกิริยาออกซิเดชันของพอลิเมอร์ พี6 พอลิเมอร์เหล่านี้มีค่าการดูดกลืนแสงยูวีวิสิเบิลที่ค่าความยาวคลื่นสูงสุดในช่วง 328 ถึง 958 นาโนเมตร

จุฬาลงกรณ์มหาวิทยาลัย
CHULALONGKORN UNIVERSITY

สาขาวิชา เคมี
ปีการศึกษา 2561

ลายมือชื่อนิสิต
ลายมือชื่อ อ.ที่ปรึกษาหลัก

6071943123 : MAJOR CHEMISTRY

KEYWORD: direct arylation, EDOT, donor-acceptor, conjugated polymer, direct (hetero)arylation polymerization

Thanat Tiyasakulchai : DIRECT ARYLATION POLYMERIZATION OF 2'-OCTYL-3,4-ETHYLENEDIOXYTHIOPHENE FOR DONOR-ACCEPTOR CONJUGATED COPOLYMER SYNTHESIS. Advisor: Asst. Prof. YONGSAK SRITANA-ANANT, Ph.D.

Direct arylation polymerization (DArP) is a new palladium-catalyzed cross-coupling method to synthesize conjugated copolymers. This reaction can generate C-C bonds between simple arenes and dibromoarenes, without passing through organometallic intermediates. In this work, we synthesized new donor-acceptor conjugated copolymers based on 2'-octyl-3,4-ethylenedioxythiophene (OEDOT) donor coupled with 3,5-dibromo-1,2,4-triazole, 4,7-dibromo-2,1,3-benzothiadiazole, 4,7-dibromo-5,6-difluoro-2,1,3-benzothiadiazole, 4,7-dibromo-1,2,3-benzotriazole, 4,7-dibromo-2-octyl-1,2,3-benzotriazole, 1,4-dibromo-2,5-(*tert*-butyldimethylsilyloxy)benzene, 5,7-dibromothieno[3,4-*b*]pyrazine and 5,7-dibromo-2,3-diphenylthieno[3,4-*b*]pyrazine to become polymers P1-6 and P9-10, respectively in various range of yields of 16-88%. Polymer P7 was prepared from deprotection followed by oxidation of polymer P6. These copolymers exhibited various UV-Visible absorptions with λ_{max} values ranging from 328 to 958 nm.

Field of Study: Chemistry

Student's Signature

Academic Year: 2018

Advisor's Signature

ACKNOWLEDGEMENTS

I would like to express my sincere thanks to my thesis advisor, Assist. Prof. Dr. Yongsak Sritana-anant for his invaluable help and constant encouragement throughout the course of this research. I am most grateful for his teaching and advice. This thesis would not have been completed without all the support that I have always received from him.

I would like to thank the rest of my thesis committee, Assoc. Prof. Dr. Vudhichai Parasuk, Assoc. Prof. Dr. Voravee Hoven, Assoc. Prof. Dr. Tienthong Thongpanchang for their valuable comments and suggestions.

I would like to thank Assist. Prof. Dr. Chayanisa Chitichotpanya, Department of Chemistry, Faculty of Science, Mahidol University, for assistance on gel permeation chromatography measurement.

I would like to gratefully acknowledge the members of YS-research group on the fourteenth floor, Mahamakut building for their support, guidance and camaraderie.

In addition, I would like to express my sincere appreciation and gratitude to my family and Faculty of Science, Chulalongkorn University for support on laboratory.

Finally, I gratefully acknowledge the Scholarship from the Graduate School, Chulalongkorn University to commemorate the 72nd anniversary of the late his Majesty King Bhumibol Adulyadej, Rama IX.

Thanat Tiyasakulchai

TABLE OF CONTENTS

	Page
.....	iii
ABSTRACT (THAI).....	iii
.....	iv
ABSTRACT (ENGLISH).....	iv
ACKNOWLEDGEMENTS.....	v
TABLE OF CONTENTS.....	vi
LIST OF FIGURES.....	xi
LIST OF SCHEMES.....	xiii
LIST OF TABLES.....	xvi
LIST OF ABBREVIATIONS.....	xvii
CHAPTER I INTRODUCTIONS.....	1
1.1 Conjugated polymers.....	1
1.2 Synthesis of conjugated polymers.....	3
1.2.1 Heck cross-coupling reaction.....	4
1.2.2 Sonogashira cross-coupling reaction.....	4
1.2.3 Stille cross-coupling reaction.....	5
1.2.4 Suzuki cross-coupling reaction.....	5
1.2.5 Negishi cross-coupling reaction.....	6
1.2.6 Kumada cross-coupling reaction.....	6
1.3 Direct arylation polymerization (DAP).....	7
1.4 Mechanisms of direct arylation polymerization.....	8

1.4.1 Mechanisms of palladium-catalyzed cross-coupling reactions.....	8
1.4.2 The concerted metalation-deprotonation (CMD) mechanism	9
1.5 Literature review.....	10
1.6 The objective of this work.....	14
CHAPTER II EXPERIMENTS.....	16
2.1 Chemicals.....	16
2.2 Instruments and Equipment	17
2.3 Monomers synthesis.....	17
2.3.1 Diethyl thiodiglycolate (1).....	17
2.3.2 Diethyl 3,4-dihydroxythiophene-2,5-dicarboxylate (2).....	18
2.3.3 1,2-Dibromodecane	18
2.3.4 Diethyl 2-octyl-2,3-dihydrothieno[3,4- <i>b</i>][1,4]dioxine-5,7-dicarboxylate (3).....	19
2.3.5 2-Octyl-2,3-dihydrothieno[3,4- <i>b</i>][1,4]dioxine-5,7-dicarboxylic acid (4).....	19
2.3.6 2'-Octyl-3,4-ethylenedioxythiophene (OEDOT).....	20
2.3.7 4,7-Dibromo-2,1,3-benzothiadiazole (DBBTD)	20
2.3.8 1,2,3-Benzotriazole (BTZ)	21
2.3.9 4,7-Dibromo-1,2,3-benzotriazole (DBBTZ).....	21
2.3.10 4,7-Dibromo-2-octyl-1,2,3-benzotriazole (DBOBTZ).....	22
2.3.11 1,4-Dibromo-2,5-bis(<i>tert</i> -butyldimethylsilyloxy)benzene (5).....	22
2.3.12 2,5-Dibromo-3,4-dinitrothiophene (DBDNT).....	23
2.3.13 3,4-Diaminothiophene dihydrochloride (DAT.2HCl).....	23
2.3.14 Thieno[3,4- <i>b</i>]pyrazine (TP).....	24
2.3.15 5,7-Dibromothieno[3,4- <i>b</i>]pyrazine (DBTP).....	24
2.3.16 2,3-Diphenylthieno[3,4- <i>b</i>]pyrazine (DPTP)	25

2.3.17 5,7-Dibromo-2,3-diphenylthieno[3,4- <i>b</i>]pyrazine (DBDPTP).....	25
2.4 Polymers synthesis.....	26
2.4.1 Poly(2'-octyl-3,4-ethylenedioxythiophene-co-1,2,4-triazole) (P1).....	26
2.4.2 Poly(2'-octyl-3,4-ethylenedioxythiophene-co-2,1,3-benzothiadiazole) (P2)	27
2.4.3 Poly(2'-octyl-3,4-ethylenedioxythiophene-co-5,6-difluoro-2,1,3- benzothiadiazole) (P3).....	28
2.4.4 Poly(2'-octyl-3,4-ethylenedioxythiophene-co-1,2,3-benzotriazole) (P4)....	28
2.4.5 Poly(2'-octyl-3,4-ethylenedioxythiophene-co-2-octyl-1,2,3-benzotriazole) (P5).....	29
2.4.6 Poly(2'-octyl-3,4-ethylenedioxythiophene-co-1,4-bis(<i>tert</i> - butyldimethylsilanyloxy)benzene) (P6).....	30
2.4.7 Poly(2'-octyl-3,4-ethylenedioxythiophene-co-benzoquinone) (P7).....	30
2.4.8 Poly(2'-octyl-3,4-ethylenedioxythiophene-co-3,4-dinitrothiophene) (P8) .	31
2.4.9 Poly(2'-octyl-3,4-ethylenedioxythiophene-co- thieno[3,4- <i>b</i>]pyrazine) (P9)	32
2.4.10 Poly(2'-octyl-3,4-ethylenedioxythiophene-co-2,3-diphenyl-thieno[3,4- <i>b</i>]pyrazine) (P10).....	32
2.5 Molar extinction coefficient	33
2.5.1 Molar extinction coefficient of UV-visible absorption.....	33
2.5.2 Molar extinction coefficient of fluorescence emission	33
CHAPTER III RESULTS AND DISCUSSION.....	34
3.1 Monomer synthesis.....	34
3.1.1 Diethyl thiodiglycolate (1).....	34
3.1.2 Diethyl 3,4-dihydroxythiophene-2,5-dicarboxylate (2).....	34

3.1.3 1,2-Dibromodecane	35
3.1.4 Diethyl 2-octyl-2,3-dihydrothieno[3,4-b][1,4]dioxine-5,7-dicarboxylate (3)	36
3.1.5 2-Octyl-2,3-dihydrothieno [3,4-b][1,4]dioxine-5,7-dicarboxylic acid (4)	37
3.1.6 2'-Octyl-3,4-ethylenedioxythiophene (OEDOT).....	38
3.1.7 4,7-Dibromo-2,1,3-benzothiadiazole (DBBTD)	38
3.1.8 1,2,3-Benzotriazole (BTZ)	39
3.1.9 4,7-Dibromo-1,2,3-benzotriazole (DBBTZ).....	39
3.1.10 4,7-Dibromo-2-octyl-1,2,3-benzotriazole (DBOBTZ).....	40
3.1.11 1,4-Dibromo-2,5-bis(<i>tert</i> -butyldimethylsilyloxy)benzene (5).....	40
3.1.12 2,5-Dibromo-3,4-dinitrothiophene (DBDNT).....	40
3.1.13 3,4-Diaminothiophene dihydrochloride (DAT.2HCl).....	41
3.1.14 Thieno[3,4- <i>b</i>]pyrazine (TP).....	41
3.1.15 5,7-Dibromothieno[3,4- <i>b</i>]pyrazine (DBTP).....	42
3.1.16 2,3-Diphenylthieno[3,4- <i>b</i>]pyrazine (DPTP)	42
3.1.17 5,7-Dibromo-2,3-diphenylthieno[3,4- <i>b</i>]pyrazine (DBDPTP).....	43
3.2 Polymer synthesis	43
3.2.1 Poly(2'-octyl-3,4-ethylenedioxythiophene-co-1,2,4-triazole) (P1).....	43
3.2.2 Poly(2'-octyl-3,4-ethylenedioxythiophene-co-2,1,3-benzothiadiazole) (P2)	50
3.2.3 Poly(2'-octyl-3,4-ethylenedioxythiophene-co-5,6-difluoro-2,1,3- benzothiadiazole) (P3).....	52
3.2.4 Poly(2'-octyl-3,4-ethylenedioxythiophene-co-1,2,3-benzotriazole) (P4)....	53
3.2.5 Poly(2'-octyl-3,4-ethylenedioxythiophene-co-2-octyl-1,2,3-benzotriazole) (P5).....	54

3.2.6 Poly(2'-octyl-3,4-ethylenedioxythiophene-co-1,4-bis((tert-butyl)dimethylsilyloxy)benzene) (P6).....	55
3.2.7 Poly(2'-octyl-3,4-ethylenedioxythiophene-co-benzoquinone) (P7).....	56
3.2.8 Poly(2'-octyl-3,4-ethylenedioxythiophene-co-3,4-dinitrothiophene) (P8) .	57
3.2.9 Poly(2'-octyl-3,4-ethylenedioxythiophene-co- thieno[3,4-b]pyrazine) (P9)	58
3.2.10 Poly(2'-octyl-3,4-ethylenedioxythiophene-co-2,3-diphenyl-thieno[3,4- b]pyrazine) (P10).....	59
3.3 Fluorescence property of polymers P1-P7, P10	61
3.4 Molar extinction coefficient	62
3.4.1 Molar extinction coefficient of UV-visible absorption.....	62
3.4.2 Molar extinction coefficient of fluorescence emission.....	62
3.5 Band gap	63
CHAPTER IV CONCLUSION.....	64
REFERENCES	68
APPENDIX.....	76
VITA.....	119

LIST OF FIGURES

	Page
Figure 1.1 Orbital interactions of donor (D) and acceptor (A) units, resulting in low bandgaps in donor-acceptor (D-A) polymers.....	2
Figure 1.2 a) electron-rich donor units b) electron-deficient acceptor units.....	2
Figure 1.3 Examples of thiophene-based conjugated polymers	3
Figure 1.4 Traditional C-C coupling methods for synthesis of conjugated polymer	4
Figure 1.5 Direct arylation polymerization or DArP	7
Figure 1.6 General mechanism of Pd-catalyzed cross-coupling reactions	8
Figure 1.7 CMD mechanism of direct C-H arylation.....	9
Figure 1.8 Target donor-acceptor conjugated polymers	15
Figure 3.1 The UV-visible absorption spectra of polymer P1 solution in CH ₂ Cl ₂ with addition of TFA.....	45
Figure 3.2 The UV-visible absorption spectra of polymer P1 solution upon protonation and after neutralization.....	46
Figure 3.3 UV-visible absorption spectra of polymer P1 solution exposed to ambient light.....	47
Figure 3.4 UV-visible absorption spectra of protonated polymer P1 solution exposed to ambient light	47
Figure 3.5 A shift of λ_{\max} of the UV-visible absorption spectra of protonated polymer P1 solution briefly exposed to ambient light.....	48
Figure 3.6 Effect of air oxidation on the UV-visible absorption spectra of polymer P1 solution.....	49
Figure 3.7 Effect of air oxidation on the UV-visible absorption spectra of polymer P1 solution + TFA.....	49

Figure 3.8 Partial ^1H NMR spectra of P2 from 2 synthetic conditions	51
Figure 3.9 Possible branched structure of polymer of P9	59
Figure 4.1 Synthesis of OEDOT	64
Figure 4.2 Synthesis of DBBTD	64
Figure 4.3 Synthesis of DBBTZ and DBOBTZ	65
Figure 4.4 Synthesis of compound 5	65
Figure 4.5 Synthesis of DBTP and DBDPTP	66



LIST OF SCHEMES

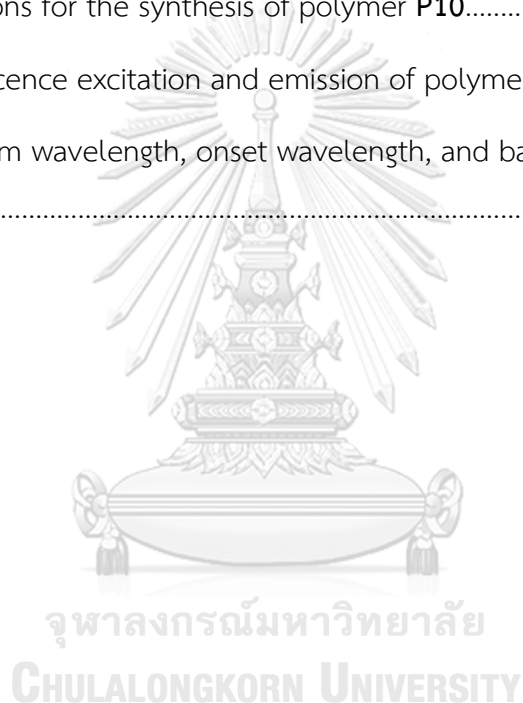
	Page
Scheme 1.1 Heck cross-coupling polymerization between 1,4-diketo-2,5-dihexyl-3,6-bis(4-bromophenyl)pyrrolo[3,4-c]pyrrole and p-divinylbenzene.....	4
Scheme 1.2 Sonogashira cross-coupling polymerization of 2,3-diphenylthieno[3,4-b]pyrazine and 3,4-didodecyl-2,5-diethynylthiophene.....	5
Scheme 1.3 Stille cross-coupling polymerization between cyclopentadithiophene derivative and 5-fluoro-[2,1,3]-benzothiadiazole.....	5
Scheme 1.4 Suzuki cross-coupling polymerization between fluorene and benzothiadiazole derivatives.....	6
Scheme 1.5 Negishi cross-coupling polymerization of fluorene derivative.....	6
Scheme 1.6 Kumada cross-coupling polymerization of 3-hexylthiophene derivative..	7
Scheme 1.7 Synthesis of oligo(3-alkylthiophene) via direct arylation.....	10
Scheme 1.8 Polycondensation of 2-bromo-3-hexylthiophene.....	10
Scheme 1.9 DArP of 2,2'-bithiophene and a fluorene derivative.....	11
Scheme 1.10 DArP of 2,4-propylenedioxythiophenes (ProDOT) and EDOT.....	11
Scheme 1.11 DArP of 2,7-dibromo-9,9-dioctylfluorene and EDOT.....	12
Scheme 1.12 DArP of EDOT and 5,8-dibromo-2,3-diphenylquinoxaline.....	12
Scheme 1.13 Synthesis of polymers A , B and C	13
Scheme 1.14 DArP of 4,7-dibromobenzothiadiazole and 2,2'-(2,5-bis((2-hexyldecyl)oxy)-1,4-phenylene)dithiophene.....	13
Scheme 1.15 DArP of 4,4-di(2-ethylhexyl)-cyclopenta[2,1-b:3,4-b']dithiophene and 4,7-dibromobenzothiadiazole.....	14
Scheme 3.1 Synthesis of diethyl thiodiglycolate (1)	34
Scheme 3.2 Synthesis of diethyl 3,4-dihydroxythiophene-2,5-dicarboxylate (2)	34

Scheme 3.3 Mechanism of Hinsberg reaction	35
Scheme 3.4 Synthesis of 1,2-dibromodecane	35
Scheme 3.5 Synthesis of diethyl 2-octyl-2,3-dihydrothieno[3,4-b][1,4]dioxine-5,7-dicarboxylate (3).....	36
Scheme 3.6 Synthesis of 2-octyl-2,3-dihydrothieno [3,4-b][1,4]dioxine-5,7-dicarboxylic acid (4).....	37
Scheme 3.7 Synthesis of 2'-octyl-3,4-ethylenedioxythiophene (OEDOT)	38
Scheme 3.8 Synthesis of 4,7-dibromo-2,1,3-benzothiadiazole (DBBTD)	38
Scheme 3.9 Synthesis of 1,2,3-benzotriazole (BTZ).....	39
Scheme 3.10 Synthesis of 4,7-dibromo-1,2,3-benzotriazole (DBBTZ)	39
Scheme 3.11 Synthesis of 4,7-dibromo-2-octyl-1,2,3-benzotriazole (DBOBTZ)	40
Scheme 3.12 Synthesis of compound 5	40
Scheme 3.13 Synthesis of 2,5-dibromo-3,4-dinitrothiophene (DBDNT).....	40
Scheme 3.14 Synthesis of 3,4-diaminothiophene dihydrochloride (DAT.2HCl).....	41
Scheme 3.15 Synthesis of thieno[3,4-b]pyrazine (TP).....	41
Scheme 3.16 Synthesis of 5,7-dibromothieno[3,4-b]pyrazine (DBTP)	42
Scheme 3.17 Synthesis of 2,3-diphenylthieno[3,4-b]pyrazine (DPTP).....	42
Scheme 3.18 Synthesis of 5,7-Dibromo-2,3-diphenylthieno[3,4-b]pyrazine (DBDPTP).....	43
Scheme 3.19 Synthesis of poly(2'-octyl-3,4-ethylenedioxythiophene-co-1,2,4-triazole) (P1)	43
Scheme 3.20 The mechanism of Pd/Cu-catalyzed direct arylation between DBTZ and OEDOT.....	44
Scheme 3.21 Protonation and tautomerization of the triazole ring in polymer P1	45
Scheme 3.22 Synthesis of poly(2'-octyl-3,4-ethylenedioxythiophene-co-2,1,3-benzothiadiazole) (P2)	50

Scheme 3.23 Synthesis of poly(2'-octyl-3,4-ethylenedioxythiophene-co-5,6-difluoro-2,1,3-benzothiadiazole) (P3)	52
Scheme 3.24 Synthesis of poly(2'-octyl-3,4-ethylenedioxythiophene-co-1,2,3-benzotriazole) (P4).....	53
Scheme 3.25 Synthesis of poly(2'-octyl-3,4-ethylenedioxythiophene-co-2-octyl-1,2,3-benzotriazole) (P5).....	54
Scheme 3.26 Synthesis of poly(2'-octyl-3,4-ethylenedioxythiophene-co-1,4-bis((tert-butyl)dimethylsilyloxy)benzene) (P6).....	55
Scheme 3.27 Synthesis of poly(2'-octyl-3,4-ethylenedioxythiophene-co-benzoquinone) (P7)	56
Scheme 3.28 Unsuccessful synthesis of poly(2'-octyl-3,4-ethylenedioxythiophene-co-3,4-dinitrothiophene) (P8)	57
Scheme 3.29 Nucleophilic aromatic substitution (S_NAr) of DBDNT	57
Scheme 3.30 Synthesis of poly(2'-octyl-3,4-ethylenedioxythiophene-co- thieno[3,4-b]pyrazine) (P9).....	58
Scheme 3.31 Synthesis of poly(2'-octyl-3,4-ethylenedioxythiophene-co-2,3-diphenyl-thieno[3,4-b]pyrazine) (P10).....	59

LIST OF TABLES

	Page
Table 3.1 Conditions for the synthesis of compound 3	36
Table 3.2 Conditions for the synthesis of polymer P1	44
Table 3.3 Conditions for the synthesis of polymer P2	51
Table 3.4 Conditions for the synthesis of polymer P3	53
Table 3.5 Conditions for the synthesis of polymer P10	60
Table 3.6 Fluorescence excitation and emission of polymers P1-P7, P10	61
Table 3.7 Maximum wavelength, onset wavelength, and band gap of polymer P1-7 and P10	63



LIST OF ABBREVIATIONS

acetone-d ₆	: deuterated acetone
cm ⁻¹	: unit of wavenumber (IR)
CDCl ₃	: deuterated chloroform
Cs ₂ CO ₃	: cesium carbonate
°C	: degree Celsius
¹³ C NMR	: carbon-13 nuclear magnetic resonance spectroscopy
d	: doublet (NMR)
BTD	: 2,1,3-benzothiadiazole
BTZ	: 1,2,3-benzotriazole
DArP	: direct arylation polymerization
DAT	: 3,4-diaminothiophene dihydrochloride
DBBTD	: 4,7-dibromo-2,1,3-benzothiadiazole
DBBTZ	: 4,7-dibromo-1,2,3-benzotriazole
DBDNT	: 2,5-dibromo-3,4-dinitrothiophene
DBOBTZ	: 4,7-dibromo-2-octyl-1,2,3-benzotriazole
DBDFBTD	: 4,7-dibromo-5,6-difluoro-2,1,3-benzothiadiazole
DBDPTP	: 5,7-dibromo-2,3-diphenylthieno[3,4- <i>b</i>]pyrazine
DBTP	: 5,7-dibromothieno[3,4- <i>b</i>]pyrazine
DBU	: 1,8-diazabicyclo(5.4.0)undec-7-ene
DCM	: dichloromethane
DDQ	: 2,3-dichloro-5,6-dicyanobenzoquinone
DMA	: dimethylacetamide

DMAP	: 4-dimethylaminopyridine
DMF	: dimethylformamide
DMSO-d ₆	: deuterated dimethyl sulfoxide
DPTP	: 2,3-diphenylthieno[3,4-b]pyrazine
EDOT	: 3,4-ethylenedioxythiophene
E _g	: band gap
Et ₃ N	: triethylamine
EtOAc	: ethyl acetate
¹⁹ F NMR	: fluorine-19 nuclear magnetic resonance spectroscopy
g	: gram (s)
GPC	: gel permeation chromatography
h	: hour (s)
¹ H NMR	: proton nuclear magnetic resonance spectroscopy
HCl	: hydrochloric acid
HNO ₃	: nitric acid
H ₂ SO ₄	: sulfuric acid
Hz	: hertz (s)
IR	: infrared spectroscopy
J	: J-coupling (NMR)
K ₂ CO ₃	: potassium carbonate
lit.	: literature
M	: molar (s)
m	: multiplet (NMR)
M _n	: the number average molecular weight

MeOH	: methanol
MgSO ₄	: magnesium sulfate
min	: minute
mL	: milliliter (s)
mmol	: millimole (s)
Mp	: melting point
MS	: mass spectrometry
MW	: microwave
m/z	: mass per charge ratio
Na ₂ CO ₃	: sodium carbonate
NaHCO ₃	: sodium hydrogen carbonate
NaOH	: sodium hydroxide
NBS	: N-bromosuccinimide
nm	: nanometer (s)
Pd ₂ (dba) ₃	: tris(dibenzylideneacetone)dipalladium(0)
Pd(OAc) ₂	: palladium(II) acetate
PivOH	: pivalic acid
PPh ₃	: triphenylphosphine
ppm	: parts per million (unit of chemical shift)
q	: quartet (NMR)
rt	: room temperature
s	: singlet (NMR)
t	: triplet (NMR)
TBAB	: tetrabutylammonium bromide

TBSCl	: <i>tert</i> -butyl(chloro)dimethylsilane
TFA	: trifluoroacetic acid
TP	: thieno[3,4- <i>b</i>]pyrazine
TZ	: 3,5-dibromo-1,2,4-triazole
UV-Vis	: ultra-violet and visible spectroscopy
W	: watt
δ	: chemical shift
ϵ	: molar extinction coefficient
λ_{\max}	: maximum wavelength
λ_{onset}	: onset wavelength

CHAPTER I

INTRODUCTIONS

1.1 Conjugated polymers

Conjugated polymers are materials with π -conjugated systems along their backbones. These π -electrons can delocalize when a conjugated polymer is excited, resulted in the conductive and many related properties. Conjugated polymers combine the conductive properties of inorganic semiconductors and physical properties of organic polymers such as solubility in organic solvent. [1] Owing to their solubility, These polymers can be easily processed to form thin and lightweight films using inkjet printing or spray-coating. [2-3] Their applications appear in many electronic devices such as sensors,[4] transistors, [5] organic light emitting diodes (OLED) [6] and organic photovoltaic cells (OPV). [7] Conjugated polymers must be designed and prepared to suit the need of particular applications such as their aromatic backbones functionalized with electron-donating or electron-withdrawing moieties for suitable optical and electronic properties. [8] Moreover, the non-conjugated side-chains are usually required to improve solubility and added functional groups. [9-10] Donor-acceptor polymers, which contain alternating electron-rich donor and electron-deficient acceptor units on the backbones, are one of the most popular types of conjugated polymers. Donor-acceptor polymers were found to have significantly decreased bandgaps as explained by hybridizations of frontier orbitals as shown in **Figure 1.1**. [11-12] The interactions between orbitals of donor and acceptor units induce more planar backbones of the polymers and increase the π -electrons delocalizations. [13] Furthermore, these donor-acceptor polymers often have a relatively broad absorption spectrum. [14]

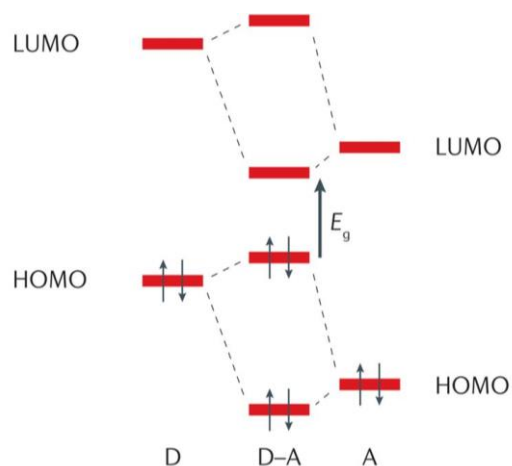


Figure 1.1 Orbital interactions of donor (D) and acceptor (A) units, resulting in low bandgaps in donor-acceptor (D-A) polymers

Examples of the electron-rich donor units often found in conjugated polymers include 3,4-ethylenedioxythiophene (EDOT), [15] fluorene, [14, 16] carbazoles, [17-18] and cyclopenta-dithiophene. [19-20] For the electron-deficient acceptor units, benzothiadiazole (BTD), [21-22] benzotriazole (BTZ), [23] thienopyrazine (TP) [24] and thienopyrroledione [25] are among those that are mostly used in conjugated polymers.

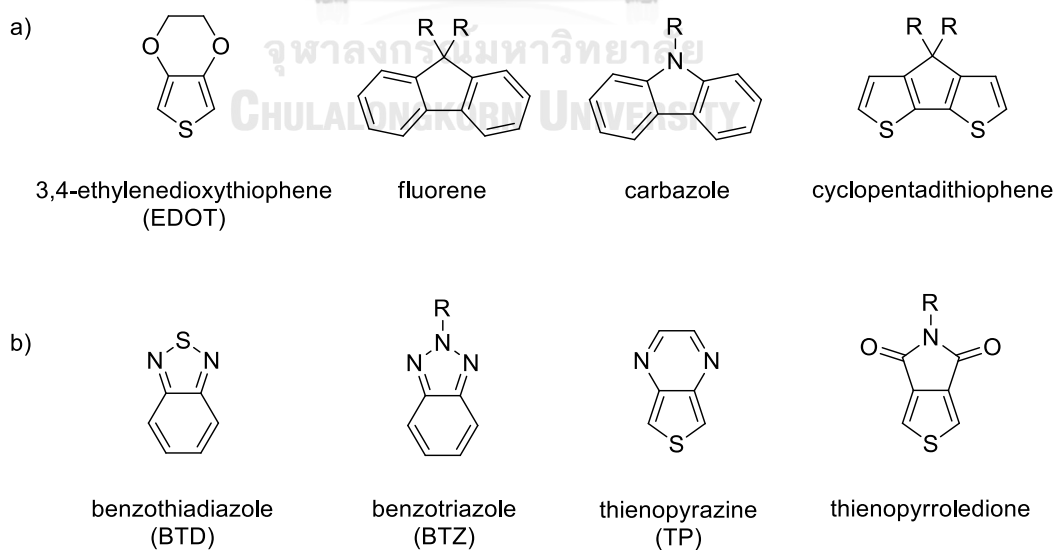


Figure 1.2 a) electron-rich donor units b) electron-deficient acceptor units

Thiophene-based polymers are the most popular conjugated polymers. With good optical properties, wide range in UV visible absorption and stable in ambient environment, [26] they are quite suitable to be developed into many electronic devices. Examples of some of the successful polymers of this type are shown in **Figure 1.3**.

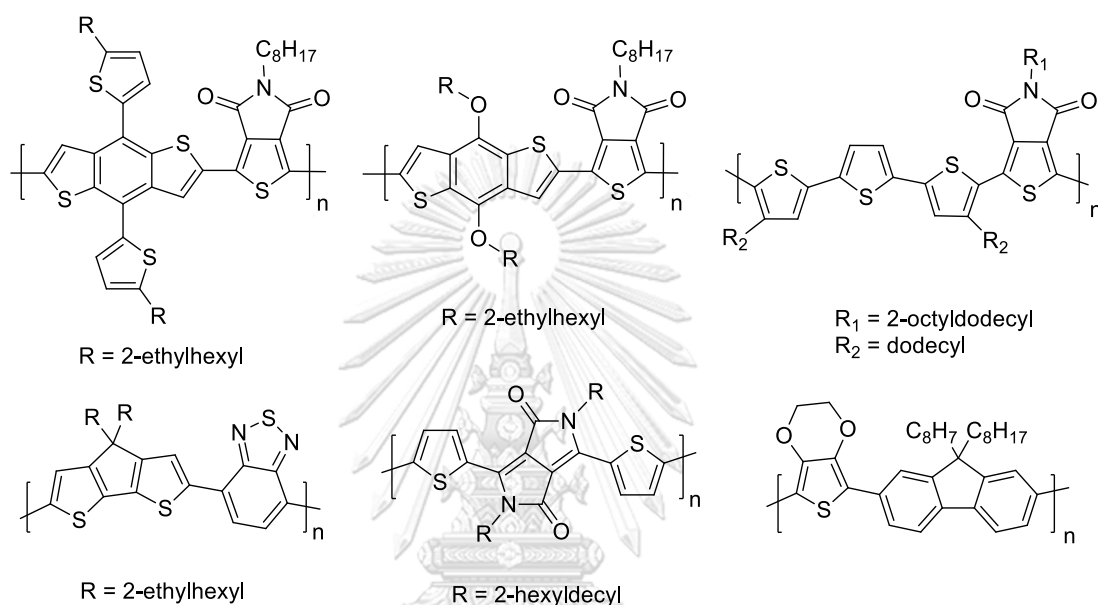


Figure 1.3 Examples of thiophene-based conjugated polymers

1.2 Synthesis of conjugated polymers

To obtain conjugated polymers, formations of C-C bonds are generally needed. Palladium catalyzed cross-coupling reactions are the most efficient and useful methods for such requirement. (**Figure 1.4**) These reaction mostly allow couplings between two sp^2 or sp hybridized carbons. Aryl halides and organometallic aryl derivatives were commonly used as the precursors.

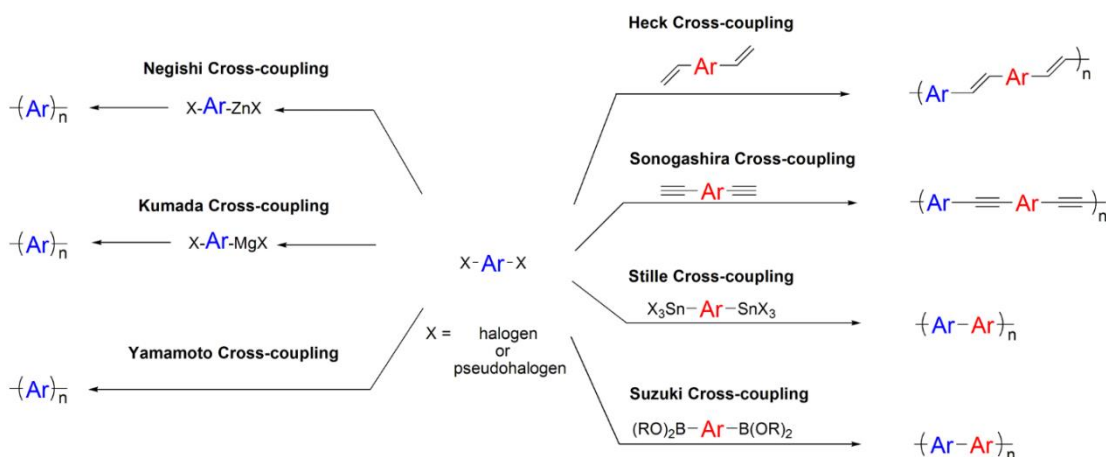
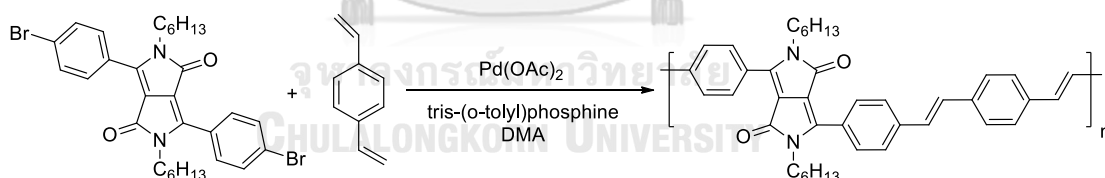


Figure 1.4 Traditional C-C coupling methods for synthesis of conjugated polymer

1.2.1 Heck cross-coupling reaction

Heck cross-coupling reaction is a reaction of an aryl halide with an alkene in the presence of a palladium catalyst. In 2005, Tieke and coworkers [27] used this method to synthesize diphenylpyrrolopyrrole (DPP)-based polymers. (**Scheme 1.1**) The polymer presented the maximum wavelength (λ_{max}) of 529 nm and emission wavelength of 598 nm.

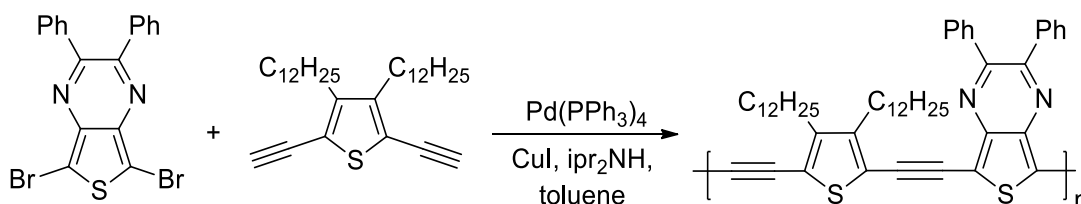


Scheme 1.1 Heck cross-coupling polymerization between 1,4-diketo-2,5-dihexyl-3,6-bis(4-bromophenyl)pyrrolo[3,4-c]pyrrole and p-divinylbenzene

1.2.2 Sonogashira cross-coupling reaction

Sonogashira cross-coupling reaction is a reaction that forms a C-C bond between an aryl halide and a terminal alkyne. In 2006, Sensfuss and coworkers [28] synthesized thieno[3,4-b]pyrazines based polymer using this method. (**Scheme 1.2**) The

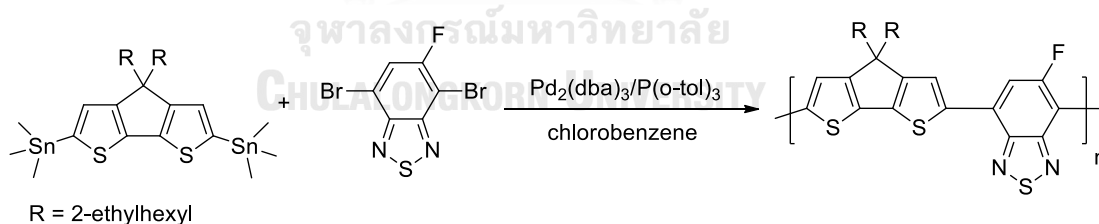
polymer was made into an organic solar cell and presented power conversion efficiency (%PCE) of 2.37 %.



Scheme 1.2 Sonogashira cross-coupling polymerization of 2,3-diphenylthieno[3,4-b]pyrazine and 3,4-didodecyl-2,5-diethynylthiophene

1.2.3 Stille cross-coupling reaction

Stille cross-coupling is a versatile C-C bond forming reaction between aryl halide and organostannane, with few limitations. This reaction is the popular and highly efficient method for synthesis of conjugated polymer. In 2012, Jen and coworkers [29] used Stille cross-coupling reaction for the synthesis of polymer from cyclopentadithiophene derivative and 5-fluoro-[2,1,3]-benzothiadiazole. (**Scheme 1.3**) The polymer presented %PCE at 5.81%.

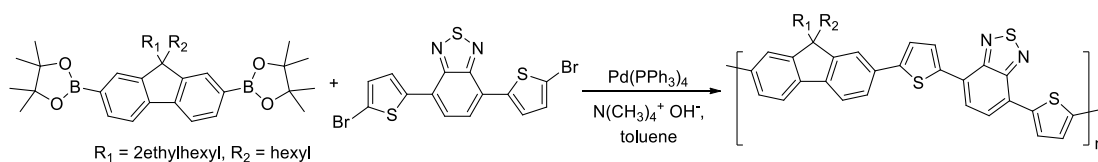


Scheme 1.3 Stille cross-coupling polymerization between cyclopentadithiophene derivative and 5-fluoro-[2,1,3]-benzothiadiazole

1.2.4 Suzuki cross-coupling reaction

Suzuki cross-coupling is a catalyzed reaction between organoborane (boronic acid or boronic ester) and aryl halide under basic condition. In 2003, Andersson and

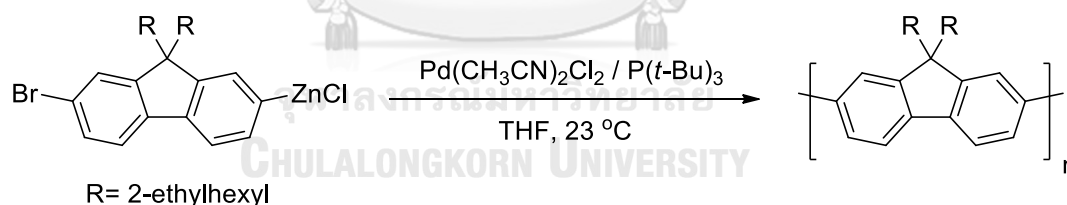
coworkers [30] successfully synthesized a conjugated polymer for organic solar cell using this method. **(Scheme 1.4)** The polymer has low band gap and broad optical absorption spectrum.



Scheme 1.4 Suzuki cross-coupling polymerization between fluorene and benzothiadiazole derivatives

1.2.5 Negishi cross-coupling reaction

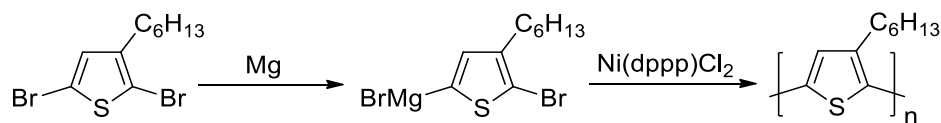
Negishi cross-coupling reaction is Ni- or Pd-catalyzed cross-coupling of organozinc compounds with aryl halides. In 2014, Kiriya and coworkers [31] synthesized a homopolymer from AB-type fluorene monomer using Negishi cross-coupling reaction in mild condition. **(Scheme 1.5)** The polymer was obtained in high molecular weight.



Scheme 1.5 Negishi cross-coupling polymerization of fluorene derivative

1.2.6 Kumada cross-coupling reaction

Kumada cross-coupling reaction is a reaction of Grignard reagents with aryl halide in the presence of Ni- or Pd- catalyst. In 2011, Kiriya and coworkers [32] synthesized homopolymer of 3-hexylthiophene by this method. **(Scheme 1.6)**



Scheme 1.6 Kumada cross-coupling polymerization of 3-hexylthiophene derivative

1.3 Direct arylation polymerization (DAP)

All of traditional methods can produce conjugated polymers in high yields. But they suffer some disadvantages especially the requirement of preparations of their corresponding organometallic precursors, which are difficult or expensive to synthesize, use or give toxic compounds or by-products, or too sensitive in ambient environment. [33] Even though Heck and Sonogashira cross-coupling polymerizations do not require organometallic precursors, both of these reactions must use monomers that have terminal alkene or alkyne. Recently, a new cross-coupling method called direct arylation polymerization or DAP was discovered and introduced as an alternative method for synthesis of conjugated polymers. (Figure 1.5) [34-36]

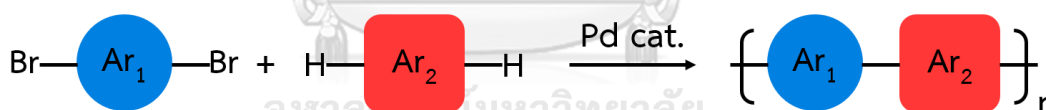


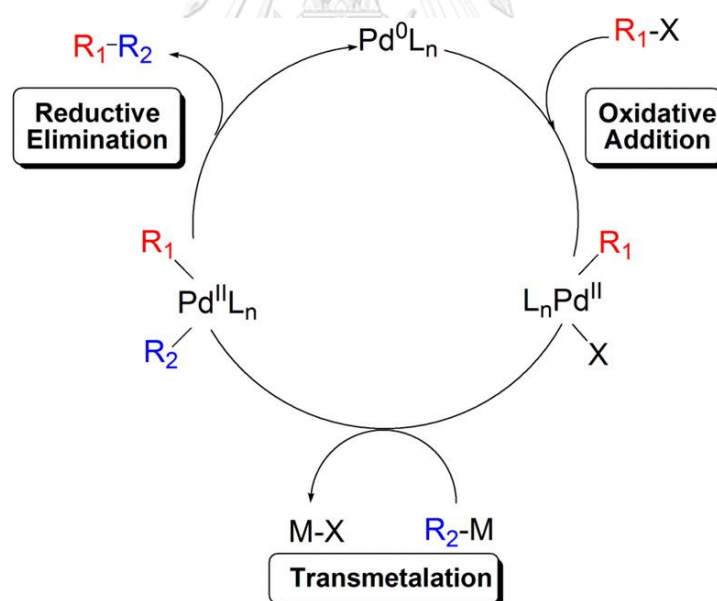
Figure 1.5 Direct arylation polymerization or DAP

DAP can form C-C bonds between two arene compounds through C-Br bonds of an aryl bromide directly onto C-H bonds of the other arenes. This method does not require organometallic precursors, which can eliminate the associated disadvantages of traditional methods from organometallic compounds, reduce synthetic steps and avoid metal toxic wastes.

1.4 Mechanisms of direct arylation polymerization

1.4.1 Mechanisms of palladium-catalyzed cross-coupling reactions

As shown in **Figure 1.6**, most palladium-catalyzed cross-coupling reactions involve the same catalytic cycle consisting three steps. The first step is usually an oxidative addition of a Pd(0) complex and electrophilic aromatic compound (R_1-X) to form intermediate L_nR_1PdX , where X is a halogen (i.e., Cl, Br, I). This is often the rate-limiting step in this catalytic cycle. [37] (except Stille coupling, where the rate-limiting step is the next transmetalation step. [38]) Then the Pd(II) intermediate reacts with nucleophilic organometallic aryl compound (R_2-M), transferring the aryl group (R_2) onto palladium-catalyst to form another intermediate $L_nR_1PdR_2$ and eliminating of $M-X$ as called a transmetalation step. The last step is a reductive elimination of the product R_1-R_2 and regeneration of active catalyst PdL_n .

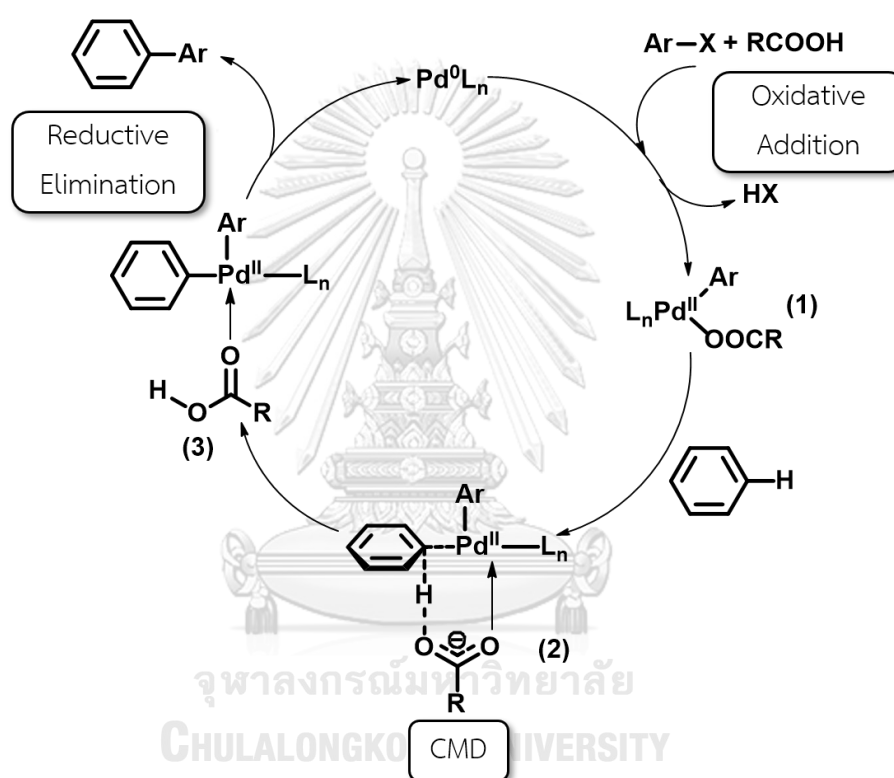


where, R_1 and R_2 are arene derivatives
 X represents an halogen or a pseudo-halogen
 M represents an organometallic functional compound

Figure 1.6 General mechanism of Pd-catalyzed cross-coupling reactions

1.4.2 The concerted metalation-deprotonation (CMD) mechanism

The mechanism of DARP is close to the above general mechanism of Pd-catalyzed cross-coupling reactions. Except in the second step, transmetalation is replaced by a process called concerted metalation-deprotonation (CMD). CMD was proposed by Fagnou and Lafrance upon studying direct C-H arylation of benzene and phenyl bromide using $\text{Pd}(\text{OAc})_2$ catalyst and pivalic acid additive. [39]



where, Ar represents an aryl group of aryl halide

X represents an halogen

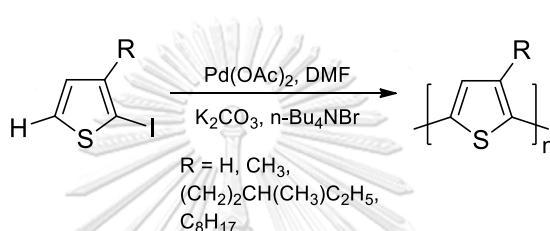
Figure 1.7 CMD mechanism of direct C-H arylation

From **Figure 1.7**, after the initial oxidative addition, palladium complex (1) reacts with aryl halide (Ar-X) to form activated complex (2) stabilized by a carboxylate (or carbonate). This step is the most important step to drive the reaction. The arene compound is deprotonated by the carboxylate forming the usually

formed diaryl palladium intermediate (3). Reductive elimination occurs in the last step to give the coupling product and regenerate the catalyst.

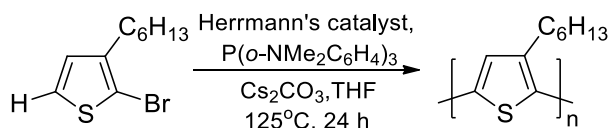
1.5 Literature review

In 1999, Lemaire and coworkers [40] successfully synthesized oligothiophene from 2-iodo-3-alkylthiophene from DArP using Heck-type condition and $\text{Pd}(\text{OAc})_2$ as the catalyst. (Scheme 1.7)



Scheme 1.7 Synthesis of oligo(3-alkylthiophene) via direct arylation

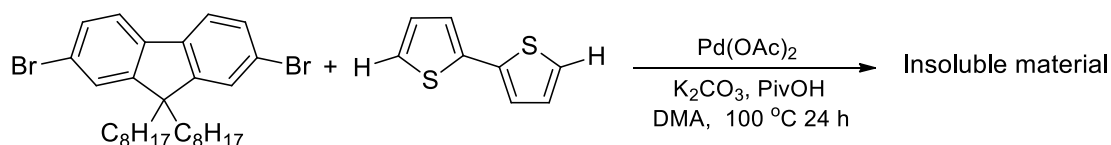
In 2010 Ozawa and coworkers [41] synthesized poly(3-hexylthiophene) from polycondensation of 2-bromo-3-hexylthiophene using Herrmann's catalyst ($\text{trans-di}(\mu\text{-acetato})\text{bis}[o\text{-(di-}o\text{-tolylphosphino)benzyl}]dipalladium(\text{II})$) and $\text{P}(o\text{-NMe}_2\text{C}_6\text{H}_4)_3$. (Scheme 1.8) The reaction gave a head-to-tail connected poly(3-hexylthiophene) with $M_n = 30600$. It is the first example of high molecular weight poly(3-hexylthiophene) from DArP.



Scheme 1.8 Polycondensation of 2-bromo-3-hexylthiophene

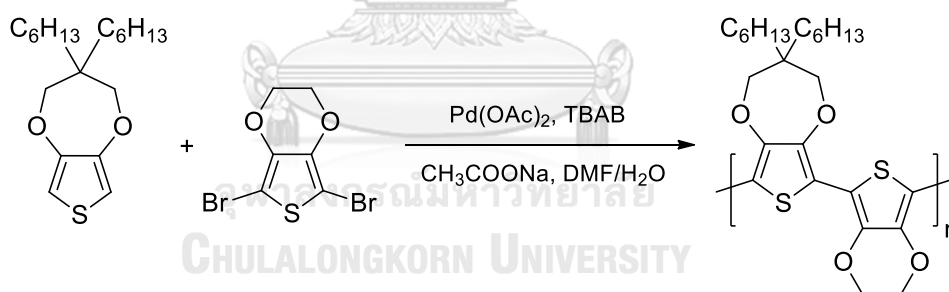
In 2011, Kanbara and coworkers [42] synthesized conjugated polymers between 2,2'-bithiophene and a fluorene derivative using direct arylation polymerization. (Scheme 1.9) An insoluble product was obtained. They presumed that the product contained an extensive cross-linked structure due to cross-couplings

onto C-H bonds at β -positions of thiophene rings or β -defect. To circumvent the β -defect problem, a β -protected arene, which is an arene that has substitution groups on β -positions, was employed. 3,4-Ethylenedioxythiophene (EDOT) and their derivatives are popular β -protected arenes that widely used in DArP.



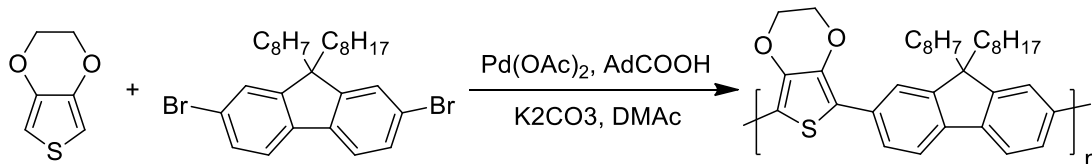
Scheme 1.9 DArP of 2,2'-bithiophene and a fluorene derivative

The first example of using EDOT in DArP was reported by Kuma and Kuma. [43] (**Scheme 1.10**) They synthesized conjugated polymer from 3,4-propylenedioxythiophenes (ProDOT) and EDOT using Pd(OAc)_2 as the catalyst. The product was obtained in high molecular weight and found be an alternated copolymer.



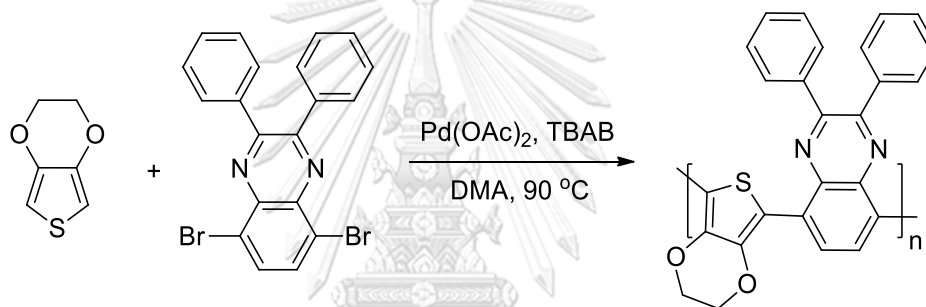
Scheme 1.10 DArP of 2,4-propylenedioxythiophenes (ProDOT) and EDOT

In 2013, Kanbara and coworkers [44] optimized the condition of DArP of EDOT and 2,7-dibromo-9,9-dioctyl-9H-fluorene, where Pd-catalyst and carboxylic acid additive were varied. (**Scheme 1.11**) They found that the reaction using Pd(OAc)_2 and 1-adamantanecarboxylic acid gave the highest molecular weight of 42700 in 87% yield.



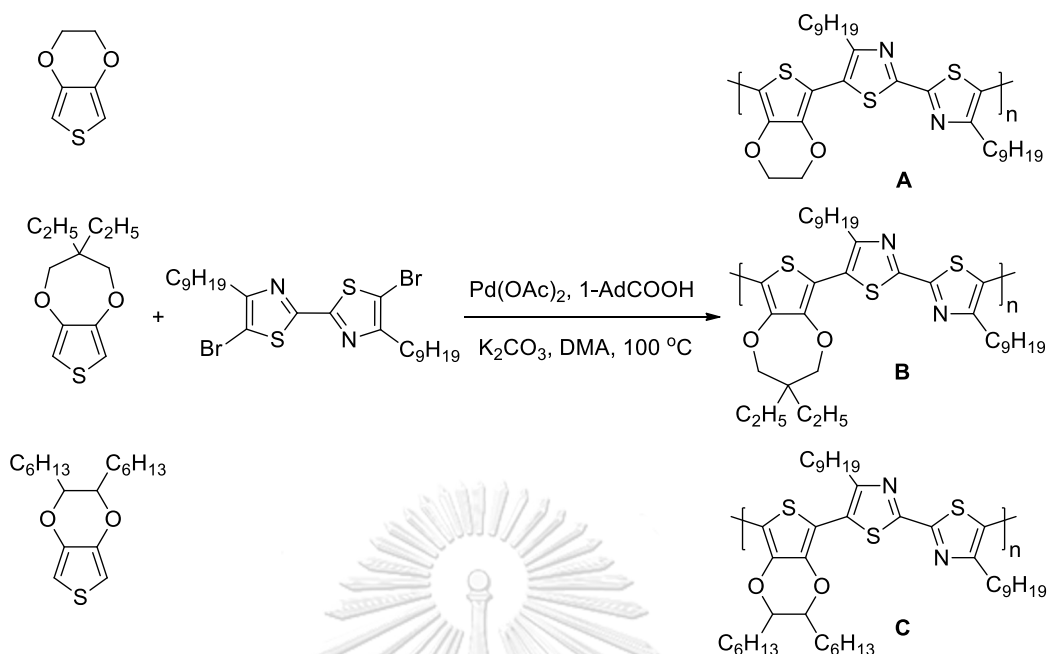
Scheme 1.11 DARp of 2,7-dibromo-9,9-dioctylfluorene and EDOT

In 2015, Joseph and coworkers [45] synthesized a donor-acceptor conjugated polymer between EDOT and 5,8-dibromo-2,3-diphenylquinoxaline via DARp. (**Scheme 1.12**) The product exhibited maximum wavelength absorption (λ_{\max}) at 561 nm, $M_n = 3207$ and low band gap 1.0 eV.



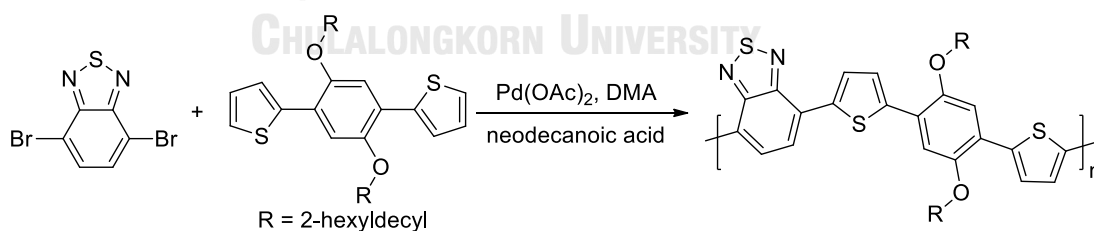
Scheme 1.12 DARp of EDOT and 5,8-dibromo-2,3-diphenylquinoxaline

Kanbara and coworkers [46] performed the polymerizations between 5,5'-dibromo-4,4'-dinyonyl-2,2'-bithiazole and three EDOT derivatives. Polymers **A**, **B** and **C** showed $M_n = 4300$, 4400 and 13100, $\lambda_{\max} = 501$, 484 and 510 nm, respectively. The best polymer is **C** that contains the dihexyl-EDOT units.



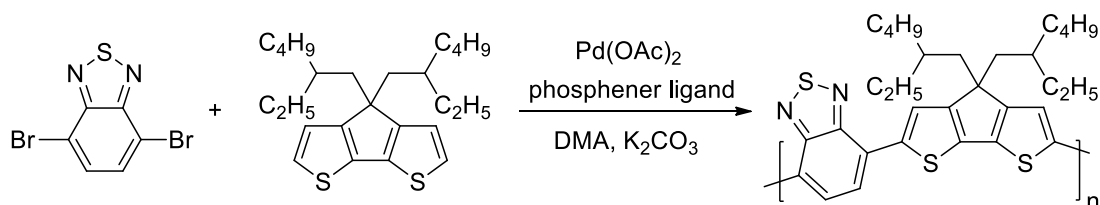
Scheme 1.13 Synthesis of polymers **A**, **B** and **C**

In parts of acceptor units, benzothiadiazole (BTD) is interesting acceptor for synthesis conjugated polymer. Bundgaard and coworkers [47] synthesized donor-acceptor conjugated polymer of 4,7-dibromobenzothiadiazole and 2,2'-(2,5-bis((2-hexyldecyl)oxy)-1,4-phenylene)dithiophene via DArP. The polymer exhibited good optical property with $\lambda_{\text{max}} = 650$ nm.



Scheme 1.14 DArP of 4,7-dibromobenzothiadiazole and 2,2'-(2,5-bis((2-hexyldecyl)oxy)-1,4-phenylene)dithiophene

Scherf and coworkers [48] synthesized conjugate polymer between 4,4-di(2-ethylhexyl)-cyclopenta[2,1-b:3,4-b']dithiophene and 4,7-dibromobenzothiadiazole using DArP. The product was obtained in high molecular weight (M_n) of 40300.



Scheme 1.15 DArP of 4,4-di(2-ethylhexyl)-cyclopenta[2,1-b:3,4-b']dithiophene and 4,7-dibromobenzothiadiazole

From literature reported, EDOT and derivatives can use as precursor in DArP and give polymers that have high molecular weight, low band gap and wide range of UV visible absorption and high conductivity. EDOT is a strong donor due to oxygen can donate electron to thiophene ring. Moreover, EDOT is β -protected arene that can solve problem about β -defect. In this work, we would like to synthesize EDOT-base donor-acceptor conjugated polymers via DArP. EDOT with long chain alkyl group was selected to use in this work. The presence of long chain alkyl group increases solubility of polymer. It was coupled with 7 selected dibromoarenes.

1.6 The objective of this work

The objective of this research are synthesis new donor-acceptor conjugated polymers based on 2'-octyl-3,4-ethylenedioxythiophene (OEDOT) from direct arylation polymerization (DArP) with selected dibromoarenes as shown in **Figure 1.8**.

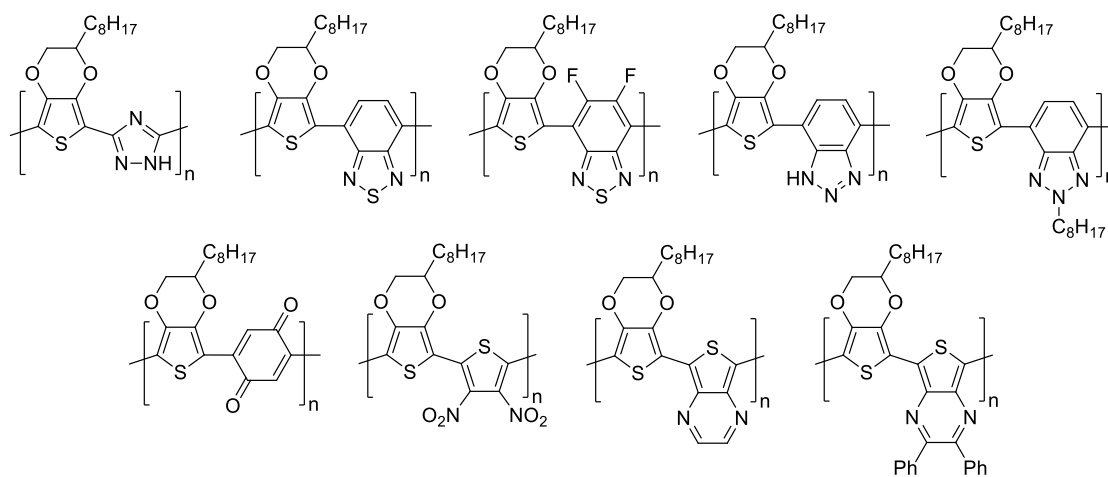


Figure 1.8 Target donor-acceptor conjugated polymers



CHAPTER II

EXPERIMENTS

2.1 Chemicals

Thin layer Chromatography (TLC) was performed on aluminum sheets precoated with silica gel (Merck Kieselgel 60 F₂₅₄, Merck KGaA, Darmstadt, Germany). Column chromatography was performed using 0.040-0.060 mm or 40-60 mesh ASTM silica gel 60 (Merck Kieselgel 60 G, Merck KGaA, Darmstadt, Germany). Solvents used in synthesis were reagent or analytical grades. Solvents used in column chromatography were distilled from commercial grade prior to use. Other reagents were purchased from the following vendors:

- Acros Organics (New Jersey, USA): *tert*-butyl(chloro)dimethylsilane, dimethylacetamide (DMA), imidazole, *o*-phenylenediamine, tri-*n*-butylamine
- Aldrich (USA): 1,8-diazabicyclo(5.4.0)undec-7-ene (DBU), 2,5-dibromobenzene-1,4-diol, diethyl oxalate, 4-dimethylaminopyridine (DMAP), ethyl chloroacetate, liquid bromine, tris(dibenzylideneacetone)dipalladium(0) (Pd₂(dba)₃), Sn powder, sodium metal, potassium carbonate (K₂CO₃), triphenylphosphine (PPh₃)
- Carlo Erba (Milan, Italy): diethyl ether, sodium hydroxide (NaOH)
- Eurisotop (USA): deuterated acetone (acetone-d₆), deuterated chloroform (CDCl₃), deuterated dimethylsulfoxide (DMSO-d₆)
- Heraeus (Hanau, Germany): palladium(II) acetate (Pd(OAc)₂)
- Intellect co. (Thailand): sodium sulfide nonahydrate (Na₂S·9H₂O)
- Merck Co. (Darmstadt, Germany): concentrated hydrochloric acid, fuming nitric acid, concentrated sulfuric acid
- Panreac (Spain): anhydrous magnesium sulfate (MgSO₄)
- RCI Labscan (Bangkok, Thailand): acetone, acetic acid, acetonitrile, dichloromethane (DCM), dimethylformamide (DMF), hexane, ethyl acetate (EtOAc), methanol, sodium hydrogen carbonate (NaHCO₃), toluene

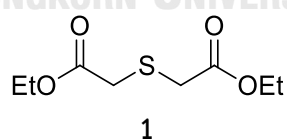
- TCI (Japan): 1-bromooctane, 2,1,3-benzothiadiazole (BTD), N-bromosuccinimide (NBS), 1-decene, 3,5-dibromo-1,2,4-triazole, 4,7-dibromo-5,6-difluoro-2,1,3-benzothiadiazole, 8.8 M glyoxal, pivalic acid (PivOH), trifluoroacetic acid (TFA)

2.2 Instruments and Equipment

The FT-IR spectra were recorded on a Nicolet 6700 FT-IR spectrometer. ^1H NMR spectra were obtained from Varian Mercury NMR spectrometer operated at 400.00 MHz. ^{13}C NMR spectra were obtained from Bruker Avance 400 operated at 100.00 MHz. The UV-Vis absorption spectra were recorded on an Agilent 8453E UV-Visible spectroscopy. The mass data were measured with ESI-MS (Quattro microTM API) or Matrix assisted laser desorption ionization-time of flight mass spectrometry (Bruker MicroFlex MALDI-TOF) or Gel permeation chromatography (GPC) (Tosoh Ecosec HLC-8320GPC and Waters 2414 refractive index (RI) detector with Styragel HR5E). Melting points were determined with a Stuart Scientific Melting Point apparatus SMP20 (Bibby Sterlin Ltd., Staffordshire, UK).

2.3 Monomers synthesis

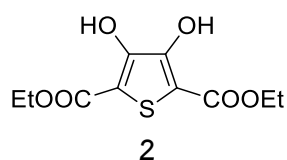
2.3.1 Diethyl thiodiglycolate (**1**)



A solution of $\text{Na}_2\text{S}\cdot 9\text{H}_2\text{O}$ (12.0 g, 50 mmol) in water (30 mL) was added dropwise to the solution of ethyl chloroacetate (13.24 g, 55 mmol) in acetone (50 mL). The reaction was refluxed under nitrogen atmosphere for 3 h. After cooling to room temperature, the reaction was extracted by diethyl ether. The separated organic layer was dried over anhydrous MgSO_4 and evaporated to give **1** as yellow liquid (7.07 g, 62% yield). [49] ^1H NMR (400 MHz, CDCl_3): δ (ppm) 4.05 (q, $J = 6.8$ Hz,

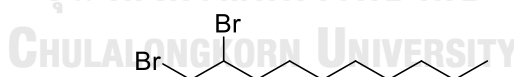
4H), 3.24 (s, 4H), 1.16 (t, $J = 7.2$ Hz, 6H). (Figure A.1, Appendix) ^{13}C NMR (100 MHz, CDCl_3): δ (ppm) 169.5, 61.1, 33.3, 13.9. (Figure A.2, Appendix)

2.3.2 Diethyl 3,4-dihydroxythiophene-2,5-dicarboxylate (2)



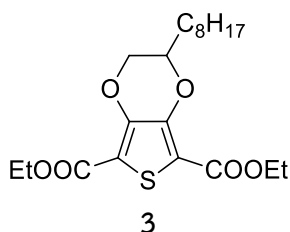
Sodium metal (2.4 g, 0.21 mol) was dissolved in ethanol (75 mL) and the solution was added dropwise to a mixture of **1** (2.00 g, 0.010 mol) and diethyl oxalate (4.5 g, 0.03 mol) for 30 min in ice bath. The reaction was refluxed under nitrogen atmosphere for 3 h. Then the reaction was cooled to room temperature, added water (400 mL), and acidified by conc. HCl (15 mL) to obtain a white solid of **2** (2.299 g, 76% yield). mp. 134-135 °C (lit. 135 °C). [50] ^1H NMR (400 MHz, CDCl_3): δ (ppm) 9.35 (s, 2H), 4.39 (q, $J = 7.0$ Hz, 4H), 1.36 (t, $J = 7.0$ Hz, 6H). (Figure A.3, Appendix) ^{13}C NMR (100 MHz, CDCl_3): δ (ppm) 165.5, 151.6, 107.1, 61.7, 14.0. (Figure A.4, Appendix) IR (ATR, cm^{-1}): 3305, 2981, 1690, 1663. (Figure A.5, Appendix)

2.3.3 1,2-Dibromodecane



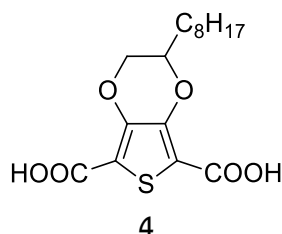
A solution of 1-decene (14.27 g, 100 mmol) in dichloromethane (DCM) (50 mL) was added liquid bromine (6 mL, 117 mmol) dropwise until the yellow color permanently appeared. Then the reaction was extracted with DCM and was evaporated to give to light-yellow liquid of 1,2-dibromodecane (40.26 g, 92% yield). [51] ^1H NMR (400 MHz, CDCl_3): δ (ppm) 4.16 (m, 1H), 3.84 (dd, $J = 10.2, 4.4$ Hz, 1H), 3.62 (t, $J = 10.0$ Hz, 1H), 2.12 (m, 1H), 1.77 (m, 1H), 1.63 – 1.10 (m, 14H), 0.88 (t, $J = 6.6$ Hz, 3H). (Figure A.6, Appendix)

2.3.4 Diethyl 2-octyl-2,3-dihydrothieno[3,4-b][1,4]dioxine-5,7-dicarboxylate (3)



A mixture of **2** (3.25 g, 12.5 mmol), tri-*n*-butylamine (6.94 g, 37.5 mmol) and 4-dimethylaminopyridine (DMAP) (1.07 g, 8.75 mmol) was dissolved in dimethylformamide (DMF) (30 mL) and heated to 100 °C under nitrogen atmosphere. Subsequently, it was added 1,2-dibromodecane (11.25 g, 37.5 mmol) and heated for 24 h. The reaction was quenched by adding 10% HCl and extracted with ethyl acetate (EtOAc). Organic layer was dried over anhydrous MgSO₄ and evaporated. The crude product was purified by column chromatography, eluted with EtOAc:hexane (1:9) to give the product as white solid (1.397 g, 28% yield). mp. 94-95 °C (lit. 92-94 °C). [52] ¹H NMR (400 MHz, CDCl₃): δ (ppm) 4.40 (m, 6H), 4.05 (m, 1H), 1.81-1.43 (m, 20H), 0.89 (t, 3H). (Figure A.7, Appendix) ¹³C NMR (100 MHz, CDCl₃): δ (ppm) 161.0, 160.9, 145.3, 145.0, 111.8, 111.5, 74.2, 68.4, 61.2, 61.1, 31.8, 30.4, 29.4, 29.3, 29.2, 25.1, 22.6, 14.2, 14.0. (Figure A.8, Appendix) IR (ATR, cm⁻¹): 2916, 2849, 1698, 1503 (Figure A.9, Appendix)

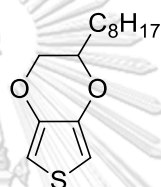
2.3.5 2-Octyl-2,3-dihydrothieno[3,4-b][1,4]dioxine-5,7-dicarboxylic acid (4)



Compound **3** (1.086 g, 2.73 mmol) was mixed with 3 mL of EtOH and 30 mL of 1 M NaOH. The mixture was refluxed under nitrogen atmosphere for 3 h. It was

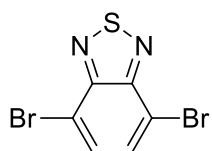
cooled to room temperature and quenched by added 15 mL of 10% HCl. The product was filtered to obtain a white solid of **4** (0.858 g, 92% yield). mp. 218-221 °C (lit. 216-220 °C). [52] ^1H NMR (400 MHz, DMSO-d_6): δ (ppm) 4.39 (m, 1H), 4.30 (m, 1H), 3.98 (m, 1H), 1.56-1.18 (m, 14H), 0.83 (t, 3H). (**Figure A.10, Appendix**) ^{13}C NMR (100 MHz, DMSO-d_6): δ (ppm) 161.7, 144.8, 144.6, 111.5, 111.4, 73.7, 67.4, 31.2, 29.6, 28.8, 28.7, 28.5, 24.2, 22.0, 13.9. (**Figure A.11, Appendix**) IR (ATR, cm^{-1}): 3364, 2913, 2849, 1718, 1671, 1574. (**Figure A.12, Appendix**)

2.3.6 2'-Octyl-3,4-ethylenedioxythiophene (OEDOT)



A mixture of **4** (0.342 g, 1 mmol) and 1,8-diazabicyclo(5.4.0)undec-7-ene (DBU) (1.2 mL, 8 mmol) in dimethylacetamide (DMA) (2 mL) was heated in a sealed vessel in a microwave reactor at 150 °C, 200 W for 1 h. Then the reaction was cooled down to room temperature and added 10% HCl and extracted with EtOAc. The separated organic layer was dried over anhydrous MgSO_4 and evaporated. The crude product was purified by column chromatography, eluted with hexane to give yellow oil of OEDOT (0.172 g, 68% yield). [53] ^1H NMR (400 MHz, CDCl_3): δ (ppm) 6.30 (s, 2H), 4.13 (m, 2H), 3.87 (m, 1H), 1.79 – 1.18 (m, 14H), 0.88 (t, $J = 6.4$ Hz, 3H). (**Figure A.13, Appendix**) IR (ATR, cm^{-1}): 2919.71, 2852.00, 1483.24. (**Figure A.14, Appendix**)

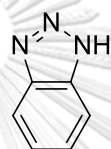
2.3.7 4,7-Dibromo-2,1,3-benzothiadiazole (DBBTD)



2,1,3-Benzothiadiazole (BTD) (0.501 g, 3.68 mmol) was mixed with N-bromosuccinimide (NBS) (1.483 g, 8.464 mmol) and conc. H_2SO_4 (5 mL). The mixture

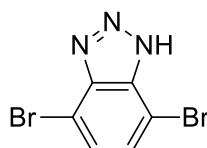
was heated to 60 °C for 4 h. The reaction was cooled in ice bath and added water (25 mL) dropwise and extracted with toluene. After separated the organic layer and evaporated, the crude product was purified by column chromatography, eluted with hexane to give the white solid of DBBTD (0.698 g, 64% yield). mp. 185-186 °C (lit. 187-188 °C). [54-55] ^1H NMR (400 MHz, CDCl_3): δ (ppm) 7.73 (s, 2H). (Figure A.15, Appendix) IR (ATR, cm^{-1}): 3078, 3043, 1583. (Figure A.16, Appendix) MS: m/z 291.73 (M^+), 293.68 ($\text{M}+2$), 295.68 ($\text{M}+4$). (Figure A.17, Appendix)

2.3.8 1,2,3-Benzotriazole (BTZ)



A solution of *o*-phenylenediamine (1.08 g, 10 mmol) in glacial acetic acid (35 mL) was cooled in ice bath and added a cold solution of NaNO_2 (1.035 g, 15 mmol) in water (20 mL). The reaction was stirred at 0 °C for 30 min and then 1 M NaOH was added until the solution turned neutral. The product was extracted into EtOAc, separated, evaporated and purified by column chromatography, eluted with EtOAc:hexane (1:1) to give the product as light-yellow solid (0.761 g, 63.75 %yield). mp. 99-101 °C (lit. 99-100 °C). [56] ^1H NMR (400 MHz, CDCl_3): δ (ppm) 7.96 (dd, $J = 6.1, 2.7$ Hz, 2H), 7.47 (dd, $J = 6.3, 2.9$ Hz, 2H). (Figure A.18, Appendix) IR (ATR, cm^{-1}): 3338, 3244, 2790. (Figure A.19, Appendix)

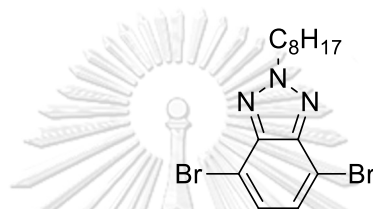
2.3.9 4,7-Dibromo-1,2,3-benzotriazole (DBBTZ)



Following the same procedure as in section 2.3.7, a reaction of BTZ (0.460 g, 3.86 mmol) and NBS (1.437 g, 8.106 mmol) yielded the crude product, which was

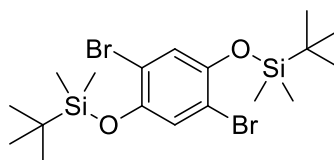
purified by column chromatography, eluted with EtOAc:hexane (1:1) to obtain the white solid of DBBTZ (0.693 g, 65% yield). mp. 247-252 °C (lit. 248-250 °C). [57] ^1H NMR (400 MHz, acetone- d_6): δ (ppm) 7.64 (s, 2H). (Figure A.20, Appendix) IR (ATR, cm^{-1}): 3113.98, 3063.94, 3013.90, 2975.63, 2910.88, 2819.62, 1612.76, 1500.90. (Figure A.21, Appendix) MS: m/z 275.75 (M^+), 277.70 ($M+2$), 279.72 ($M+4$). (Figure A.22, Appendix)

2.3.10 4,7-Dibromo-2-octyl-1,2,3-benzotriazole (DBOBTZ)



DBBTZ (1.396 g, 5.04 mmol) was mixed with 1-bromooctane (1.168 g, 6.05 mmol), K_2CO_3 (2.089 g, 15.12 mmol) and DMF (5 mL). It was heated to 60 °C for 3 h and cooled to room temperature. It was extracted with EtOAc and evaporated. The crude product was purified by column chromatography, eluted with EtOAc:hexane (1:19) to obtain the product as colorless oil (1.166 g, 59% yield). [23] ^1H NMR (400 MHz, CDCl_3): δ (ppm) 7.44 (s, 2H), 4.78 (t, $J = 7.4$ Hz, 2H), 2.14 (dd, $J = 14.3, 7.2$ Hz, 2H), 1.48 – 1.08 (m, 10H), 0.87 (t, $J = 6.5$ Hz, 3H). (Figure A.23, Appendix) IR (ATR, cm^{-1}): 2949.14, 2922.65, 2849.06, 1492.07. (Figure A.24, Appendix) MS: m/z 387.53 (M^+), 389.67 ($M+2$), 392.19 ($M+4$). (Figure A.25, Appendix)

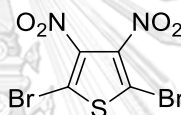
2.3.11 1,4-Dibromo-2,5-bis(*tert*-butyldimethylsilyloxy)benzene (5)



5

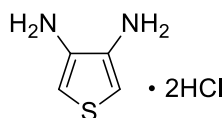
A mixture of 2,5-dibromobenzene-1,4-diol (0.134 g, 0.5 mmol), imidazole (0.136 g, 2 mmol) and *tert*-butyl(chloro)dimethylsilane (TBSCl) (0.301 g, 2 mmol) in 1:1 DCM:DMF (10 mL) was stirred at room temperature for 19 h. The reaction was quenched by 1 M NaOH and extracted with DCM. Organic layer was dried over anhydrous MgSO₄ and evaporated. The crude product was purified by column chromatography, eluted with hexane to give the product as white solid (0.133 g, 52% yield). [58] mp. 90-91 °C. ¹H NMR (400 MHz, CDCl₃): δ (ppm) 6.82 (s, 2H), 0.82 (s, 18H), 0.02 (s, 12H). **(Figure A.26, Appendix)** IR (ATR, cm⁻¹): 2952, 2943, 1468. **(Figure A.27, Appendix)**

2.3.12 2,5-Dibromo-3,4-dinitrothiophene (DBDNT)



3,4-Dibromothiophene (2 mL, 17.74 mmol) was added dropwise to conc. H₂SO₄ (30 mL) in ice bath. The mixture was added fuming HNO₃ (7 mL) dropwise and stirred at room temperature for 3 h. Then the reaction was quenched by NaHCO₃ powder in ice bath. and extracted with EtOAc. Organic layer was dried over anhydrous MgSO₄ and evaporated. The crude product was purified by column chromatography, eluted with EtOAc:hexane (1:9) to obtain yellow solid (2.009 g, 34% yield). mp. 135-138 °C (lit. 134-136 °C). [59] ¹³C NMR (100 MHz, CDCl₃): δ (ppm) 139.2, 113.8. **(Figure A.28, Appendix)** IR (ATR, cm⁻¹): 1538, 1315. **(Figure A.29, Appendix)** MS: m/z 330.68 (M⁺), 332.63 (M+2), 334.64 (M+4). **(Figure A.30, Appendix)**

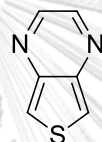
2.3.13 3,4-Diaminothiophene dihydrochloride (DAT.2HCl)



A mixture of DBDNT (0.996 g, 3 mmol) and conc. HCl (18.5 mL) was cooled in ice bath. Sn powder (2.490 g, 21 mmol) was added in small portion to maintain the

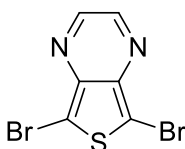
temperature at 25 °C and then stirred at room temperature for 2 h. The reaction was cooled overnight in freezer. The precipitated product was filtered and washed with diethyl ether and acetonitrile to give a light gray solid (0.319 g, 56.75 % yield). [60] The product in salt form cannot characterize. So, the product was changed to free amino form by adding 0.89 M KOH and characterized with ^1H NMR spectroscopy. ^1H NMR (400 MHz, CDCl_3): δ (ppm) 6.14 (s, 2H), 2.28 (s, 4H) ppm. (**Figure A.31, Appendix**) The free amino product is very susceptible to oxidation. It must use immediately after synthesis.

2.3.14 Thieno[3,4-*b*]pyrazine (TP)



DAT.2HCl (0.523 g, 2.8 mmol) was dissolved in 5% Na_2CO_3 solution (30 mL). 39% w/w glyoxal (0.45 mL, 4 mmol) was added into the solution and stirred at room temperature for 3 h. The reaction was extracted with DCM. Organic layer was dried over anhydrous MgSO_4 and evaporated. The crude product was purified by column chromatography, eluted with EtOAc:hexane (1:1) to obtain yellow solid (0.129 g, 34% yield). mp. 46-48 °C (lit. 47.3-48.1°C). [61] ^1H NMR (400 MHz, CDCl_3): δ (ppm) 8.50 (s, 2H), 8.02 (s, 2H). (**Figure A.32, Appendix**) The product is very susceptible to self-polymerization. It must use immediately after synthesis.

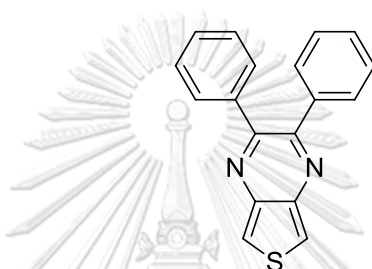
2.3.15 5,7-Dibromothieno[3,4-*b*]pyrazine (DBTP)



A solution of TP (0.053 g, 0.39 mmol) and NBS (0.208 g, 1.17 mmol) in DCM (10 mL) was stirred in ice bath under N_2 atmosphere for 15 min. The reaction was

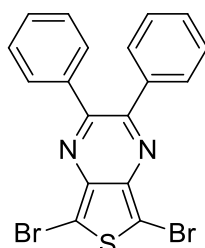
extracted with DCM, dried over anhydrous MgSO_4 , evaporated and purified by column chromatography, eluted with DCM:hexane (1:1) to obtain yellow solid (0.028 g, 24% yield). mp. 204-206 °C (lit. 205 °C). [62] ^1H NMR (400 MHz, CDCl_3): δ (ppm) 8.54 (s, 2H). **(Figure A.33, Appendix)** MS: m/z 291.82 (M^+), 293.77 ($\text{M}+2$), 295.83 ($\text{M}+4$). **(Figure A.34, Appendix)** The product is very susceptible to self-polymerization. It must use immediately after synthesis.

2.3.16 2,3-Diphenylthieno[3,4-*b*]pyrazine (DPTP)



DAT.2HCl (0.187 g, 1 mmol), Benzil (0.231 g, 1.1 mmol) and Et_3N (0.42 mL, 3 mmol) was dissolved in EtOH (20 mL). The mixture was stirred overnight at room temperature. The crude product was evaporated to dry and purified by column chromatography, eluted with EtOAc:hexane (1:9) to obtain yellow solid (0.207 g, 72% yield). Mp 190-192 °C (lit. 190-191 °C). [63] ^1H NMR (400 MHz, acetone- d_6): δ (ppm) 8.21 (s, 2H), 7.64 – 7.01 (m, 10H). **(Figure A.35, Appendix)** IR (ATR, cm^{-1}): 3082, 3055, 1439. **(Figure A.36, Appendix)** The product is very susceptible to self-polymerization. It must use immediately after synthesis.

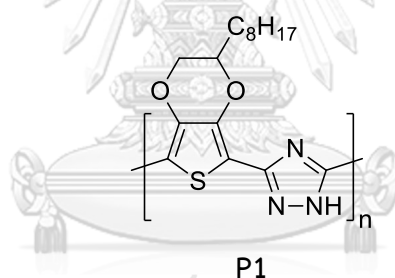
2.3.17 5,7-Dibromo-2,3-diphenylthieno[3,4-*b*]pyrazine (DBDPTP)



DPTP (0.230 g, 0.8 mmol) and NBS (0.299 g, 1.68 mmol) was dissolved in DCM (6 mL) and stirred at room temperature for 1 h. The reaction was extracted with DCM, dried over anhydrous MgSO_4 , evaporated and purified by column chromatography, eluted with DCM:hexane (1:1) to give a greenish-yellow solid (0.218 g, 61% yield). mp. 170-172 °C (lit. 169.1-171.0 °C). [63-64] ^1H NMR (400 MHz, CDCl_3): δ (ppm) 7.57 (m, 4H), 7.52 – 7.30 (m, 6H). (Figure A.37, Appendix) ^{13}C NMR (100 MHz, CDCl_3): δ (ppm) 154.7, 139.4, 138.3, 129.9, 129.4, 128.1, 105.0. (Figure A.38, Appendix) IR (ATR, cm^{-1}): 3049, 1521. (Figure A.39, Appendix) MS: m/z 444.81 (M^+), 446.81 ($\text{M}+2$), 448.70 ($\text{M}+4$). (Figure A.40, Appendix) The product is very susceptible to self-polymerization. It must use immediately after synthesis.

2.4 Polymers synthesis

2.4.1 Poly(2'-octyl-3,4-ethylenedioxythiophene-co-1,2,4-triazole) (P1)

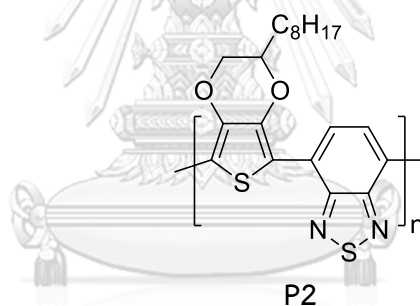


OEDOT (0.076 g, 0.30 mmol), 3,5-dibromo-1,2,4-triazole (0.068 g, 0.30 mmol), palladium(II) acetate ($\text{Pd}(\text{OAc})_2$) (0.0034 g, 0.015 mmol), Copper(I) iodide (CuI) (0.0028 g, 0.015 mmol), K_2CO_3 (0.099 g, 0.72 mmol), triphenylphosphine (PPh_3) (0.0079 g, 0.03 mmol) and pivalic acid (PivOH) (0.003 g, 0.03 mmol) were dissolved in DMA (5 mL). The mixture was heated to 110 °C for 48 h. The reaction was cooled down to room temperature and the solution was extracted by EtOAc. After evaporating the separated organic layer, the crude product was purified by column chromatography, eluted with EtOAc:hexane (1:1) to obtain the yellow solid of **P1** (0.034 g, 44% yield).

OEDOT (0.062 g, 0.244 mmol), 3,5-dibromo-1,2,4-triazole (0.055 g, 0.244 mmol), tris(dibenzylideneacetone)dipalladium(0) ($\text{Pd}_2(\text{dba})_3$) (0.0056 g, 0.0061 mmol),

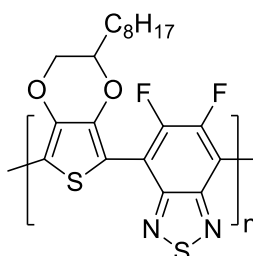
K_2CO_3 (0.08 g, 0.586 mmol), triphenylphosphine (PPh_3) (0.0062 g, 0.0244 mmol) and pivalic acid (PivOH) (0.0029 g, 0.0244 mmol) were dissolved in DMA (5 mL). The mixture was heated to 110 °C for 72 h. The reaction was cooled down to room temperature and the solution was extracted by EtOAc. After evaporating the separated organic layer, the crude product was purified by column chromatography, eluted with EtOAc:hexane (1:1) to obtain the yellow solid of **P1** (0.051 g, 65% yield). 1H NMR (400 MHz, $CDCl_3$): δ (ppm) 3.93 (3H), 2.43-0.89 (17H). (**Figure A.41, Appendix**) IR (ATR, cm^{-1}): 2920, 2849, 1639. (**Figure A.42, Appendix**) MALDI-TOF MS: m/z = 894.414, 725.912. (**Figure A.43, Appendix**) UV-visible : λ_{max} = 259 nm, with shoulder absorbance at 346 nm. (**Figure A.44, Appendix**)

2.4.2 Poly(2'-octyl-3,4-ethylenedioxythiophene-co-2,1,3-benzothiadiazole) (P2)



The mixture of OEDOT (0.203 g, 0.8 mmol), DBBTD (0.102 g, 0.35 mmol), $Pd(OAc)_2$ (0.009 g, 0.04 mmol), Cs_2CO_3 (0.632 g, 1.94 mmol), PPh_3 (0.021 g, 0.08 mmol) and PivOH (0.008 g, 0.08 mmol) was dissolved in toluene (5 mL). It was refluxed for 20 h, then cooled to room temperature, extracted into DCM and evaporated. The crude polymer was purified by two Soxhlet extractions with hexane and then methanol to give a dark blue solid (0.110 g, 82% yield). 1H NMR (400 MHz, $CDCl_3$): δ (ppm) 8.42 (2H), 4.30 (3H), 2.06 (2H), 1.28(12H), 0.88 (3H). (**Figure A.45, Appendix**) IR (ATR, cm^{-1}): 2923, 2846, 1557, 1483. (**Figure A.46, Appendix**) MALDI-TOF MS: m/z = 3606.503, 2825.845. (**Figure A.47, Appendix**) M_n (GPC) = 3114. UV-visible : λ_{max} = 630 nm. (**Figure A.48, Appendix**)

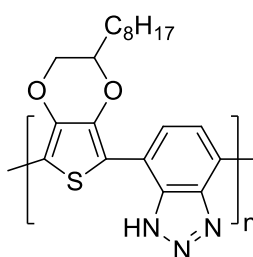
2.4.3 Poly(2'-octyl-3,4-ethylenedioxythiophene-co-5,6-difluoro-2,1,3-benzothiadiazole) (P3)



P3

OEDOT (0.0508 g, 0.2 mmol), 4,7-dibromo-5,6-difluoro-2,1,3-benzothiadiazole (DBDFBTD) (0.033 g, 0.1 mmol), Pd₂(dba)₃ (0.002 g, 0.0025 mmol), K₂CO₃ (0.05 g, 0.36 mmol) and acetic acid (0.006 mL, 0.1 mmol) was mixed in DMA (5 mL). It was heated to 110 °C for 24 h. It was then cooled to room temperature, extracted into DCM and evaporated. The crude product was purified by two Soxhlet extractions with hexane and then methanol to obtain the product as a red solid (0.016 g, 38% yield). ¹H NMR (400 MHz, CDCl₃): δ (ppm) 4.11 (3H), 1.48 (14H), 0.87 (3H). (Figure A.49, Appendix) IR (ATR, cm⁻¹): 2923, 2852, 1492. (Figure A.52, Appendix) MALDI-TOF MS: m/z = 2527.052, 1648.291. (Figure A.53, Appendix) M_n (GPC) = 2421. UV-visible : λ_{max} = 461 nm. (Figure A.55, Appendix)

2.4.4 Poly(2'-octyl-3,4-ethylenedioxythiophene-co-1,2,3-benzotriazole) (P4)

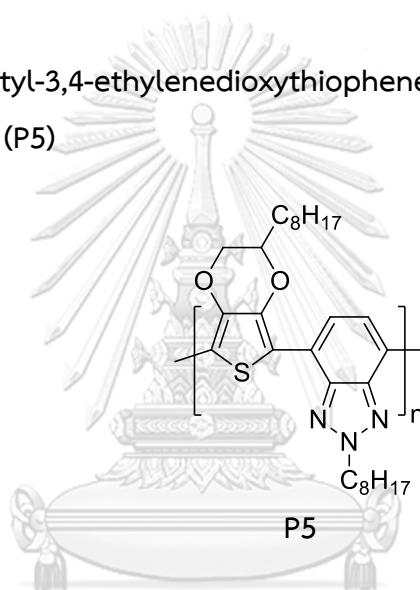


P4

A mixture of OEDOT (0.127 g, 0.5 mmol), DBBTZ (0.178 g, 0.5 mmol), Pd(OAc)₂ (0.006 g, 0.025 mmol), K₂CO₃ (0.17 g, 1.2 mmol), PPh₃ (0.013 g, 0.05 mmol) and PivOH

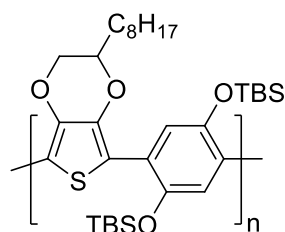
(0.005 g, 0.05 mmol) was mixed in DMA (5 mL). It was heated to 110 °C for 48 h, cooled to room temperature, extracted into DCM and evaporated. The product was purified by column chromatography, eluted with EtOAc:hexane (1:4) to obtain the yellow solid of **P4** (0.693 g, 65% yield). ^1H NMR (400 MHz, CDCl_3): δ (ppm) 7.55 (2H), 4.26 (3H), 1.25 (14H), 0.89 (3H). (**Figure A.56, Appendix**) IR (ATR, cm^{-1}): 2923, 2852. (**Figure A.57, Appendix**) MALDI-TOF MS: $m/z = 2212.910, 1245.524$. (**Figure A.58, Appendix**) UV-visible : $\lambda_{\text{max}} = 293$ nm, with shoulder absorbance at 331 nm. (**Figure A.59, Appendix**)

2.4.5 Poly(2'-octyl-3,4-ethylenedioxythiophene-co-2-octyl-1,2,3-benzotriazole) (**P5**)



OEDOT (0.127 g, 0.5 mmol), DBOBTZ (0.195 g, 0.5 mmol), $\text{Pd}(\text{OAc})_2$ (0.006 g, 0.025 mmol), Cs_2CO_3 (0.39 g, 1.2 mmol), PPh_3 (0.013 g, 0.05 mmol) and PivOH (0.005 g, 0.05 mmol) was mixed in toluene (5 mL). The reaction was heated to reflux for 22 h. Then it was cooled to room temperature, extracted into DCM and evaporated. The polymer was purified by two Soxhlet extractions with hexane and then methanol to obtain the red solid of **P5** (0.224 g, 87.5% yield). ^1H NMR (400 MHz, CDCl_3): δ (ppm) 8.10 (2H), 4.87 (2H), 4.42 (2H), 4.09 (1H), 2.29 (2H), 1.28 (12H), 0.86 (3H). (**Figure A.60, Appendix**) IR (ATR, cm^{-1}): 2920, 2852, 1566, 1504. (**Figure A.61, Appendix**) MALDI-TOF MS: $m/z = 5306.861, 2488.815$. (**Figure A.62, Appendix**) M_n (GPC) = 3670. UV-visible : $\lambda_{\text{max}} = 506$ nm. (**Figure A.63, Appendix**)

2.4.6 Poly(2'-octyl-3,4-ethylenedioxythiophene-co-1,4-bis(*tert*-butyldimethylsilyloxy)benzene) (P6)

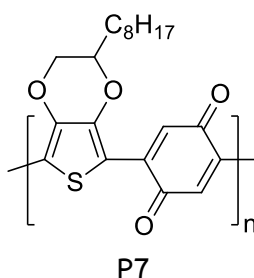


TBS = *tert*-butyldimethylsilyl

P6

OEDOT (0.073 g, 0.29 mmol), compound **5** (0.144 g, 0.29 mmol), Pd₂(dba)₃ (0.0064 g, 0.007 mmol), Cs₂CO₃ (0.203 g, 0.624 mmol), PPh₃ (0.0075 g, 0.029 mmol) and PivOH (0.003 g, 0.029 mmol) were dissolved in toluene (5 mL). The mixture was heated to reflux for 48 h. The reaction was cooled down to room temperature and the solution was extracted by DCM. After evaporating the separated organic layer, the crude product was purified by column chromatography, eluted with EtOAc:hexane (1:4) to obtain the brown solid of **P6** (0.693 g, 65% yield). ¹H NMR (400 MHz, CDCl₃): δ (ppm) 6.56-6.26 (2H), 4.12 (2H), 3.88 (1H), 2.43– 1.06 (14H), 0.89 (21H), 0.10 (12H). (Figure A.64, Appendix) IR (ATR, cm⁻¹): 2949, 2923, 2849, 1463. (Figure A.65, Appendix) MALDI-TOF MS: m/z = 2983.895, 2964.360. (Figure A.66, Appendix) UV-visible : λ_{max} = 296 nm, with shoulder absorbance at 353 nm. (Figure A.67, Appendix)

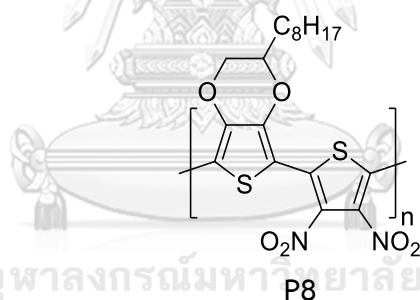
2.4.7 Poly(2'-octyl-3,4-ethylenedioxythiophene-co-benzoquinone) (P7)



P7

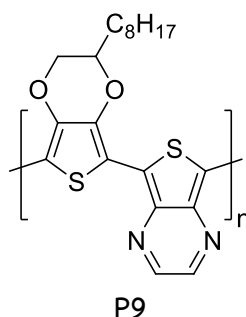
Polymer **P6** (0.013 g, 0.022 mmol), KF (0.0038 g 0.044 mmol), 33% HBr (0.011 mL, 0.044 mmol), tetrabutylammonium bromide (TBAB) (0.007 g, 0.0022 mmol) and 2,3-dichloro-5,6-dicyanobenzoquinone (DDQ) (0.005 g, 0.022 mmol) was dissolved in 5 mL DCM:DMF (1:1). The mixture was stirred at room temperature for 48 h. Then it was extracted into DCM and evaporated. The product was purified by column chromatography, eluted with EtOAc:DCM (1:4) to obtain the brown solid (0.006 g, 76% yield). ^1H NMR (400 MHz, CDCl_3): δ (ppm) 5.45–4.73 (2H), 4.47–3.23 (3H), 1.97 (2H), 1.28 (12H), 0.81 (3H). (Figure A.68, Appendix) IR (ATR, cm^{-1}): 2952, 2931, 2852, 1725, 1707, 1465. (Figure A.69, Appendix) MALDI-TOF MS: m/z = 829.665, 580.343. (Figure A.70, Appendix) UV-visible : λ_{max} = 289 nm, with shoulder absorbance at 336 nm. (Figure A.71, Appendix)

2.4.8 Poly(2'-octyl-3,4-ethylenedioxythiophene-co-3,4-dinitrothiophene) (P8)



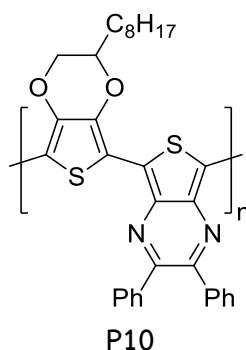
OEDOT (0.076 g, 0.3 mmol), DBDNT (0.0996 g, 0.3 mmol), $\text{Pd}(\text{OAc})_2$ (0.003 g, 0.015 mmol), Cs_2CO_3 (0.234 g, 0.72 mmol) and PivOH (0.0015 g, 0.015 mmol) were dissolved in toluene (5 mL). The reaction was heated to reflux for 2 h. After heating, DBDNT disappeared in TLC and only orange precipitate was obtained. This product was later identified not to be the desired polymer **P8**.

2.4.9 Poly(2'-octyl-3,4-ethylenedioxythiophene-co- thieno[3,4-b]pyrazine)
(P9)



OEDOT (0.012 g, 0.048 mmol), DBTP (0.014 g, 0.047 mmol), Pd(OAc)₂ (0.0005 g, 0.0024 mmol), Cs₂CO₃ (0.038 g, 0.1152 mmol), PPh₃ (0.0012 g, 0.0048 mmol) and PivOH (0.0005 g, 0.0048 mmol) were dissolved in toluene (5 mL). The mixture was heated to reflux for 24 h. The reaction was cooled down to room temperature and was extracted by DCM. After evaporating the separated organic layer, the crude product was purified by Soxhlet extraction with hexane to obtain the product as a dark green solid (0.003 g, 16% yield). ¹H NMR (400 MHz, CDCl₃): δ (ppm) 8.77 (2H), 7.49 (1H), 4.64 – 3.23 (3H), 1.19 (14H), 0.81 (3H). (Figure A.72, Appendix) UV-visible : λ_{max} = 845 nm. (Figure A.73, Appendix)

2.4.10 Poly(2'-octyl-3,4-ethylenedioxythiophene-co-2,3-diphenyl-
thieno[3,4-b]pyrazine) (P10)



OEDOT (0.073 g, 0.29 mmol), DBDTP (0.035 g, 0.075 mmol), Pd₂(dba)₃ (0.02 g, 0.0019 mmol), Cs₂CO₃ (0.058 g, 0.18 mmol), PPh₃ (0.002 g, 0.0075 mmol) and PivOH

(0.0008 g, 0.0075 mmol) were dissolved in toluene (5 mL). The reaction was heated to reflux for 20 h. Then it was cooled to room temperature, extracted into DCM and evaporated. The crude product was purified by Soxhlet extraction with hexane to obtain the product as a dark green solid (0.016 g, 34% yield). ^1H NMR (400 MHz, acetone- d_6): δ (ppm) 7.78 – 6.63 (10H), 4.91 – 3.13 (3H), 1.72 – 0.87 (14H), 0.75 (3H). (Figure A.74, Appendix) IR (ATR, cm^{-1}): 2914, 2849, 1483, 1439. (Figure A.75, Appendix) M_n (GPC) = 1886. UV-visible : λ_{max} = 958 nm. (Figure A.76, Appendix)

2.5 Molar extinction coefficient

2.5.1 Molar extinction coefficient of UV-visible absorption

The polymer **P2** solutions were prepared in five concentration: 0.02, 0.04, 0.06, 0.08, and 0.10 mM. The polymer **P5** solutions were prepared in five concentration: 0.02, 0.03, 0.04, 0.05, and 0.06 nM. All solutions were measured the absorbance values at 630 nm for **P2** and 506 nm for **P5**. The data were plot into liner graph between absorbance and concentration by Microsoft Excel.

2.5.2 Molar extinction coefficient of fluorescence emission

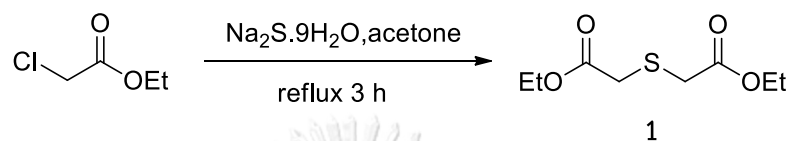
The polymer **P5** solutions were prepared in four concentration: 0.005, 0.01, 0.015, and 0.02 mM. All solutions were measured the intensity values at 610 nm. The data were plot into liner graph between intensity and concentration by Microsoft Excel.

CHAPTER III

RESULTS AND DISCUSSION

3.1 Monomer synthesis

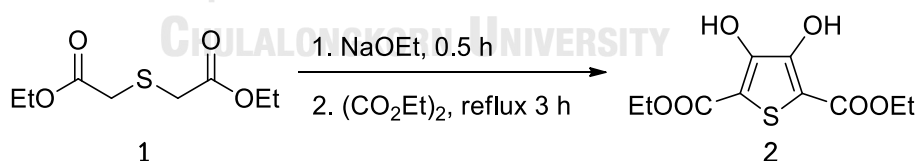
3.1.1 Diethyl thiodiglycolate (1)



Scheme 3.1 Synthesis of diethyl thiodiglycolate (1)

Compound **1** was synthesized in 62% yield from double substitution reaction between sodium sulfide and ethyl chloroacetate. (**Scheme 3.1**) The ¹H NMR spectrum showed the singlet signal at 3.24 ppm of the methylene protons, and the quartet and triplet signals of the ethyl groups at 4.05 and 1.16 ppm, respectively. (**Figure A.1, Appendix**) The ¹³C NMR (**Figure A.2, Appendix**) spectrum also confirmed the structure with the signals that matched those in a previous report. [49]

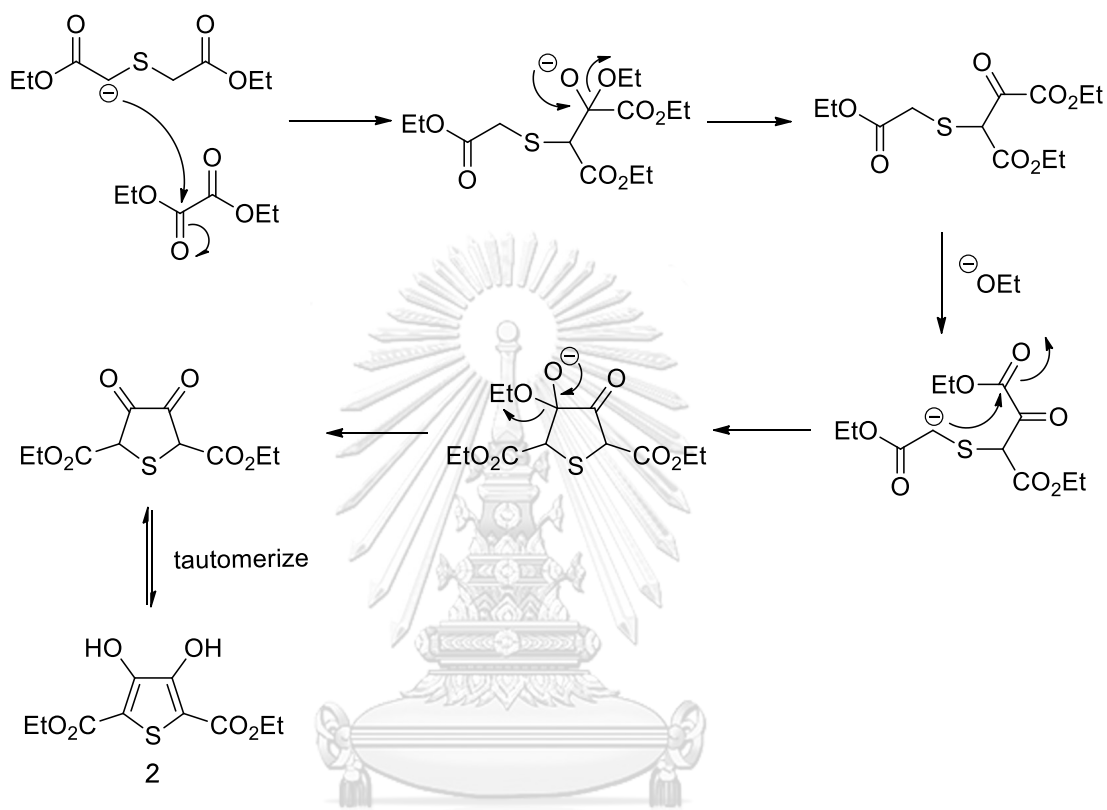
3.1.2 Diethyl 3,4-dihydroxythiophene-2,5-dicarboxylate (2)



Scheme 3.2 Synthesis of diethyl 3,4-dihydroxythiophene-2,5-dicarboxylate (2)

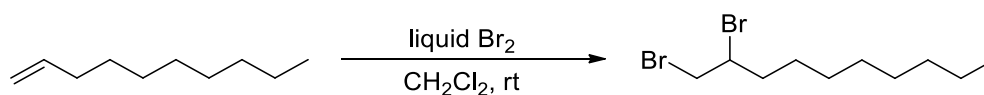
Compound **2** was successfully synthesized in 76% yield through Hinsberg reaction. [65] (**Scheme 3.2**) The mechanism of this reaction is the consecutive Claisen condensation reactions of compound **1** and diethyl oxalate to produce a diketone compound, which readily tautomerizes to dihydroxythiophene of product **2**. (**Scheme 3.3**) The ¹H NMR spectrum exhibited a broad singlet signal of -OH group at 9.35 ppm and signals of ethyl groups at 4.39 and 1.36 ppm. (**Figure A.3, Appendix**)

The ^{13}C NMR spectrum showed the $\beta\text{-C-OH}$ at 151.6 ppm, and the carbonyl carbon at 165.5 ppm. (Figure A.4, Appendix) The IR spectrum displayed a broad peak of -OH stretching at 3305 cm^{-1} . (Figure A.5, Appendix) [50]



Scheme 3.3 Mechanism of Hinsberg reaction

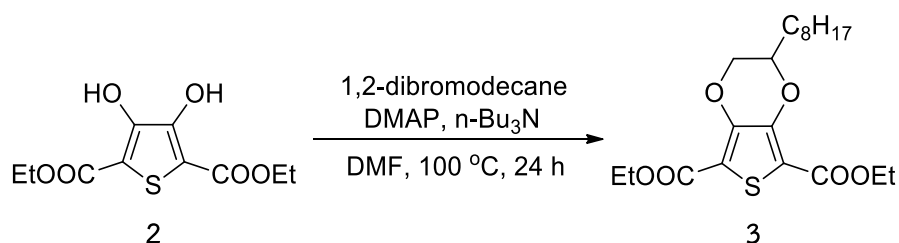
3.1.3 1,2-Dibromodecane



Scheme 3.4 Synthesis of 1,2-dibromodecane

1,2-Dibromodecane was prepared from bromination of 1-decene in excellent yield. (92%, Scheme 3.4) The structure of product was confirmed with ^1H NMR spectrum. (Figure A.6, Appendix) [51]

3.1.4 Diethyl 2-octyl-2,3-dihydrothieno[3,4-b][1,4]dioxine-5,7-dicarboxylate (3)



Scheme 3.5 Synthesis of diethyl 2-octyl-2,3-dihydrothieno[3,4-b][1,4]dioxine-5,7-dicarboxylate (3)

Compound **2** reacted with 1,2-dibromodecane presumably via S_N2 mechanism to produce compound **3**. (**Scheme 3.5**) The conditions for several attempted synthesis of compound **3** were shown in **Table 3.1**.

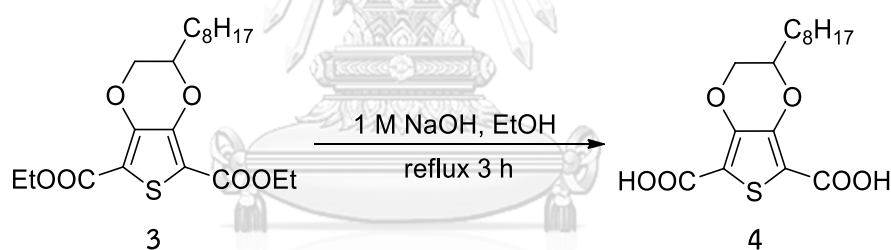
Table 3.1 Conditions for the synthesis of compound **3**

Entry	Solvent	Catalyst	Temperature ($^\circ\text{C}$)	%yield
1	ACN	none	82	no reaction
2	ACN	DMAP	82	0.51
3	DMF	DMAP	85	23.7
4	DMF	DMAP	100	28.1
5	DMF	DMAP	120	21.7

The mixture in ACN without catalyst resulted in no reaction (**Entry 1, Table 3.1**), while the presence of DMAP gave the product **3** in low yield. (**Entry 2, Table 3.1**) Comparison between the two solvents, the reaction using DMF gave higher yield. The best temperature was at 100 $^\circ\text{C}$, giving the product up to 28.1 %yield. (**Entries 3-5, Table 3.1**) Lower temperature gave lower yield due to uncompleted reaction.

Higher temperature at 120 °C might cause the reactant or the product to partly decompose and reduce the product yield. However, the product yield was still low. Increasing the reaction time or increasing the equivalent of 1,2-dibromodecane might solve this problem. Its ^1H NMR spectrum showed multiplet signals at 4.40 and 4.05 ppm from CH_2 of ethyl group and ethylenedioxy group ($-\text{O}-\text{CH}_2-\text{CH}-\text{O}-$), and signals at 1.81-1.43 and 0.89 ppm from CH_3 of ethyl group and octyl group. **(Figure A.7, Appendix)** The ^{13}C NMR spectrum exhibited two carbonyl carbon signals at 161.0 and 160.9 ppm together with all signals of other carbons in the rest of the structure. **(Figure A.8, Appendix)** The IR spectrum showed a carbonyl $\text{C}=\text{O}$ stretching peak at 1698 cm^{-1} and aromatic $\text{C}=\text{C}$ stretching peak at 1503 cm^{-1} . **(Figure A.9, Appendix)** [52]

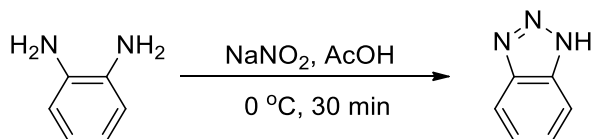
3.1.5 2-Octyl-2,3-dihydrothieno [3,4-b][1,4]dioxine-5,7-dicarboxylic acid (4)



Scheme 3.6 Synthesis of 2-octyl-2,3-dihydrothieno [3,4-b][1,4]dioxine-5,7-dicarboxylic acid (4)

Compound **4** was synthesized in high yield (92% yield) from basic hydrolysis of compound **3**. **(Scheme 3.6)** The structure of the product was confirmed by ^1H NMR spectrum **(Figure A.10, Appendix)** and ^{13}C NMR spectrum **(Figure A.11, Appendix)** by with disappearance of the ethyl group signals of the starting material **3**, supporting the successful and complete hydrolysis. The IR spectrum also displayed strong broad band of carboxylic $-\text{OH}$ stretching peak. **(Figure A.12, Appendix)** [52]

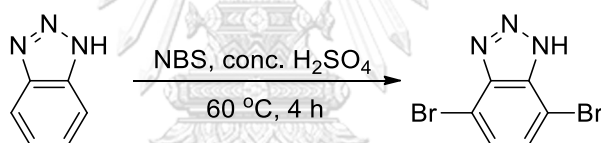
3.1.8 1,2,3-Benzotriazole (BTZ)



Scheme 3.9 Synthesis of 1,2,3-benzotriazole (BTZ)

BTZ was prepared in 63.75% yield from diazotization of *o*-phenylenediamine followed by cyclization of the diazo intermediate. (**Scheme 3.9**) The structure of the product was confirmed by the ^1H NMR spectrum that showed the two expected signals of protons on the benzene ring at 7.96 and 7.47 ppm. (**Figure A.18, Appendix**) [56]

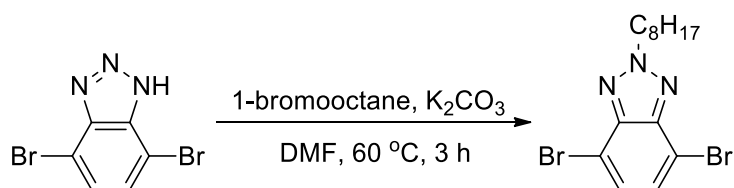
3.1.9 4,7-Dibromo-1,2,3-benzotriazole (DBBTZ)



Scheme 3.10 Synthesis of 4,7-dibromo-1,2,3-benzotriazole (DBBTZ)

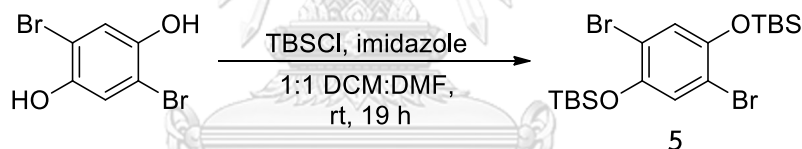
DBBTZ was synthesized in 65% yield through bromination of BTZ using the same method and condition as those of DBBTD synthesis in section 3.1.7. (**Scheme 3.10**) The ^1H NMR spectrum exhibited the singlet signal of the protons on the benzene ring at 7.64 ppm. (**Figure A.20, Appendix**) The chemical shift of this signal matched well with the data from literature. [57]

3.1.10 4,7-Dibromo-2-octyl-1,2,3-benzotriazole (DBOBTZ)



Scheme 3.11 Synthesis of 4,7-dibromo-2-octyl-1,2,3-benzotriazole (DBOBTZ)

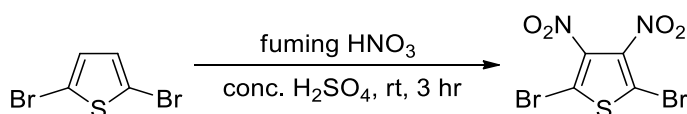
DBOBTZ was successfully synthesized in 59% yield from nucleophilic substitution reaction of DBBTZ and 1-bromooctane. (Scheme 3.11) The ^1H NMR showed the singlet signal of the protons on the benzene ring at 7.44 ppm, and signals of octyl group on the triazole ring at 4.78, 2.14, 1.48–1.08 and 0.87 ppm. (Figure A.23, Appendix) [23]

3.1.11 1,4-Dibromo-2,5-bis(*tert*-butyldimethylsilyloxy)benzene (5)

Scheme 3.12 Synthesis of compound 5

Compound 5 was synthesized in 52% yield from nucleophilic substitution reaction of TBSCl with 2,5-dibromobenzene-1,4-diol. (Scheme 3.12) The ^1H NMR spectrum exhibited the singlet signal of the 2 protons on the benzene ring at 6.82 ppm, the singlet signal of *tert*-butyl group at 0.82 ppm, and the singlet signal of methyl group at 0.02 ppm. (Figure A.26, Appendix). [58]

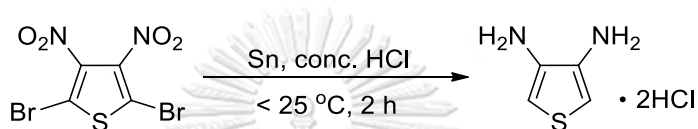
3.1.12 2,5-Dibromo-3,4-dinitrothiophene (DBDNT)



Scheme 3.13 Synthesis of 2,5-dibromo-3,4-dinitrothiophene (DBDNT)

DBDNT was synthesized in 34% yield from nitration of 3,4-dibromothiophene. **(Scheme 3.13)** The structure of the product was confirmed by IR spectrum showing strong and sharp peaks at 1538 and 1315 cm^{-1} , corresponding to the N-O stretching from the nitro groups. **(Figure A.29, Appendix)** The ^{13}C NMR spectrum displayed the signals of the two carbons of the symmetric thiophene ring at 139.2 and 113.8 ppm. **(Figure A.28, Appendix)** [59]

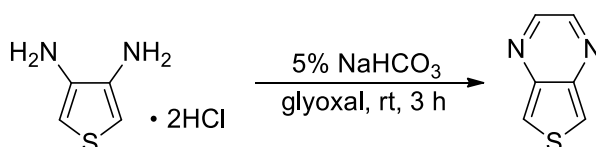
3.1.13 3,4-Diaminothiophene dihydrochloride (DAT.2HCl)



Scheme 3.14 Synthesis of 3,4-diaminothiophene dihydrochloride (DAT.2HCl)

DAT.2HCl was prepared from reduction of DBDNT with tin powder in acidic condition. **(Scheme 3.14)** The product was filtered after freezing the reaction mixture overnight. DAT.2HCl was added 0.89 M KOH to produce free amino form before characterization. The ^1H NMR spectrum of 3,4-diaminothiophene exhibited the signal of two protons in thiophene ring at 6.14 ppm, and the signal of four protons on amino groups at 2.28 ppm. **(Figure A.31, Appendix)** [60]

3.1.14 Thieno[3,4-*b*]pyrazine (TP)

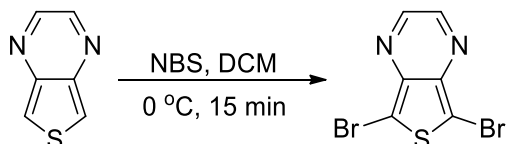


Scheme 3.15 Synthesis of thieno[3,4-*b*]pyrazine (TP)

The core structure of TP was prepared from one-pot condensation of DAT and 1,2-dicarbonyl compound. **(Scheme 3.15)** In this case, DAT.2HCl was neutralized with NaHCO_3 to convert to its free base thiophene-3,4-diamine, which readily condensed with glyoxal to give the TP product in 34% yield. The ^1H NMR spectrum

showed the singlet signal of the two protons on the pyrazine ring at 8.50 ppm, and the singlet signal of the protons on the thiophene ring at 8.02 ppm. (Figure A.32, Appendix) [61]

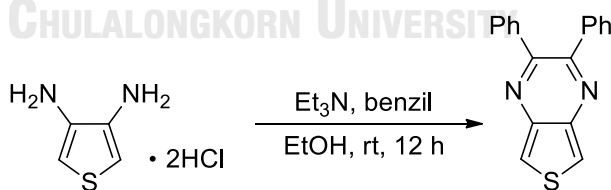
3.1.15 5,7-Dibromothieno[3,4-*b*]pyrazine (DBTP)



Scheme 3.16 Synthesis of 5,7-dibromothieno[3,4-*b*]pyrazine (DBTP)

DBTP was synthesized from mild bromination of TP. (Scheme 3.16) The product was obtained in low yield (24 %), presumably because DBTP could be prone to self-polymerization evidenced by the presence of insoluble red solid obtained during the reaction and the purification processes. The signals of the protons on the thiophene ring disappeared in the ^1H NMR spectrum of the product, which showed only the signals of the proton on the pyrazine ring at 8.54 ppm, (Figure A.33, Appendix) indicating that TP was successfully brominated. [62]

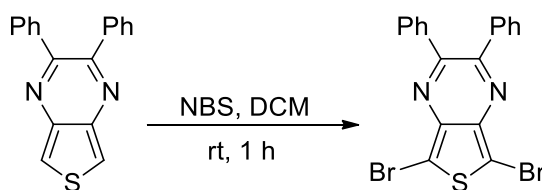
3.1.16 2,3-Diphenylthieno[3,4-*b*]pyrazine (DPTP)



Scheme 3.17 Synthesis of 2,3-diphenylthieno[3,4-*b*]pyrazine (DPTP)

Similar to TP, DPTP was synthesized in 72% yield from neutralization of DAT.2HCl, following by condensation with benzil. (Scheme 3.17) The ^1H NMR spectrum showed the singlet signal of protons on the thiophene ring at 8.21 ppm and those of the phenyl groups at 7.64–7.01 ppm. (Figure A.35, Appendix) [63]

3.1.17 5,7-Dibromo-2,3-diphenylthieno[3,4-*b*]pyrazine (DBDPTP)

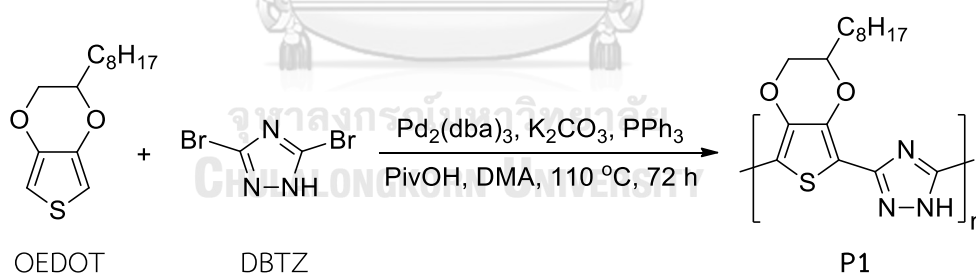


Scheme 3.18 Synthesis of 5,7-Dibromo-2,3-diphenylthieno[3,4-*b*]pyrazine (DBDPTP)

DBDPTP was successfully synthesized in 61% yield from bromination of DPTP following a modification of the method from the literature. [64] (**Scheme 3.18**) The ^1H NMR spectrum exhibited the signals of the protons on the phenyl groups at 7.57 and 7.52–7.30 ppm, with the absence of the signals of protons on the thiophene ring. (**Figure A.37, Appendix**) All signals of the ^{13}C NMR spectrum matched well with that from the literature. [64] (**Figure A.38, Appendix**)

3.2 Polymer synthesis

3.2.1 Poly(2'-octyl-3,4-ethylenedioxythiophene-co-1,2,4-triazole) (P1)



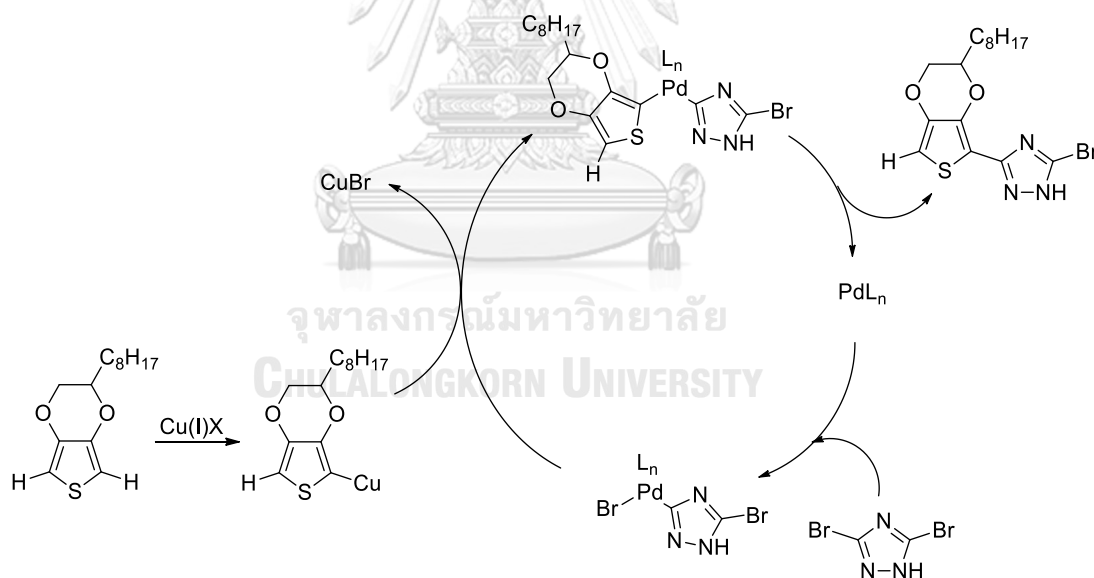
Scheme 3.19 Synthesis of poly(2'-octyl-3,4-ethylenedioxythiophene-co-1,2,4-triazole) (P1)

TZ and OEDOT were selected to be the first pair of the starting precursors of the synthesis of polymer **P1**. (**Scheme 3.19**) The first attempted reaction used $\text{Pd}(\text{OAc})_2$ as the catalyst. (**Entry 1, Table 3.2**) The reaction was heated to 110 °C for 48 h. The expected product **P1** was unfortunately not observed in this case. Using the conditions adopted from a literature [66] (**Entry 2, Table 3.2**) with CuI added into

the reaction as a co-catalyst, the reaction completed in 48 h generating the product **P1** in 44% yield. The catalytic cycle of mechanism of Pd/Cu-catalyzed direct arylation was proposed in **Scheme 3.20**. When more reactive catalyst $\text{Pd}_2(\text{dba})_3$ was used, the reaction could proceed without CuI co-catalyst and produced the product **P1** in better yield of 65%, (**Entry 3, Table 3.2**) although with longer reaction time.

Table 3.2 Conditions for the synthesis of polymer **P1**

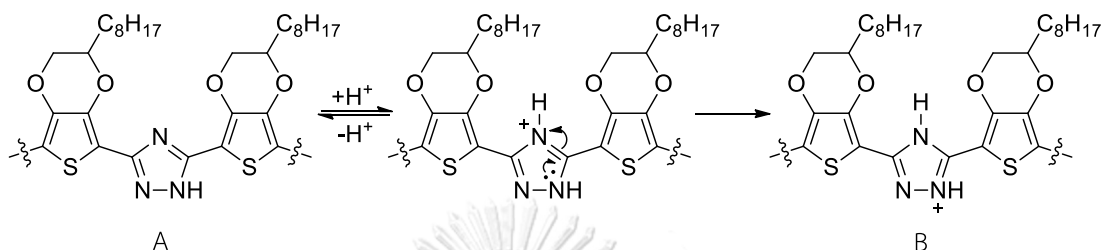
Entry	Catalyst	Additive	Time (h)	%yield
1	$\text{Pd}(\text{OAc})_2$	-	48	no reaction
2	$\text{Pd}(\text{OAc})_2$	CuI	48	44
3	$\text{Pd}_2(\text{dba})_3$	-	72	65



Scheme 3.20 The mechanism of Pd/Cu-catalyzed direct arylation between DBTZ and OEDOT

The UV-visible spectrum of the polymer **P1** solution in CH_2Cl_2 exhibited a weak absorption over 700 nm and a shoulder absorption band at 346 nm. The unexpected low wavelength and intensity of the absorbance due perhaps to the

non-conjugated system of 1H-tautomers of the triazole rings backbone of polymer. **(Structure A, Scheme 3.21)** This problem could be solved by protonations on the triazoles and tautomerization to give the form that allows full-conjugation of the π -system along the chain. **(Structure B, Scheme 3.21)**



Scheme 3.21 Protonation and tautomerization of the triazole ring in polymer **P1**

Upon protonation with trifluoroacetic acid (TFA), the UV-visible absorption of **P1** showed a new λ_{max} at 488 nm. The intensity of this absorption band increased as more TFA was added. **(Figure 3.1)** The color of this solution changed from green to red-brown. When this acidic solution was neutralized by K_2CO_3 , the absorption at 488 nm disappeared and the spectrum returned to the original spectrum of the solution before protonation. **(Figure 3.2)** This result supported the hypothesis of a reversible acid-base reaction that occurred on the triazole rings of the polymer.

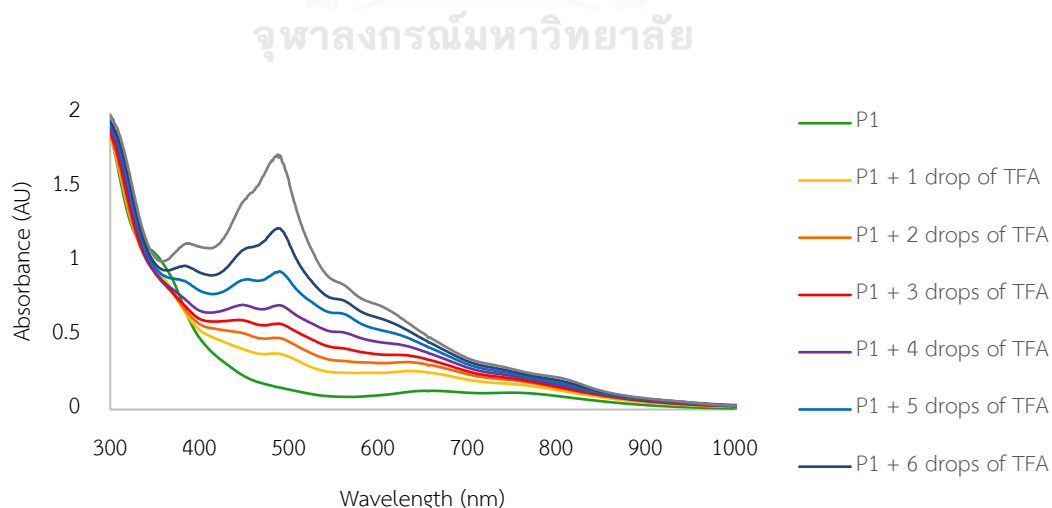


Figure 3.1 The UV-visible absorption spectra of polymer **P1** solution in CH_2Cl_2 with addition of TFA

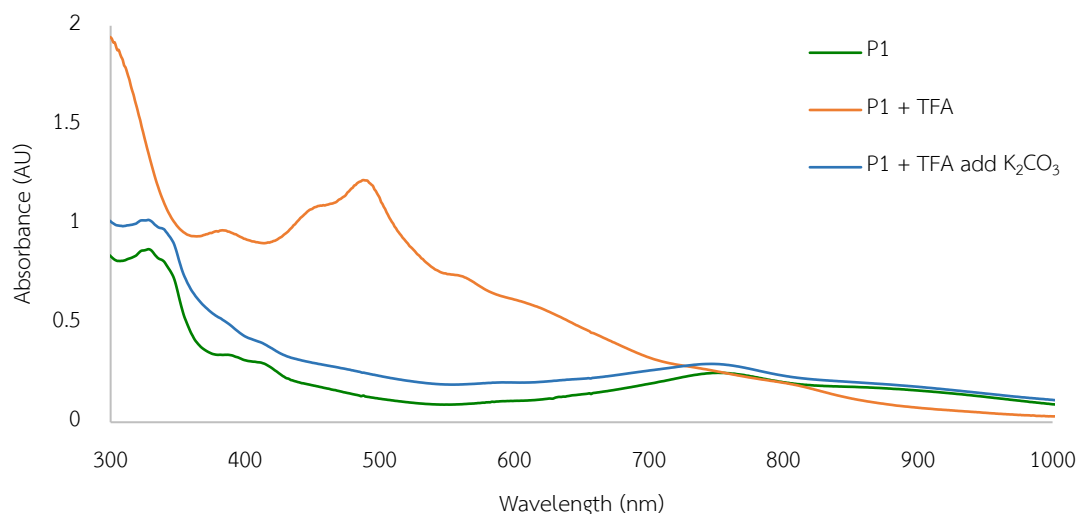


Figure 3.2 The UV-visible absorption spectra of polymer **P1** solution upon protonation and after neutralization.

In addition, when the polymer **P1** solution was kept under ambient light for one day, the UV-visible absorption of the solution changed to show a new absorption band around 500 nm, with the absorption at 752 nm disappeared. (**Figure 3.3**) This photosensitivity was also observed on the protonated form of **P1** solution. When the protonated **P1** solution was similarly kept under ambient light, a new absorption at 741 nm appeared in UV-visible absorption spectrum. (**Figure 3.4**) Both changes on the absorption of the solution did not revert back to the original spectra, indicating irreversible processes. The first process may involve a kind of photo-induced degradation of the polymer to shorter chain length, as evidenced by hypsochromic shift of its λ_{max} value. The second process may instead be an elongation process, since the λ_{max} shift went to the opposite direction. Unfortunately, just these changes in UV-visible spectra were not enough to give any more clues to the chemical processes that actually occurred.

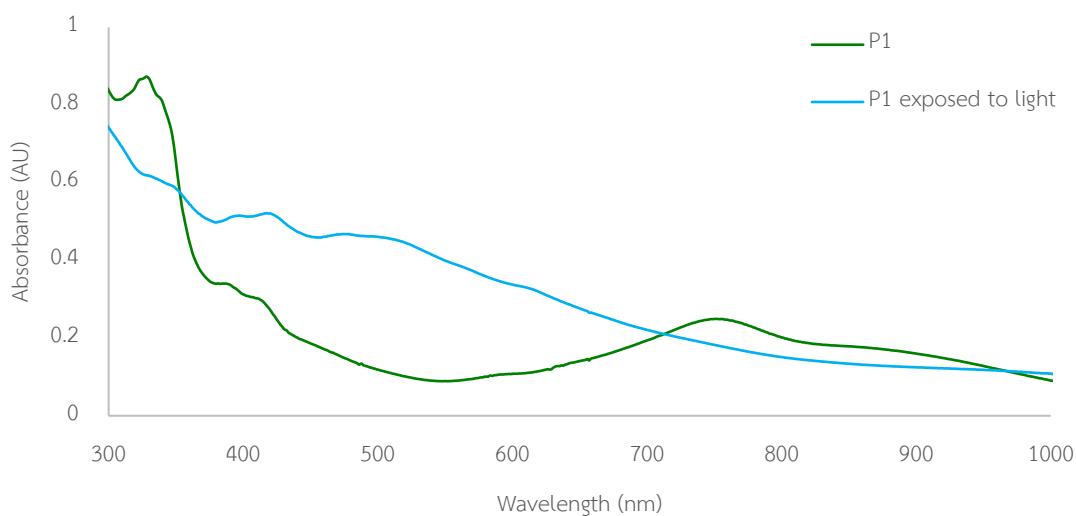


Figure 3.3 UV-visible absorption spectra of polymer **P1** solution exposed to ambient light

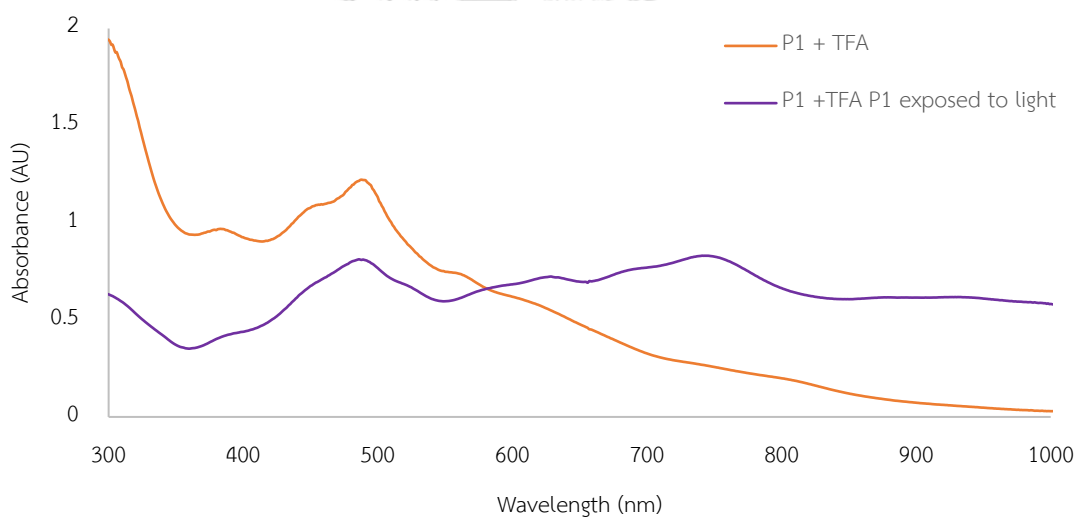


Figure 3.4 UV-visible absorption spectra of protonated polymer **P1** solution exposed to ambient light

The photosensitivity of **P1** had become a problem in the study. Even though polymer **P1** was stored in dark, it was inescapably exposed to ambient light during transfer processes. Gradual shift of the λ_{max} in the UV-visible absorption of **P1** + TFA solution from 488 to 443 nm was found in one example that was briefly exposed to light. (**Figure 3.5**).

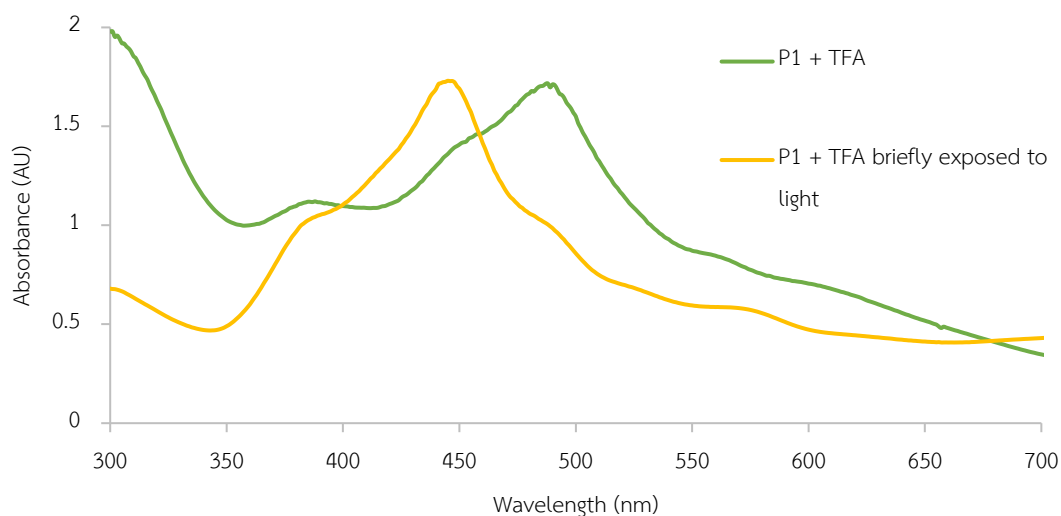


Figure 3.5 A shift of λ_{max} of the UV-visible absorption spectra of protonated polymer **P1** solution briefly exposed to ambient light

Another unexpected situation was found, when solution of polymer **P1** was kept expose to air for 1 week, a new absorption peak appeared in UV-visible absorption spectrum at 927 nm. (**Figure 3.6**) It's possible that oxidation of triazole rings of polymer **P1** occurred and shifted the position of π -bonds in triazole ring to the tautomers that improved the π -conjugated system. This air oxidation was not occurred in protonation form of **P1** solution, as its spectrum remain the same. (**Figure 3.7**) When this air-exposed **P1** + TFA solution was neutralized, the UV-visible spectrum showed the original absorption at 757 nm of the neutral form of polymer.

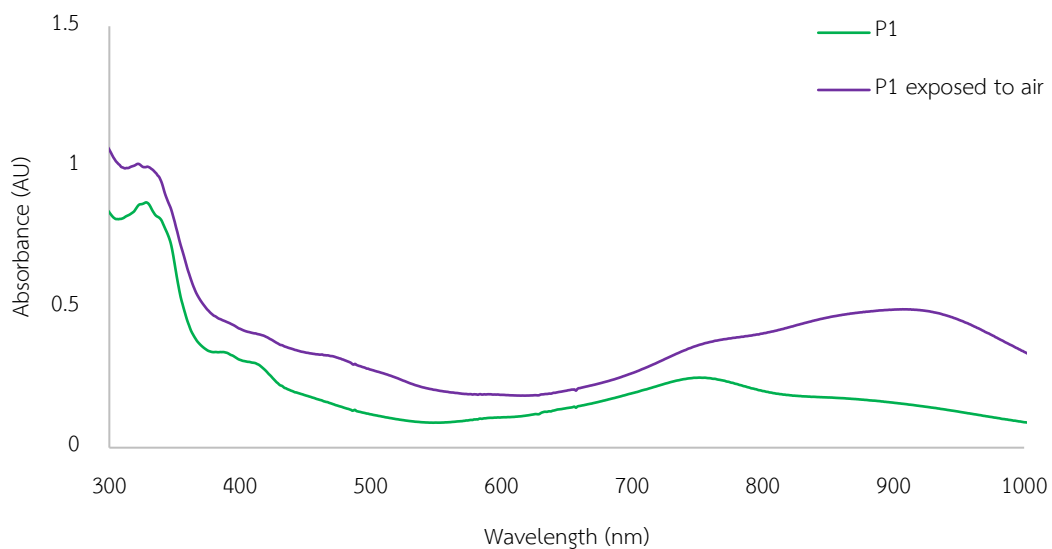


Figure 3.6 Effect of air oxidation on the UV-visible absorption spectra of polymer **P1** solution

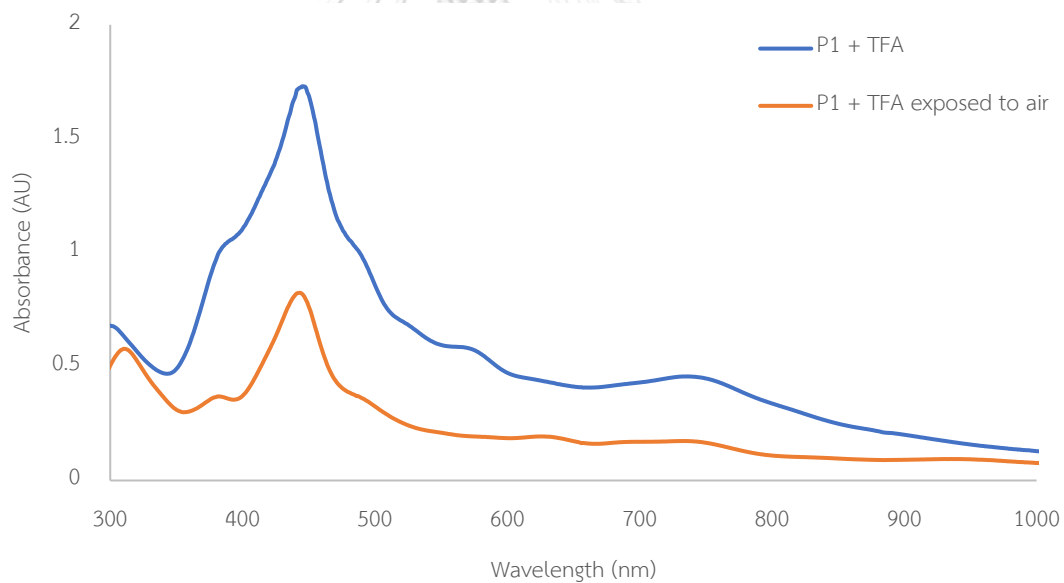
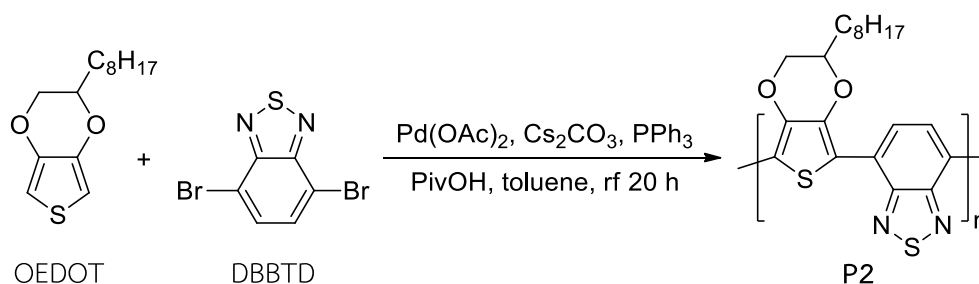


Figure 3.7 Effect of air oxidation on the UV-visible absorption spectra of polymer **P1** solution + TFA

3.2.2 Poly(2'-octyl-3,4-ethylenedioxythiophene-co-2,1,3-benzothiadiazole) (P2)

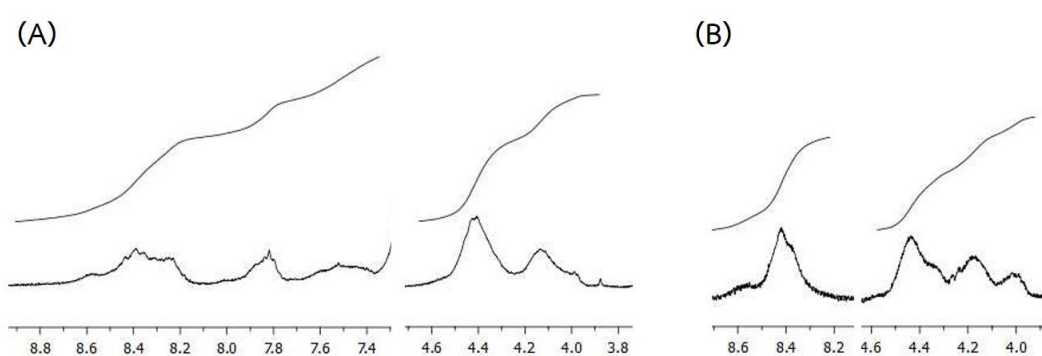


Scheme 3.22 Synthesis of poly(2'-octyl-3,4-ethylenedioxythiophene-co-2,1,3-benzothiadiazole) (**P2**)

The polymer **P2** was prepared by DARp of OEDOT and DBBTD. (**Scheme 3.22**) The first condition of this preparation used OEDOT and DBBTD in equal equivalence by mole. (**Entry 1, Table 3.3**) Considering integration in ^1H NMR spectrum of **P2**, the broad signal around 8 ppm represent the two protons on the benzene rings of BTD units in the polymer, and the signal around 4 ppm represent the three protons of the ethylenedioxy group of OEDOT. This information was used to identify the relative incorporation of OEDOT and BTD in the structure of the polymer product. The DARp of OEDOT and DBBTD in equal ratio by mole gave the integrations in ^1H NMR spectrum of the resulted product **P2** corresponding to a random copolymer with the ratio of OEDOT : BTD = 1 : 2.3. (**Figure 3.8a**) When OEDOT was increased to the ratio of OEDOT : DBBTD = 2.3 : 1, (**Entry 2, Table 3.3**) the integration of ^1H NMR spectrum of this second product presented the desired 1 : 1 ratio of the two monomeric units, likely to correspond to an alternating copolymer. (**Figure 3.8b**)

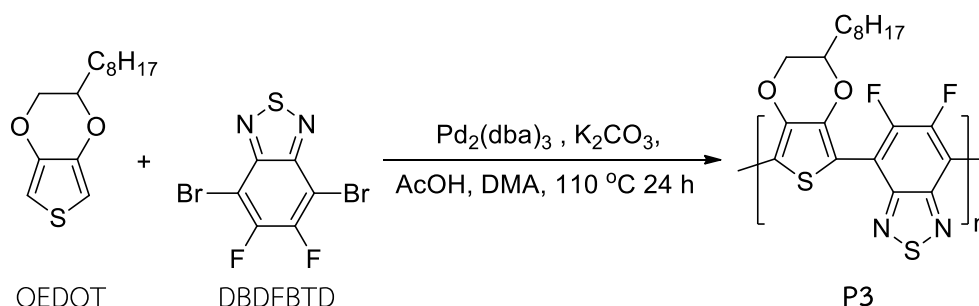
Table 3.3 Conditions for the synthesis of polymer P2

Entry	Starting OEDOT : DBBTD ratios	Incorporated ratios of OEDOT : BTD units	%yield	λ_{\max} (nm)
1	1 : 1	1 : 2.3	59	589
2	2.3 : 1	1 : 1	82	630

**Figure 3.8** Partial ^1H NMR spectra of **P2** from 2 synthetic conditions

The UV-visible spectra of **P2** products from 2 conditions exhibited λ_{\max} at 589 and 630 nm from the obtained random and alternating copolymers, respectively. This result supported that optical property of alternating donor-acceptor copolymers should be better than random copolymers. The Mass of second **P2** polymer product from MALDI-TOF MS spectrum showed m/z of 3606.503, corresponded to approximately 9 repeating donor-acceptor units in the structure.

3.2.3 Poly(2'-octyl-3,4-ethylenedioxythiophene-co-5,6-difluoro-2,1,3-benzothiadiazole) (P3)



Scheme 3.23 Synthesis of poly(2'-octyl-3,4-ethylenedioxythiophene-co-5,6-difluoro-2,1,3-benzothiadiazole) (**P3**)

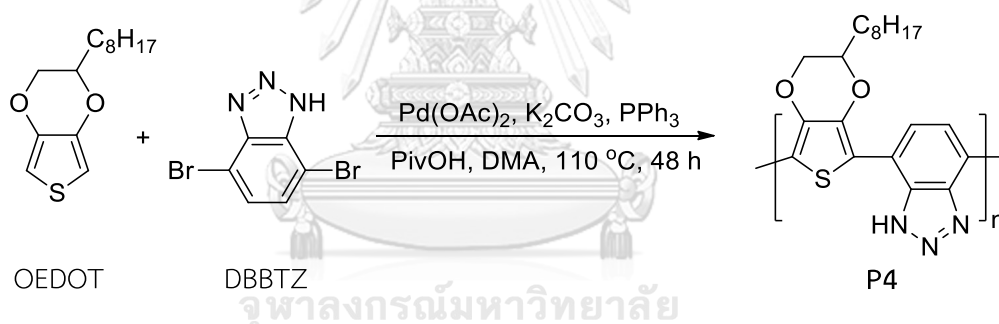
Polymer **P3** was first synthesized from DARP between OEDOT and DBDFBT (**Scheme 3.23**) using the same condition as the synthesis of **P2** in section 3.2.2. (**Entry 1, Table 3.4**) The reaction was however, gave the desired product in only 5% yield. The ^1H NMR spectrum showed the signal of the protons on the ethylenedioxy group of OEDOT at 4.11 ppm. (**Figure A.49, Appendix**) The structure of the product was confirmed with ^{19}F NMR spectrum that showed signals of fluorine nuclei of DFBT units at -120.04, -120.06, -122.81 and -123.05 ppm. (**Figure A.50, Appendix**) The UV-visible spectrum of the product showed only a shoulder absorption around 400 nm. (**Figure A.54, Appendix**) Polymer **P3** was re-synthesized following the condition from a report from Scherf and coworkers. [67] (**Entry 2, Table 3.4**) This reaction improved and gave the polymer **P3** in 38% yield. The ^{19}F NMR spectrum showed multiplet signals of fluorine nuclei in DFBT at -118.06, -119.16, -119.57, -123.46 and -124.57 ppm. (**Figure A.51, Appendix**) UV-visible absorption spectrum of the product showed λ_{max} at 461 nm (**Figure A.55, Appendix**), which also improved over the product from the first condition. The m/z obtained from MALDI-TOF MS of 2527.052 corresponded to approximately 6 repeating donor-acceptor units in the structure.

Table 3.4 Conditions for the synthesis of polymer **P3**

Entry	Catalyst	Base	Acid	Solvent	%yield	λ_{\max} (nm)
1	Pd(OAc) ₂	Cs ₂ CO ₃	PivOH	toluene	5	shoulder ~400
2	Pd ₂ (dba) ₃	K ₂ CO ₃	AcOH	DMA	38	461

Comparing to polymer **P2**, the much lower λ_{\max} value of **P3** suggested that the difluoro groups have little or even no influence on the band gap of the polymer, [68] while in this case, shorter conjugation length from shorter polymer chain length lowered the λ_{\max} value in comparison to the non-fluorinated **P2** polymer.

3.2.4 Poly(2'-octyl-3,4-ethylenedioxythiophene-co-1,2,3-benzotriazole) (P4)

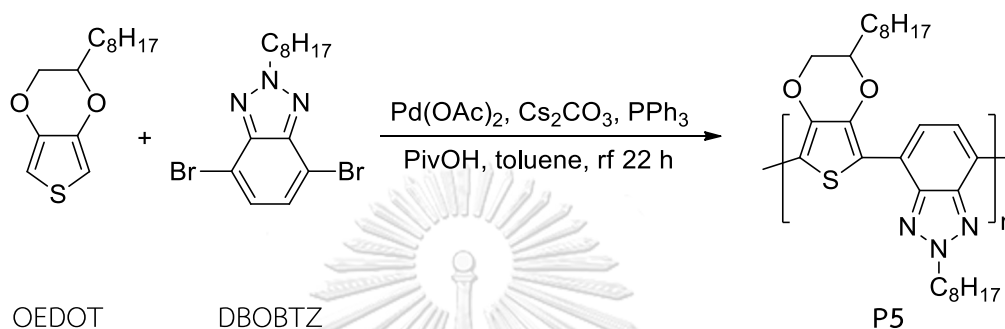


Scheme 3.24 Synthesis of poly(2'-octyl-3,4-ethylenedioxythiophene-co-1,2,3-benzotriazole) (**P4**)

Polymer **P4** was synthesized from DArP of OEDOT and DBBTZ. (**Scheme 3.24**) The structure of the product was confirmed with ¹H NMR spectrum that showed the signal of the 2 protons on the benzene rings of the BTZ units at 7.55 ppm, and the signal of the 3 protons on the ethylenedioxy group in OEDOT at 4.26 ppm. (**Figure A.56, Appendix**) The optical property of the polymer exhibited a disappointingly low absorption at $\lambda_{\max} = 331$ nm in its UV-visible spectrum. (**Figure A.59, Appendix**) It is postulated that BTZ may be a rather poor acceptor to induce an effective conjugation along the polymer chain. From MALDI-TOF MS spectrum, **P4** exhibited a

molecular weight of 2212.910, corresponded to approximately 6 repeating donor-acceptor units.

3.2.5 Poly(2'-octyl-3,4-ethylenedioxythiophene-co-2-octyl-1,2,3-benzotriazole) (P5)

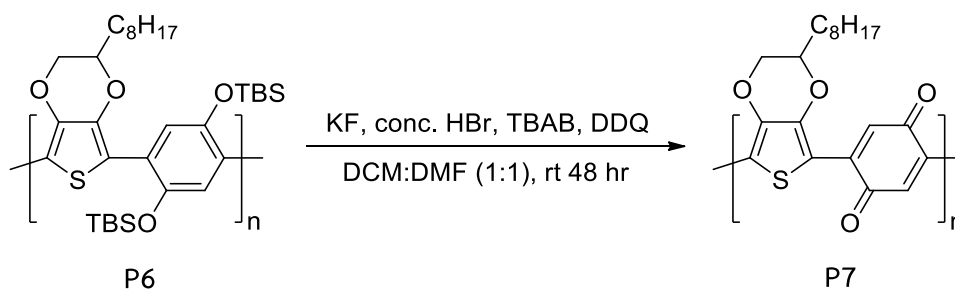


Scheme 3.25 Synthesis of poly(2'-octyl-3,4-ethylenedioxythiophene-co-2-octyl-1,2,3-benzotriazole) (**P5**)

The poor optical property of **P4** may be improved with the presence of an alkyl substituted BTZ at N2 to lock the π -bond in the tautomer that allows better conjugation to the backbone, similar to that of BTD. (section 3.2.2) Polymer **P5** was successfully synthesized from DARp of OEDOT and DBOBTZ. (**Scheme 3.25**) The reaction gave the product as red solid in excellent 87.5% yield. The ^1H NMR spectrum displayed the signal of 2 protons of the benzene rings and the 2 protons of $-\text{N-CH}_2-$ on the OBTZ units at 8.10 and 4.87 ppm, respectively. The signal of the ethylenedioxy group in OEDOT was also present at 4.42 ppm. (**Figure A.60, Appendix**) UV-visible absorption spectrum of **P5** showed the λ_{max} at 506 nm, much higher than **P4**. (**Figure A.63, Appendix**) The high molecular weight of 5306.861 was observed in its MALDI-TOF MS spectrum of polymer **P5**, corresponding to approximately 11 repeating donor-acceptor units.

The observation of improved synthetic efficiency and optical property is possibly due to the lower aromaticity of OBTZ upon forming the quinoid resonance structure in the conjugated polymeric chain, in comparison to BTZ. The resistance

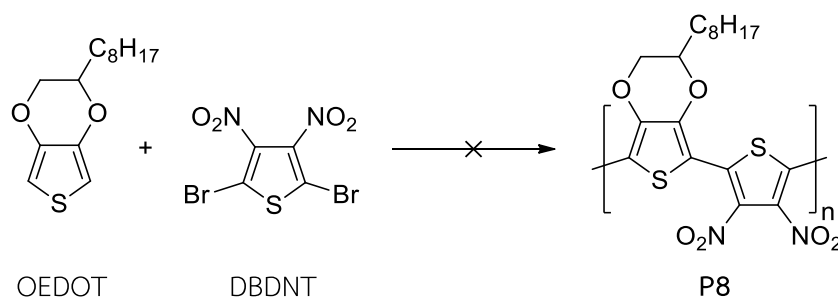
3.2.7 Poly(2'-octyl-3,4-ethylenedioxythiophene-co-benzoquinone) (P7)



Scheme 3.27 Synthesis of poly(2'-octyl-3,4-ethylenedioxythiophene-co-benzoquinone) (P7)

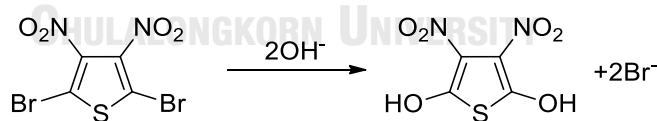
P7 was synthesized in 76% yield from deprotections of tert-butyldimethylsilyl groups from P6 using KF in acidic condition to give hydroquinone, which was then oxidized to benzoquinone units of polymer P7. The product was confirmed with ^1H NMR and IR spectra. The ^1H NMR spectrum showed the signals of the ethylenedioxy group on the OEDOT at 4.47–3.23 ppm, and the signals of the protons of the benzoquinone ring at 5.45–4.73 ppm. (Figure A.68, Appendix) IR spectrum of the product displayed the carbonyl C=O stretching peaks at 1725 and 1707 cm^{-1} . (Figure A.69, Appendix) P7 exhibited an unexpected low absorption λ_{max} at 336 nm. (Figure A.71, Appendix) Its even lower absorption than that of polymer P6 may perhaps due to the non-conjugation of the π -bonds between the benzoquinone and OEDOT units.

3.2.8 Poly(2'-octyl-3,4-ethylenedioxythiophene-co-3,4-dinitrothiophene)
(P8)



Scheme 3.28 Unsuccessful synthesis of poly(2'-octyl-3,4-ethylenedioxythiophene-co-3,4-dinitrothiophene) (**P8**)

Synthesis of polymer **P8** was attempted from DArP of OEDOT and DBDNT using $\text{Pd}(\text{OAc})_2$ as the main catalyst, Cs_2CO_3 , PivOH in toluene. After heating to reflux, an orange precipitate was immediately occurred in the reaction and only DBDNT disappeared. The precipitate occurred to derive from an unexpected side reaction of from $\text{S}_{\text{N}}\text{Ar}$ substitution on DBDNT in basic condition. (**Scheme 3.39**) Unfortunately, changing base from Cs_2CO_3 to Et_3N could not avoid the $\text{S}_{\text{N}}\text{Ar}$ of DBDNT, and the synthesis of **P8** had to be abandoned.



Scheme 3.29 Nucleophilic aromatic substitution ($\text{S}_{\text{N}}\text{Ar}$) of DBDNT

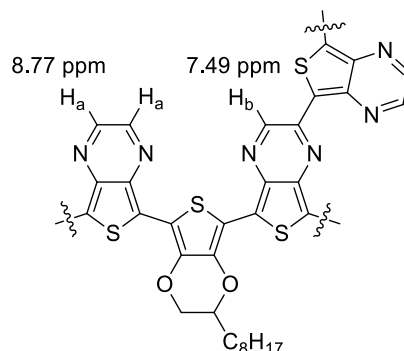
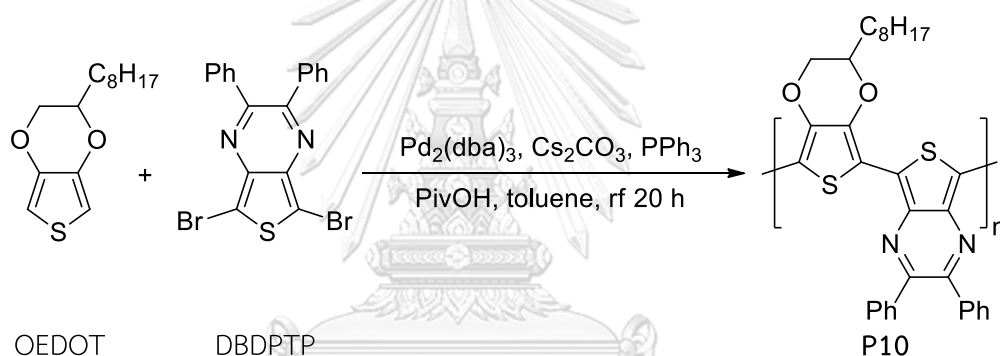


Figure 3.9 Possible branched structure of polymer of P9

3.2.10 Poly(2'-octyl-3,4-ethylenedioxythiophene-co-2,3-diphenylthieno[3,4-b]pyrazine) (P10)



Scheme 3.31 Synthesis of poly(2'-octyl-3,4-ethylenedioxythiophene-co-2,3-diphenylthieno[3,4-b]pyrazine) (P10)

Polymer **P10** was synthesized from DArP between OEDOT and DBDPTP. (Scheme 3.31) The fully substituted pyrazine on DBDPTP would prevent the formation of branching defect of polymer in **P9**. The steric phenyl groups may also reduce the potential of self-polymerization of the reactant. The reaction with equal ratio by mole of OEDOT and DBDPTP using $\text{Pd}(\text{OAc})_2$ as the catalyst (Entry 1, Table 3.5) gave higher incorporation of DPTP units into the product, corresponding to random copolymer with the ratio of OEDOT : DPTP = 1 : 4, according to the integration of signals in ^1H NMR spectrum. (Figure A.77, Appendix) The ratio of OEDOT : DPTP was obtained from comparing the signals of 10 protons of phenyl

groups on DPTP units at around 7 ppm and the signals of three protons of OEDOT units at around 4 ppm. When we increased the ratio of OEDOT : DBDPTP to 4 : 1 (**Entry 2, Table 3.5**), the signal integration of the ^1H NMR spectrum of the second product presented the improved 1 : 2 ratio of OEDOT : DPTP units, closer to the desired alternating copolymer. (**Figure A.78, Appendix**) When $\text{Pd}_2(\text{dba})_3$ was used instead as the catalyst in the reaction, and used the same ratio of OEDOT : DBDPTP as the second condition. (**Entry 3, Table 3.5**) The signal integration of the ^1H NMR spectrum of this third product showed the closest 1 : 1.23 ratio of OEDOT : DPTP units, almost reaching the fully alternating copolymer. (**Figure A.74, Appendix**) All conditions still generated some insoluble solid, assumed to be the homopolymer of DPTP from its self-polymerization, which caused low yields of the product. UV-visible spectrum of **P10** from the third condition exhibited a very high λ_{max} at 958 nm, (**Figure A.76, Appendix**) indicating an excellent property of TP units as an acceptor.

Table 3.5 Conditions for the synthesis of polymer **P10**

Entry	Catalyst	Starting OEDOT : DBDPTP ratios	Incorporated ratios of OEDOT : DPTP units	Time (h)	%yield	λ_{max} (nm)	M_n^a
1	$\text{Pd}(\text{OAc})_2$	1 : 1	1 : 4	72	7.3	746	2842
2	$\text{Pd}(\text{OAc})_2$	4 : 1	1 : 2	72	30	973	2823
3	$\text{Pd}_2(\text{dba})_3$	4 : 1	1 : 1.23	20	34	958	1886

^afrom GPC analysis

The polymer from entry 1, **Table 3.5** with 1 : 4 ratio of OEDOT : DPTP presented the value of M_n of comparable size to that of entry 2, **Table 3.5** with 1 : 2 ratio of OEDOT : DPTP. The much lower λ_{max} of the polymer from entry 1 would be an evidence to support the idea that the copolymer with the ratio of OEDOT : DPTP closer to 1 : 1 would likely to have the desirable alternating connections between

the two units and hence better optical property. It was also confirmed in the comparison between the polymers from entries 2 and 3, **Table 3.5** in which their λ_{\max} values were comparable despite their large difference in sizes, further emphasized that the polymer with ratio of the two monomeric units near 1 : 1 or alternating copolymer would have the best optical property.

3.3 Fluorescence property of polymers P1-P7, P10

The polymer **P1-P7** and **P10** in dichloromethane was measure their fluorescence emission as summarized in **Table 3.6**

Table 3.6 Fluorescence excitation and emission of polymers **P1-P7, P10**

Polymer	Excitation (nm)	Emission (nm)
P1	480	565
P2	630	710
P3	461	607
P4	420	509
P5	506	610
P6	400	472
P7	336	-
P9	845	-
P10	958	-

The polymers **P1-P6** gave various fluorescence emission values ranging from 509 to 710 nm. The polymer **P2** exhibited the highest fluorescence emission values at 710 nm. The polymers **P3** and **P5** also showed high fluorescence emission values

at 607 and 610 nm, respectively. These results showed that the presence of BTD or OBTZ units as an acceptor in structure had high value of fluorescence emission.

3.4 Molar extinction coefficient

3.4.1 Molar extinction coefficient of UV-visible absorption

Polymer **P2** and **P5** were selected to measure their molar extinction coefficient because of the high λ_{\max} values and intensities. Determination of molar extinction coefficient (ϵ) followed the Beer–Lambert law :

$$A = \epsilon cl$$

:

- A = absorbance
- ϵ = molar extinction coefficient ($\text{L}\cdot\text{mol}^{-1}\cdot\text{cm}^{-1}$)
- c = concentration (molar)
- l = path length (1 cm)

The polymer **P2** was determined to have the molar extinction coefficient at 630 nm (ϵ_{630}) = 9,400 $\text{L}\cdot\text{mol}^{-1}\cdot\text{cm}^{-1}$. (**Figure A.79, Appendix**), which the polymer **P5** had the molar extinction coefficient at 506 nm (ϵ_{506}) = 12,180 $\text{L}\cdot\text{mol}^{-1}\cdot\text{cm}^{-1}$. (**Figure A.80, Appendix**)

3.4.2 Molar extinction coefficient of fluorescence emission

Polymer **P5** was selected to measure the molar extinction coefficient of fluorescence emission because of its highest intensity of emission. Molar extinction coefficient was calculated from Beer–Lambert law similar to section 3.4.1. The polymer **P5** has molar extinction coefficient at 610 nm (ϵ_{610}) = 34811 $\times 10^{-3}$ $\text{L}\cdot\text{mol}^{-1}\cdot\text{cm}^{-1}$. (**Figure A.81, Appendix**)

3.5 Band gap

Onset wavelength (λ_{onset}) and band gap (E_g) of polymer **P1-7** and **P10** showed in **Table 3.7**

Table 3.7 Maximum wavelength, onset wavelength, and band gap of polymer **P1-7** and **P10**

Polymer	λ_{max} (nm)	λ_{onset} (nm)	E_g (eV)
P1	259	520	2.39
P2	630	925	1.34
P3	461	615	2.02
P4	293	520	2.39
P5	506	655	1.90
P6	296	575	2.16
P7	289	665	1.87
P9	845	>1100 ^a	<1.13
P10	958	>1100 ^a	<1.13

^a λ_{onset} value of **P10** exceed the limit of instrument (1100 nm)

Most polymers exhibited rather large band gap around 2 eV. In particular, conjugated polymers for OPV were suggested to should have band gaps lower than 2.0 eV to be able to absorb most of the solar energy. [70] So, these polymers can apply to make polymer solar cells.

CHAPTER IV CONCLUSION

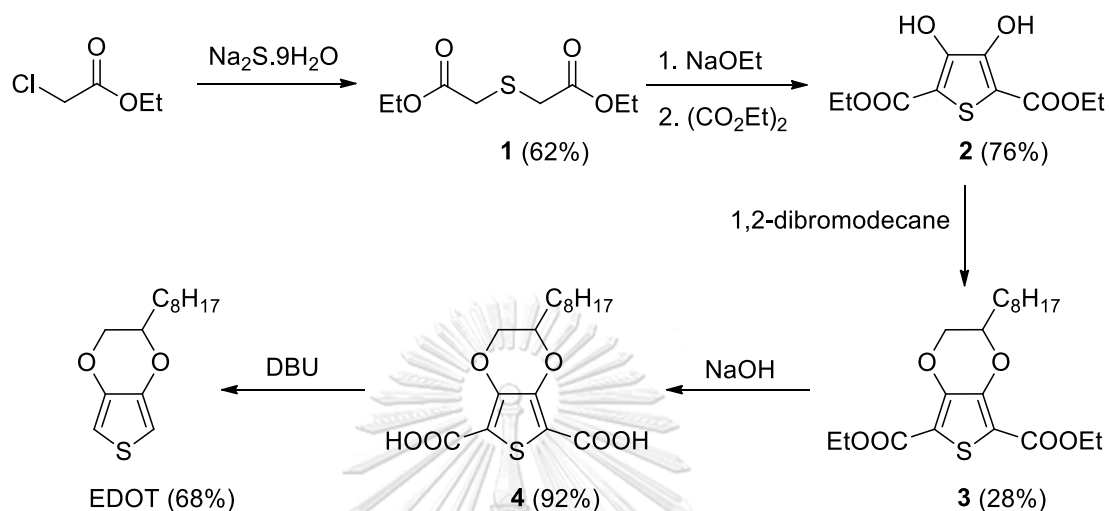


Figure 4.1 Synthesis of OEDOT

In the part of monomers synthesis, compound **1** was prepared by double $\text{S}_{\text{N}}2$ reaction between sodium sulfide and ethyl chloroacetate in 62% yield. Compound **2** was synthesized from Hinsberg reaction between compound **1** and diethyl oxalate in 76% yield. Compound **3** was synthesized from $\text{S}_{\text{N}}2$ reaction of compound **2** and 1,2-dibromodecane in 28% yield. Compound **3** was hydrolyzed by NaOH to obtain compound **4** in 92% yield, and finally, OEDOT was successfully synthesized from decarboxylation of compound **4** in 68% yield (8.3% overall yield).

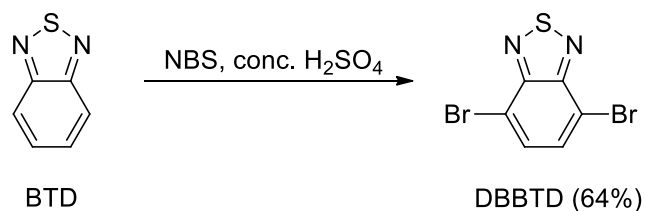


Figure 4.2 Synthesis of DBBTD

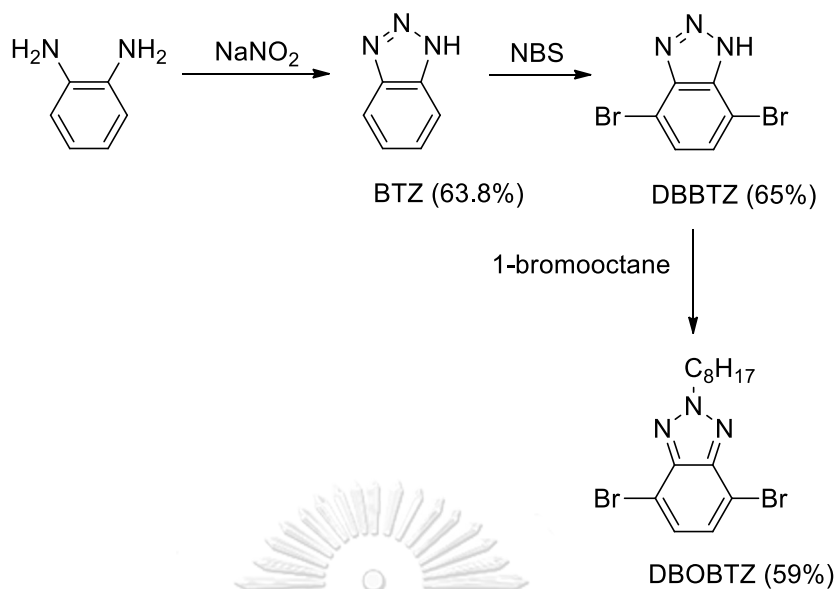


Figure 4.3 Synthesis of DBBTZ and DBOBTZ

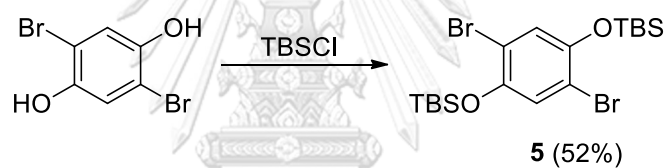


Figure 4.4 Synthesis of compound **5**

DBBTZ was successfully synthesized from bromination of BTZ with NBS in conc. H_2SO_4 in 64% yield. BTZ was prepared by diazotization and cyclization of *o*-phenylenediamine in 63.8% yield. BTZ was similarly brominated to obtain DBBTZ in 65% yield, which was then substituted with 1-bromooctane to produce DBOBTZ in 59% yield. Compound **5** was obtained from double protections of 2,5-dibromobenzene-1,4-diol in 52% yield.

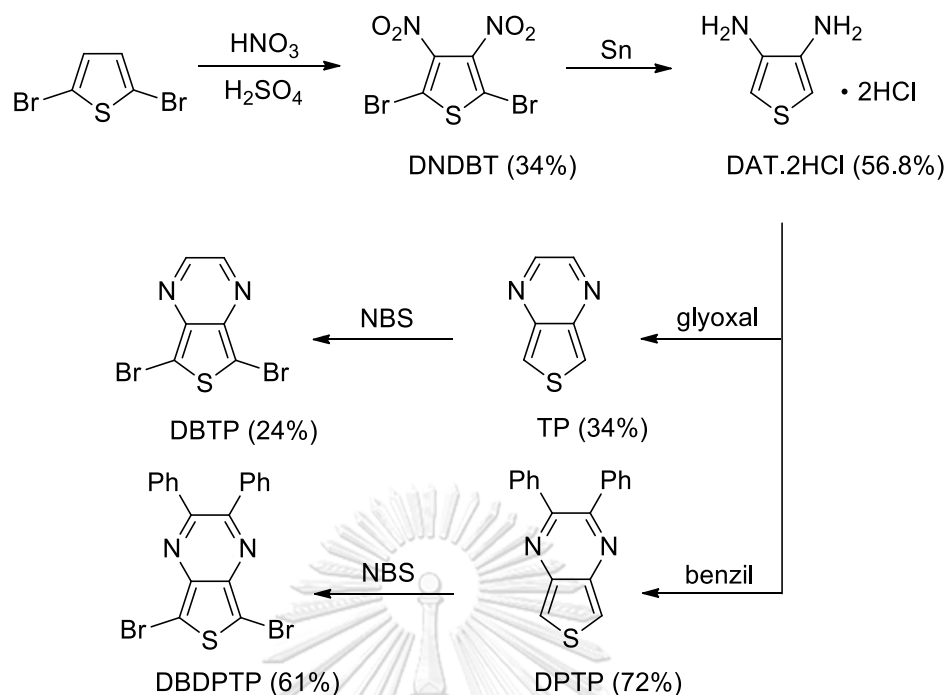


Figure 4.5 Synthesis of DBTP and DBDPTP

DBDNT was prepared by nitration of 3,4-dibromothiophene in 34% yield. DAT was synthesized from reduction of DBDNT with tin powder in 56.8% yield. TP was prepared by condensation of DTA with glyoxal in 34% yield, which was then brominated to give DBTP in 24% yield. DPTP was similarly prepared from condensation of DAT with benzil in 72% yield. DBDPTP was then obtained from bromination of DPTP in 61% yield.

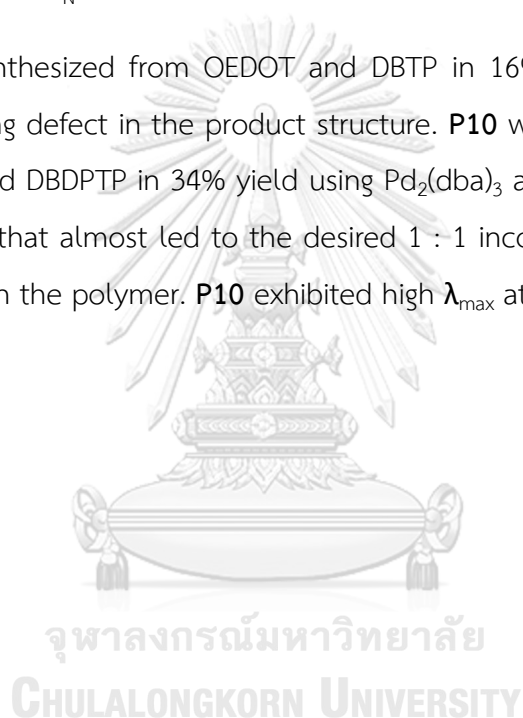
For polymers synthesis, polymer **P1** was synthesized from DARp of OEDOT and DBTZ in 65% yield. **P1** exhibited λ_{max} at 328 nm, in which upon doping with strong acid, λ_{max} moved to 488 nm. However, **P1** is unstable and can be degraded under ambient light and air.

P2 was synthesized from DARp of OEDOT and DBBTD in 82% yield. The starting ratio of OEDOT : DBBTD = 1 : 2.3 gave an alternating copolymer **P2**, that exhibited λ_{max} at 630 nm ($\epsilon_{630} = 9,400 \text{ L}\cdot\text{mol}^{-1}\cdot\text{cm}^{-1}$) and molecular weight (m/z) of 3606.50. **P3** was synthesized from DARp between OEDOT and DBDFBTD in 38% yield. The product was smaller and showed λ_{max} at 461 nm, lower than that of non-fluorinated **P2**.

P4 was synthesized from OEDOT and DBBTZ via DArP in 65% yield, which exhibited low λ_{\max} at only 293 nm. In comparison, the synthesis using octyl substituted BTZ to give **P5** showed much higher λ_{\max} at 506 nm ($\epsilon_{506} = 12,180 \text{ L}\cdot\text{mol}^{-1}\cdot\text{cm}^{-1}$). It also presented high molecular weight (m/z) of 5306.861.

P6 was synthesized from DArP of OEDOT and compound **5** in 65% yield. It showed a rather low λ_{\max} at 269 nm. Deprotection and oxidation to give polymer **P7** still gave disappointing value of λ_{\max} at 289 nm. **P8** was unsuccessfully synthesized from DArP due to the S_NAr side reaction of DBDNT monomer with base.

P9 was synthesized from OEDOT and DBTP in 16% yield, with evidence of extensive branching defect in the product structure. **P10** was similarly obtained from DArP of OEDOT and DBDPTP in 34% yield using $\text{Pd}_2(\text{dba})_3$ and starting ratio of OEDOT : DBDPTP = 4 : 1, that almost led to the desired 1 : 1 incorporation ratio of the two monomeric units in the polymer. **P10** exhibited high λ_{\max} at 985 nm.



REFERENCES

- [1]. Pouliot, J. R.; Grenier, F.; Blaskovits, J. T.; Beaupre, S.; Leclerc, M. Direct (Hetero)arylation Polymerization: Simplicity for Conjugated Polymer Synthesis. Chemical Reviews 116(22) (2016): 14225-14274.
- [2]. Hösel, M.; Dam, H. F.; Krebs, F. C. Development of Lab-to-Fab Production Equipment Across Several Length Scales for Printed Energy Technologies, Including Solar Cells. Energy Technology 3(4) (2015): 293-304.
- [3]. Reale, A.; Notte, L. L.; Salamandra, L.; Polino, G.; Susanna, G.; Brown, T. M.; Brunetti, F.; Carl, A. D. Spray Coating for Polymer Solar Cells: An Up-to-Date Overview. Energy Technology 3 (2015): 385 –406.
- [4]. Feng, X.; Liu, L.; Wang, S.; Zhu, D. Water-soluble fluorescent conjugated polymers and their interactions with biomacromolecules for sensitive biosensors. Chemical Society Reviews 39(7) (2010): 2411-2419.
- [5]. Wang, C.; Dong, H.; Hu, W.; Liu, Y.; Zhu, D. Semiconducting pi-conjugated systems in field-effect transistors: a material odyssey of organic electronics. Chemical Reviews 112(4) (2012): 2208-2267.
- [6]. Xu, R.-P.; Li, Y.-Q.; Tang, J.-X. Recent advances in flexible organic light-emitting diodes. Journal of Materials Chemistry C 4(39) (2016): 9116-9142.
- [7]. Khelifi, S.; Voroshazi, E.; Spoltore, D.; Piersimoni, F.; Bertho, S.; Aernouts, T.; Manca, J.; Lauwaert, J.; Vrielinck, H.; Burgelman, M. Effect of light induced degradation on electrical transport and charge extraction in polythiophene:Fullerene (P3HT:PCBM) solar cells. Solar Energy Materials and Solar Cells 120 (2014): 244-252.
- [8]. Roncali, J. Molecular Engineering of the Band Gap of π -Conjugated Systems: Facing Technological Applications. Macromolecular Rapid Communications 28(17) (2007): 1761-1775.
- [9]. Lei, T.; Wang, J.-Y.; Pei, J. Roles of Flexible Chains in Organic Semiconducting Materials. Chemistry of Materials 26(1) (2013): 594-603.
- [10]. Mei, J.; Bao, Z. Side Chain Engineering in Solution-Processable Conjugated

- Polymers. Chemistry of Materials 26(1) (2013): 604-615.
- [11]. Yuen, J. D.; Wudl, F. Strong acceptors in donor–acceptor polymers for high performance thin film transistors. Energy & Environmental Science 6(2) (2013): 392–406.
- [12]. Li, G.; Chang, W.-H.; Yang, Y. Low-bandgap conjugated polymers enabling solution-processable tandem solar cells. Nature Reviews Materials 2(8) (2017): 1-13.
- [13]. Zhou, H.; Yang, L.; You, W. Rational Design of High Performance Conjugated Polymers for Organic Solar Cells. Macromolecules 45(2) (2012): 607-632.
- [14]. Sharma, B.; Alam, F.; Dutta, V.; Jacob, J. Synthesis and photovoltaic studies on novel fluorene based cross-conjugated donor-acceptor type polymers. Organic Electronics 40 (2017): 42-50.
- [15]. Elsayy, W.; Son, M.; Jang, J.; Kim, M. J.; Ji, Y.; Kim, T.-W.; Ko, H. C.; Elbarbary, A.; Ham, M.-H.; Lee, J.-S. Isoindigo-Based Donor–Acceptor Conjugated Polymers for Air-Stable Nonvolatile Memory Devices. ACS Macro Letters 4(3) (2015): 322-326.
- [16]. Guo, T.; Yu, L.; Zhao, B.; Ying, L.; Wu, H.; Yang, W.; Cao, Y. Blue light-emitting hyperbranched polymers using fluorene-co-dibenzothiophene-S,S-dioxide as branches. Journal of Polymer Science Part A: Polymer Chemistry 53(8) (2015): 1043-1051.
- [17]. Park, Y. W. Editorial for the conducting polymers for carbon electronics themed issue. Chemical Society Reviews 39(7) (2010): 2399–2410.
- [18]. Kim, J.; Kwon, Y. S.; Shin, W. S.; Moon, S.-J.; Park, T. Carbazole-Based Copolymers: Effects of Conjugation Breaks and Steric Hindrance. Macromolecules 44(7) (2011): 1909-1919.
- [19]. Li, K. C.; Huang, J. H.; Hsu, Y. C.; Huang, P. J.; Chu, C. W.; Lin, J. T.; Ho, K. C.; Wei, K. H.; Lin, H. C. Tunable Novel Cyclopentadithiophene-Based Copolymers Containing Various Numbers of Bithiazole and Thienyl Units for Organic Photovoltaic Cell Applications. Macromolecules 42(11) (2009): 3681-3693.
- [20]. Moule, A. J.; Tsami, A.; Buennagel, T. W.; Forster, M.; Kronenberg, N. M.; Scharber, M.; Koppe, M.; Morana, M.; Brabec, C. J.; Meerholz, K.; Scherf, U. Two novel cyclopentadithiophene-based alternating copolymers as potential donor

- components for high-efficiency bulk-heterojunction-type solar cells. Chemistry of Materials 20(12) (2008): 4045-4050.
- [21]. Zhou, H.; Yang, L.; Price, S. C.; Knight, K. J.; You, W. Enhanced photovoltaic performance of low-bandgap polymers with deep LUMO levels. Angewandte Chemie International Edition in English 49(43) (2010): 7992 –7995.
- [22]. Wang, L.; Cai, D.; Zheng, Q.; Tang, C.; Chen, S.-C.; Yin, Z. Low Band Gap Polymers Incorporating a Dicarboxylic Imide-Derived Acceptor Moiety for Efficient Polymer Solar Cells. ACS Macro Letters 2(7) (2013): 605–608.
- [23]. Gruber, M.; Jung, S. H.; Schott, S.; Venkateshvaran, D.; Kronemeijer, A. J.; Andreasen, J. W.; McNeill, C. R.; Wong, W. W. H.; Shahid, M.; Heeney, M.; Lee, J. K.; Siringhaus, H. Enabling high-mobility, ambipolar charge-transport in a DPP-benzotriazole copolymer by side-chain engineering. Chemical Science 6(12) (2015): 6949-6960.
- [24]. Rasmussen, S. C.; Schwiderski, R. L.; Mulholland, M. E. Thieno[3,4-b]pyrazines and their applications to low band gap organic materials. Chemical Communications 47(41) (2011): 11394-11410.
- [25]. Berrouard, P.; Najari, A.; Pron, A.; Gendron, D.; Morin, P. O.; Pouliot, J. R.; Veilleux, J.; Leclerc, M. Synthesis of 5-alkyl[3,4-c]thienopyrrole-4,6-dione-based polymers by direct heteroarylation. Angewandte Chemie International Edition in English 51(9) (2012): 2068-2071.
- [26]. Kumaresan, P.; Vegiraju, S.; Ezhumalai, Y.; Yau, S.; Kim, C.; Lee, W.-H.; Chen, M.-C. Fused-Thiophene Based Materials for Organic Photovoltaics and Dye-Sensitized Solar Cells. Polymers 6(10) (2014): 2645-2669.
- [27]. Zhu, Y.; Heim, I.; Tieke, B. Red Emitting Diphenylpyrrolopyrrole (DPP)-Based Polymers Prepared by Stille and Heck Coupling. Macromolecular Chemistry and Physics 207(23) (2006): 2206-2214.
- [28]. Ashraf, R. S.; Shahid, M.; Klemm, E.; Al-Ibrahim, M.; Sensfuss, S. Thienopyrazine-Based Low-Bandgap Poly(heteroaryleneethynylene)s for Photovoltaic Devices. Macromolecular Rapid Communications 27(17) (2006): 1454-1459.
- [29]. Zhang, Y.; Zou, J.; Cheuh, C.-C.; Yip, H.-L.; Jen, A. K. Y. Significant Improved Performance of Photovoltaic Cells Made from a Partially Fluorinated

- Cyclopentadithiophene/Benzothiadiazole Conjugated Polymer.
Macromolecules 45(13) (2012): 5427-5435.
- [30]. Svensson, M.; Zhang, F.; Veenstra, S. C.; Verhees, W. J. H.; Hummelen, J. C.; Kroon, J. M.; Inganäs, O.; Andersson, M. R. High-Performance Polymer Solar Cells of an Alternating Polyfluorene Copolymer and a Fullerene Derivative. Advanced Materials 15(12) (2003): 988-991.
- [31]. Tkachov, R.; Senkovskyy, V.; Beryozkina, T.; Boyko, K.; Bakulev, V.; Lederer, A.; Sahre, K.; Voit, B.; Kiriya, A. Palladium-catalyzed chain-growth polycondensation of AB-type monomers: high catalyst turnover and polymerization rates. Angewandte Chemie International Edition in English 53(9) (2014): 2402-2407.
- [32]. Kiriya, A.; Senkovskyy, V.; Sommer, M. Kumada Catalyst-Transfer Polycondensation: Mechanism, Opportunities, and Challenges. Macromolecular Rapid Communications 32(19) (2011): 1503-1517.
- [33]. Li, C.; Bo, Z., CHAPTER 1. New Chemistry for Organic Photovoltaic Materials. In Polymer Photovoltaics, pp. 1-31: RSC Publishing, 2015.
- [34]. Ueda, K.; Yanagisawa, S.; Yamaguchi, J.; Itami, K. A general catalyst for the beta-selective C-H bond arylation of thiophenes with iodoarenes. Angewandte Chemie International Edition in English 49(47) (2010): 8946-8949.
- [35]. Yanagisawa, S.; Ueda, K.; Sekizawa, H.; Itami, K. Programmed Synthesis of Tetraarylthiophenes through Sequential C-H Arylation. Journal of the American Chemical Society 131(41) (2009): 14622-14623.
- [36]. Join, B.; Yamamoto, T.; Itami, K. Iridium catalysis for C-H bond arylation of heteroarenes with iodoarenes. Angewandte Chemie International Edition in English 48(20) (2009): 3644-3647.
- [37]. GARCÍA-MELCHOR, G.; BRAGA, A. A. C.; LLEDOS, A.; UJAQUE, G.; MASERAS, G. Computational Perspective on Pd-Catalyzed C-C Cross-Coupling Reaction Mechanisms. ACCOUNTS OF CHEMICAL RESEARCH 46(11) (2013): 2626-2634.
- [38]. Carsten, B.; He, F.; Son, H. J.; Xu, T.; Yu, L. Stille polycondensation for synthesis of functional materials. Chemical Reviews 111(3) (2011): 1493-1528.
- [39]. Lafrance, M.; Fagnou, K. Palladium-catalyzed benzene arylation: Incorporation of catalytic pivalic acid as a proton shuttle and a key element in catalyst

- design. Journal of the American Chemical Society 128(51) (2006): 16496-16497.
- [40]. Sevignon, M.; Papillon, J.; Schulz, E.; Lemaire, M. New synthetic method for the polymerization of alkylthiophenes. Tetrahedron Letters 40(32) (1999): 5873-5876.
- [41]. Wang, Q.; Takita, R.; Kikuzaki, Y.; Ozawa, F. Palladium-catalyzed dehydrohalogenative polycondensation of 2-bromo-3-hexylthiophene: an efficient approach to head-to-tail poly(3-hexylthiophene). Journal of the American Chemical Society 132(33) (2010): 11420-11421.
- [42]. Fujinami, Y.; Kuwabara, J.; Lu, W.; Hayashi, H.; Kanbara, T. Synthesis of Thiophene- and Bithiophene-Based Alternating Copolymers via Pd-Catalyzed Direct C–H Arylation. ACS Macro Letters 1(1) (2012): 67–70.
- [43]. Kumar, A.; Kumar, A. Single step reductive polymerization of functional 3,4-propylenedioxythiophenes via direct C–H arylation catalyzed by palladium acetate. Polymer Chemistry 1(3) (2010): 286-288.
- [44]. Yamazaki, K.; Kuwabara, J.; Kanbara, T. Detailed optimization of polycondensation reaction via direct C-H arylation of ethylenedioxythiophene. Macromolecular Rapid Communications 34(1) (2013): 69-73.
- [45]. Narayanan, S.; Raghunathan, S. P.; Mathew, S.; Mahesh Kumar, M. V.; Abbas, A.; Sreekumar, K.; Kartha, C. S.; Joseph, R. Synthesis and third-order nonlinear optical properties of low band gap 3,4-ethylenedioxythiophene–quinoxaline copolymers. European Polymer Journal 64 (2015): 157-169.
- [46]. Lu, W.; Kuwabara, J.; Kuramochi, M.; Kanbara, T. Synthesis of bithiazole-based crystalline polymers via palladium-catalyzed direct C-H arylation. Journal of Polymer Science Part A: Polymer Chemistry 53(11) (2015): 1396-1402.
- [47]. Livi, F.; Gobalasingham, N. S.; Thompson, B. C.; Bundgaard, E. Analysis of diverse direct arylation polymerization (DArP) conditions toward the efficient synthesis of polymers converging with stille polymers in organic solar cells. Journal of Polymer Science Part A: Polymer Chemistry 54(18) (2016): 2907-2918.
- [48]. Kowalski, S.; Allard, S.; Scherf, U. Synthesis of Poly(4,4-dialkyl-cyclopenta[2,1-b:3,4-b']dithiophene-alt-2,1,3-benzothiadiazole) (PCPDTBT) in a Direct Arylation

- Scheme. ACS Macro Letters 1(4) (2012): 465-468.
- [49]. C. G. Overberger, H. J. M. a. R. F. Cyclic Sulfones. II. The Polymerization of Styrene in the Presence of 3,4-Diphenylthiophene-1 -dioxide and 3,4-Di- (p-chlorophenyl) -thiophene-1 -dioxide. Journal of American Chemical Society 72 (1950): 4958- 4961.
- [50]. Guo, K.; Hao, J.; Zhang, T.; Zu, F.; Zhai, J.; Qiu, L.; Zhen, Z.; Liu, X.; Shen, Y. The synthesis and properties of novel diazo chromophores based on thiophene conjugating spacers and tricyanofuran acceptors. Dyes and Pigments 77(3) (2008): 657-664.
- [51]. Kikushima, K.; Moriuchi, T.; Hirao, T. Vanadium-catalyzed oxidative bromination promoted by Brønsted acid or Lewis acid. Tetrahedron 66(34) (2010): 6906-6911.
- [52]. Sankaran, B.; Reynolds, J. R. High-Contrast Electrochromic Polymers from Alkyl-Derivatized Poly(3,4-ethylenedioxythiophenes). Macromolecules 30 (1997): 2582-2588.
- [53]. Wolfs, M.; Darmanin, T.; Guittard, F. Versatile Superhydrophobic Surfaces from a Bioinspired Approach. Macromolecules 44(23) (2011): 9286-9294.
- [54]. Heiskanen, J. P.; Vivo, P.; Saari, N. M.; Hukka, T. I.; Kastinen, T.; Kaunisto, K.; Lemmetyinen, H. J.; Hormi, O. E. Synthesis of Benzothiadiazole Derivatives by Applying C-C Cross-Couplings. The Journal of Organic Chemistry 81(4) (2016): 1535-1546.
- [55]. DaSilveira Neto, B. A.; Lopes, A. S. A.; Ebeling, G.; Gonçalves, R. S.; Costa, V. E. U.; Quina, F. H.; Dupont, J. Photophysical and electrochemical properties of π -extended molecular 2,1,3-benzothiadiazoles. Tetrahedron 61(46) (2005): 10975-10982.
- [56]. Bhardwaj, B.; Jain, S. C. Synthesis and Antimicrobial Activities of Novel Aminoalkylated 2H-benzotriazoles. American Chemical Science Journal 5 (2014): 576-586.
- [57]. Bretner, M.; Baier, A.; Kopanska, K.; Najda, A.; Schoof, A.; Reinholz, M.; Lipniacki, A.; Piasek, A.; Kulikowski, T.; Borowski, P. Synthesis and biological activity of 1H-

- benzotriazole and 1H-benzimidazole analogues – inhibitors of the NTPase/helicase of HCV and of some related Flaviviridae. Antiviral Chemistry & Chemotherapy 16(5) (2005): 315–326.
- [58]. Ko, H. C.; Kim, S.; Lee, H.; Moon, B. Multicolored Electrochromism of a Poly{1,4-bis[2-(3,4-ethylenedioxy)thienyl]benzene} Derivative Bearing Viologen Functional Groups. Advanced Functional Materials 15(6) (2005): 905-909.
- [59]. Zou, Y.; Wan, M.; Sang, G.; Ye, M.; Li, Y. An Alternative Copolymer of Carbazole and Thieno[3,4b]-Pyrazine: Synthesis and Mercury Detection. Advanced Functional Materials 18(18) (2008): 2724-2732.
- [60]. McNamara, L. E.; Liyanage, N.; Peddapuram, A.; Murphy, J. S.; Delcamp, J. H.; Hammer, N. I. Donor-Acceptor-Donor Thienopyrazines via Pd-Catalyzed C-H Activation as NIR Fluorescent Materials. The Journal of Organic Chemistry 81(1) (2016): 32-42.
- [61]. Kenning, D. D.; Mitchell, K. A.; Calhoun, T. R.; Funfar, M. R.; Sattler, D. J.; Rasmussen, S. C. Thieno[3,4-b]pyrazines: synthesis, structure, and reactivity. The Journal of Organic Chemistry 67(25) (2002): 9073-9076.
- [62]. Casado, J.; Ortiz, R. P.; Ruiz Delgado, M. C.; Hernandez, V.; Lopez Navarrete, J. T.; Raimundo, J. M.; Blanchard, P.; Allain, M.; Roncali, J. Alternated quinoid/aromatic units in terthiophenes building blocks for electroactive narrow band gap polymers. Extended spectroscopic, solid state, electrochemical, and theoretical study. The Journal of Physical Chemistry B 109(35) (2005): 16616-16627.
- [63]. Shahid, M.; Ashraf, R. S.; Klemm, E.; Sensfuss, S. Synthesis and properties of novel low-band-gap thienopyrazine-based poly(heteroarylenevinylene)s. Macromolecules 39(23) (2006): 7844-7853.
- [64]. Jeong, J.; Kumar, R. S.; Naveen, M.; Son, Y.-A. Synthesis and characterization of triphenylamine-based polymers and their application towards solid-state electrochromic cells. RSC Advances 6(82) (2016): 78984-78993.
- [65]. Wynberg, H.; Kooreman, H. J. The Mechanism of the Hinsberg Thiophene Ring Synthesis. Journal of the American Chemical Society 87 (1965): 1739–1742.
- [66]. Demory, E.; Farran, D.; Baptiste, B.; Chavant, P. Y.; Blandin, V. Fast Pd- and

- Pd/Cu-catalyzed direct C-H arylation of cyclic nitrones. Application to the synthesis of enantiopure quaternary alpha-amino esters. The Journal of Organic Chemistry 77(18) (2012): 7901-7912.
- [67]. Kowalski, S.; Allard, S.; Scherf, U. Scope and limitations of a direct arylation polycondensation scheme in the synthesis of PCPDTBT-type copolymers. Macromolecular Rapid Communications 36(11) (2015): 1061-1068.
- [68]. Kim, J.; Chae, S.; Yi, A.; Hong, S.; Kim, H. J.; Suh, H. Characterization of push-pull type of conjugated polymers containing 8H-thieno[2,3-b]indole for organic photovoltaics. Synthetic Metals 245 (2018): 267-275.
- [69]. Larina, L. I., Tautomerism and Structure of Azoles. In Advances in Heterocyclic Chemistry, pp. 233-321: Elsevier Inc., 2018.
- [70]. Nunzi, J. M. Organic photovoltaic materials and devices. Comptes Rendus Physique 3 (2002): 523-542.



APPENDIX

จุฬาลงกรณ์มหาวิทยาลัย
CHULALONGKORN UNIVERSITY

Calculation of band gap (E_g)

Band gap of polymer can calculate from Planck relation

$$E_g = hc/\lambda_{\text{onset}} \quad : \quad E_g = \text{band gap (J)}$$

h = Plank's constant (6.626×10^{-34} J/s)
 c = speed of light (3×10^8 m/s)
 λ_{onset} = onset wavelength (m)

λ_{onset} is the intersection between tangent line of low energetic edge of adsorption spectrum and tangent line of baseline as showed in **Figure A.44**, **Figure A.48**, **Figure A.55**, **Figure A.59**, **Figure A.63**, **Figure A.67**, and **Figure A.71**

Example, calculation of E_g of polymer P1

$$\begin{aligned}
 E_g &= hc/\lambda_{\text{onset}} \\
 &= (6.626 \times 10^{-34} \text{ J/s}) \cdot (3.00 \times 10^8 \text{ m/s}) / (520 \times 10^{-9} \text{ m}) \\
 &= 3.82 \times 10^{-19} \text{ J}
 \end{aligned}$$

Convert J to eV ($1 \text{ eV} = 1.6 \times 10^{-19} \text{ J}$)

$$\begin{aligned}
 &= (3.82 \times 10^{-19}) / (1.6 \times 10^{-19}) \text{ eV} \\
 &= 2.39 \text{ eV}
 \end{aligned}$$

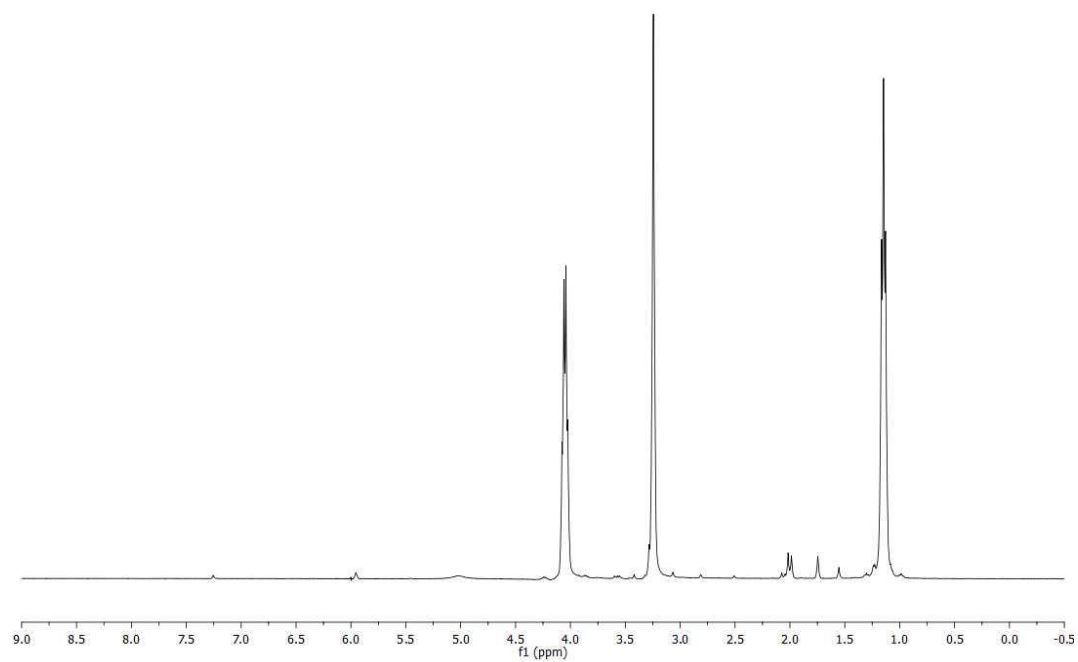


Figure A.1 ^1H NMR (CDCl_3) spectrum of compound **1**

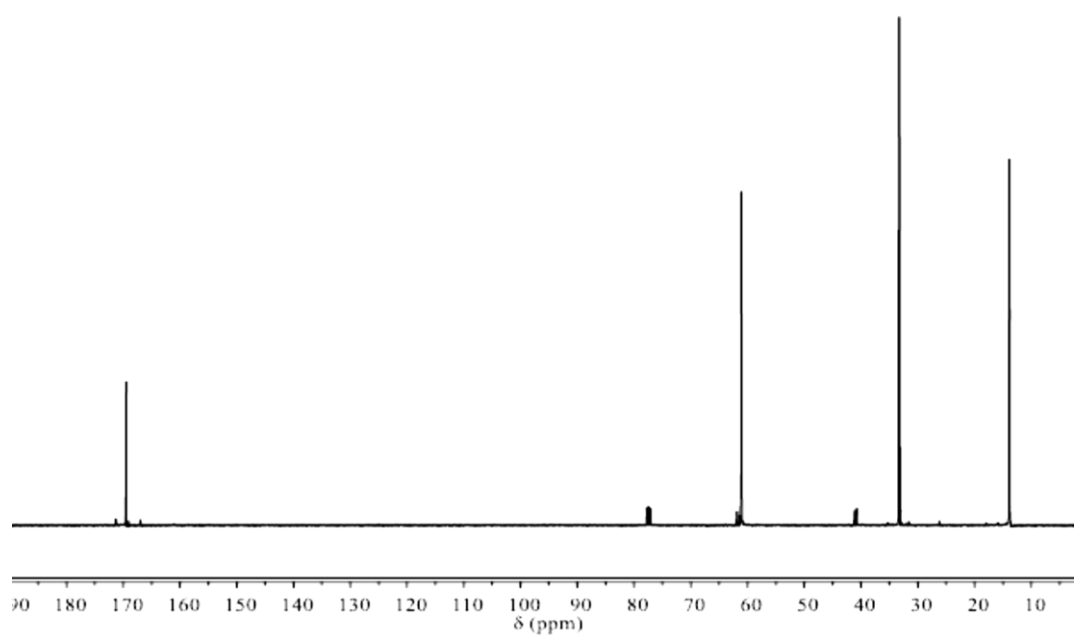


Figure A.2 ^{13}C NMR (CDCl_3) spectrum of compound **1**

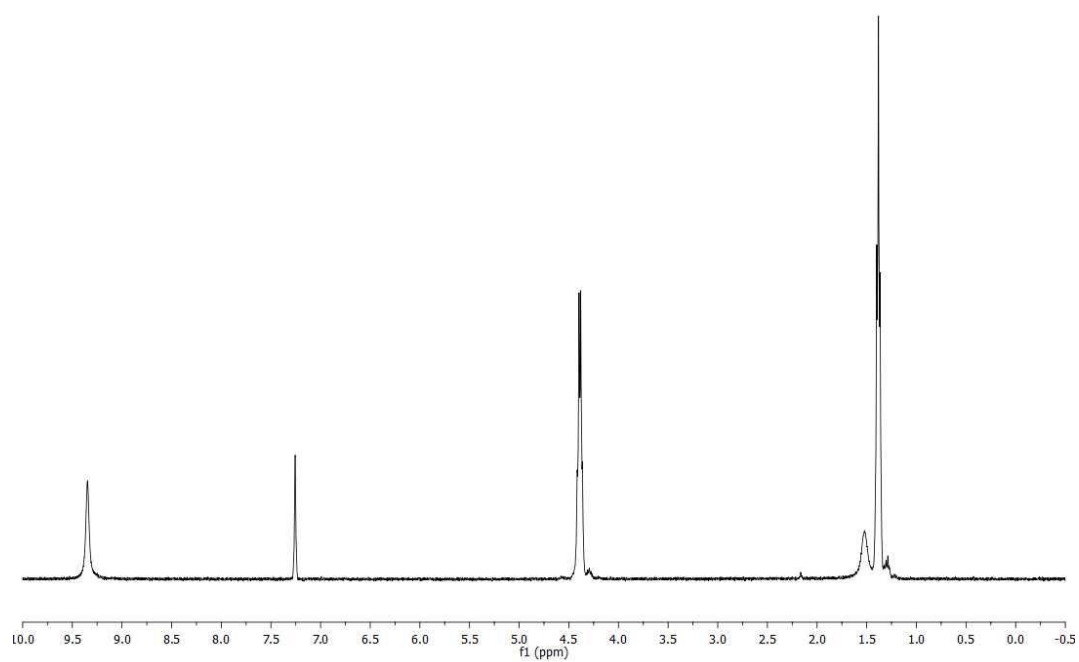


Figure A.3 ^1H NMR (CDCl_3) spectrum of compound 2

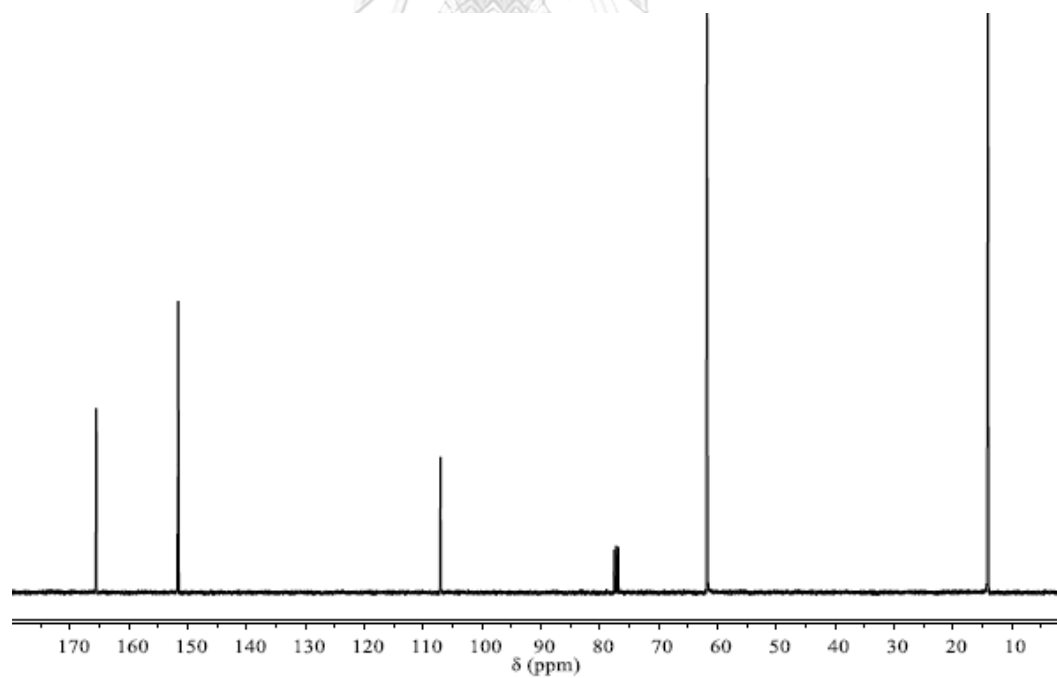


Figure A.4 ^{13}C NMR (CDCl_3) spectrum of compound 2

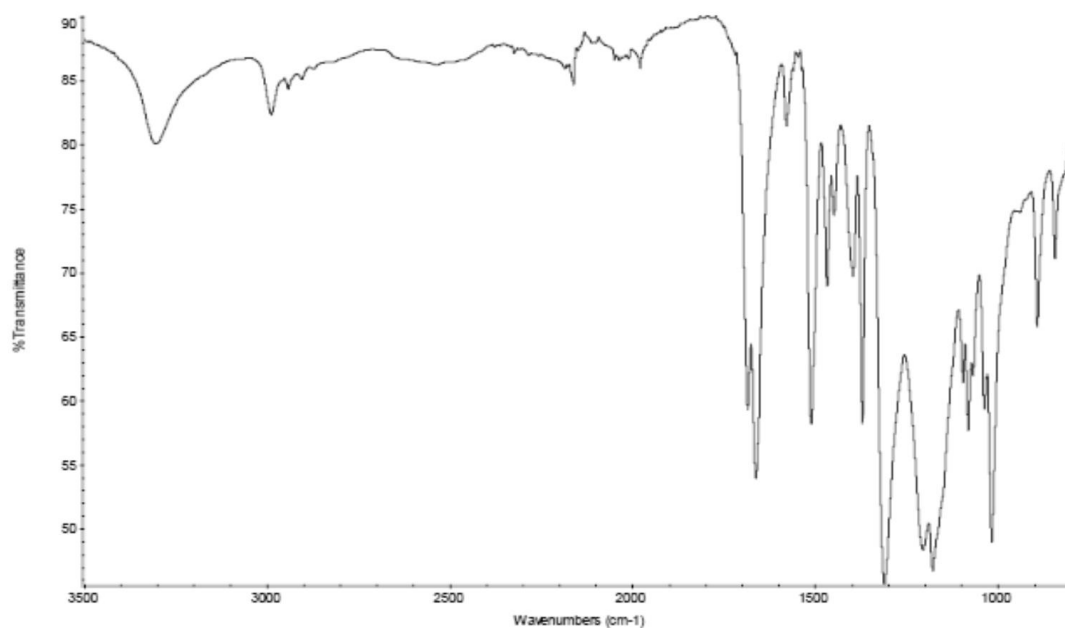


Figure A.5 IR spectrum of compound 2

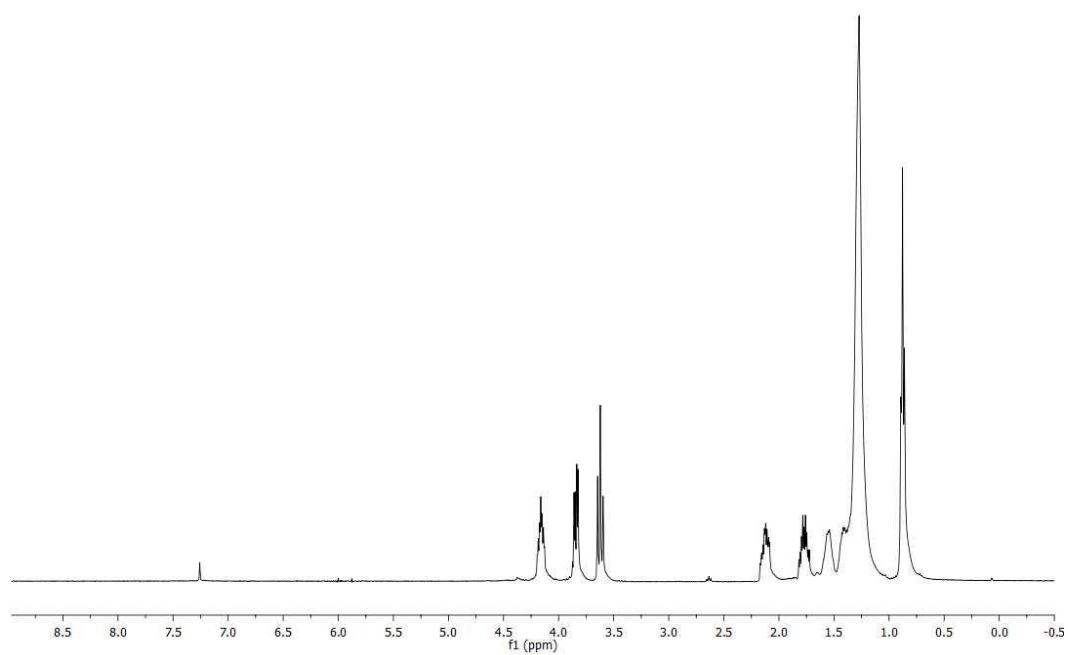


Figure A.6 ¹H NMR (CDCl₃) spectrum of 1,2-dibromodecane

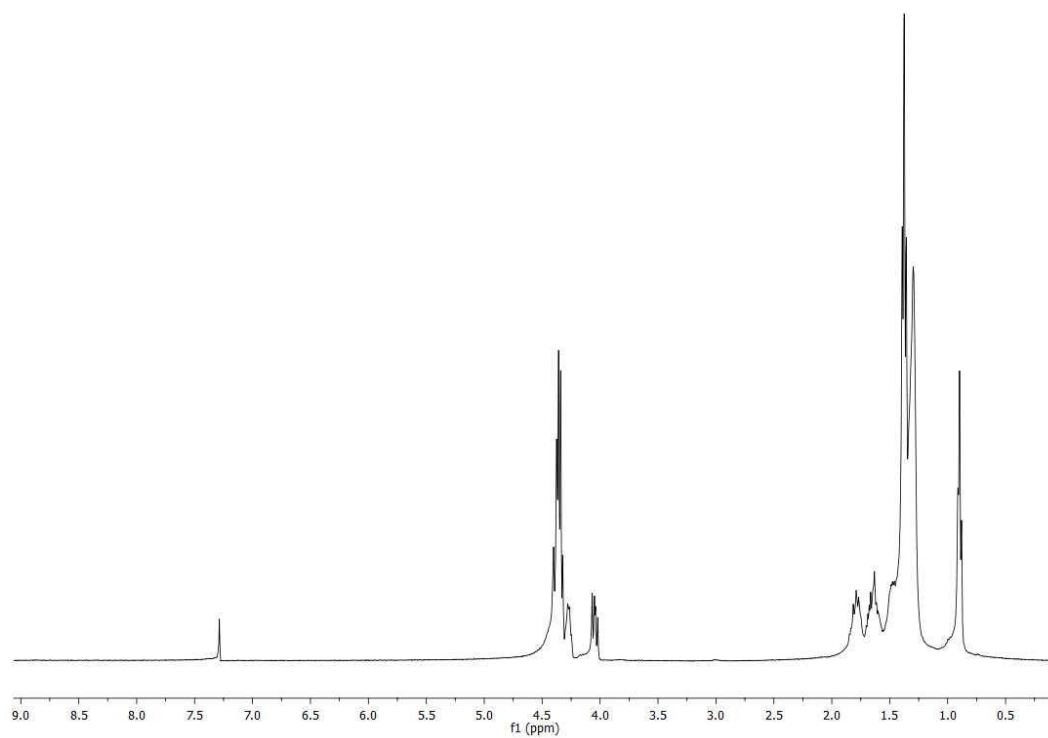


Figure A.7 ^1H NMR (CDCl_3) spectrum of compound **3**

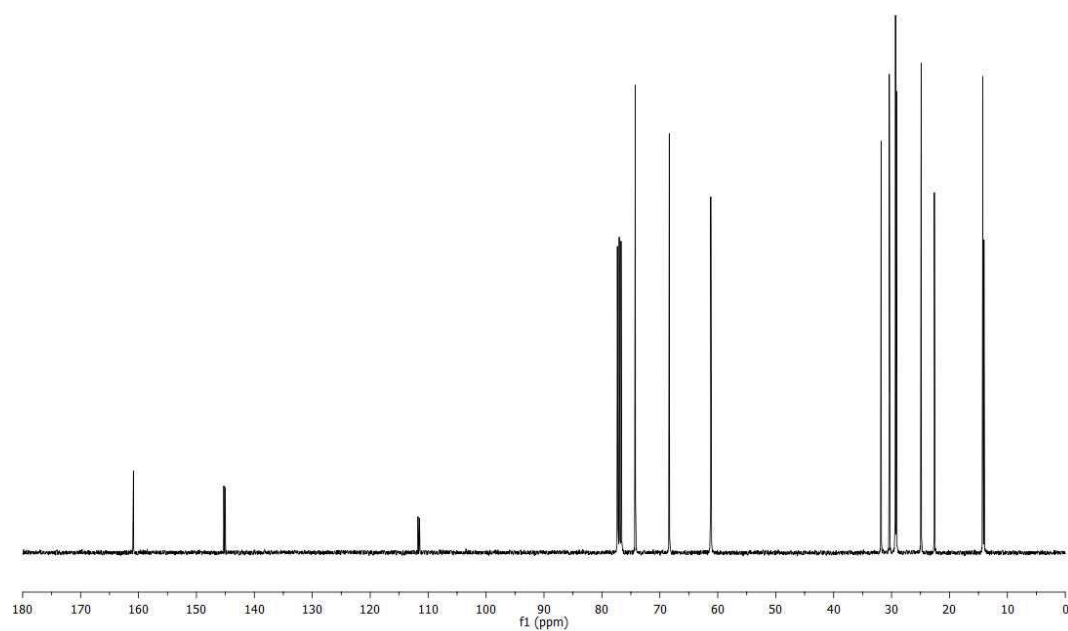


Figure A.8 ^{13}C NMR (CDCl_3) spectrum of compound **3**

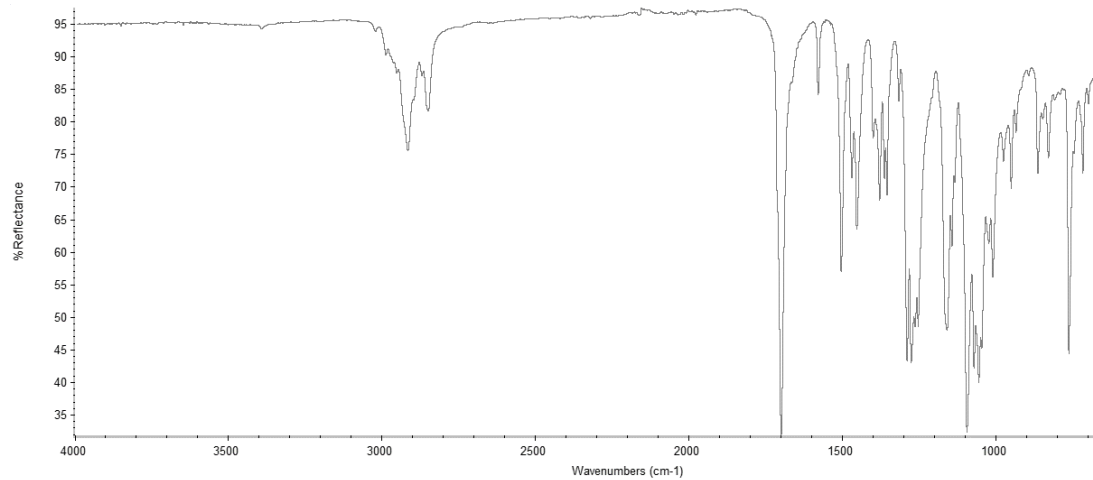


Figure A.9 IR spectrum of compound 3

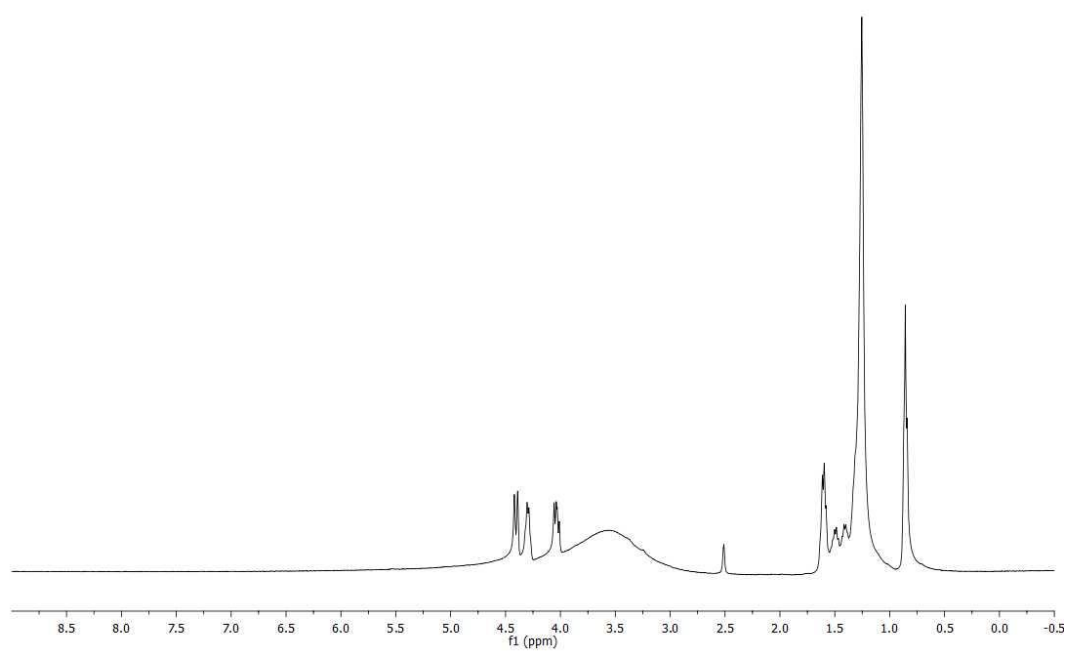


Figure A.10 ¹H NMR (DMSO-d₆) spectrum of compound 4

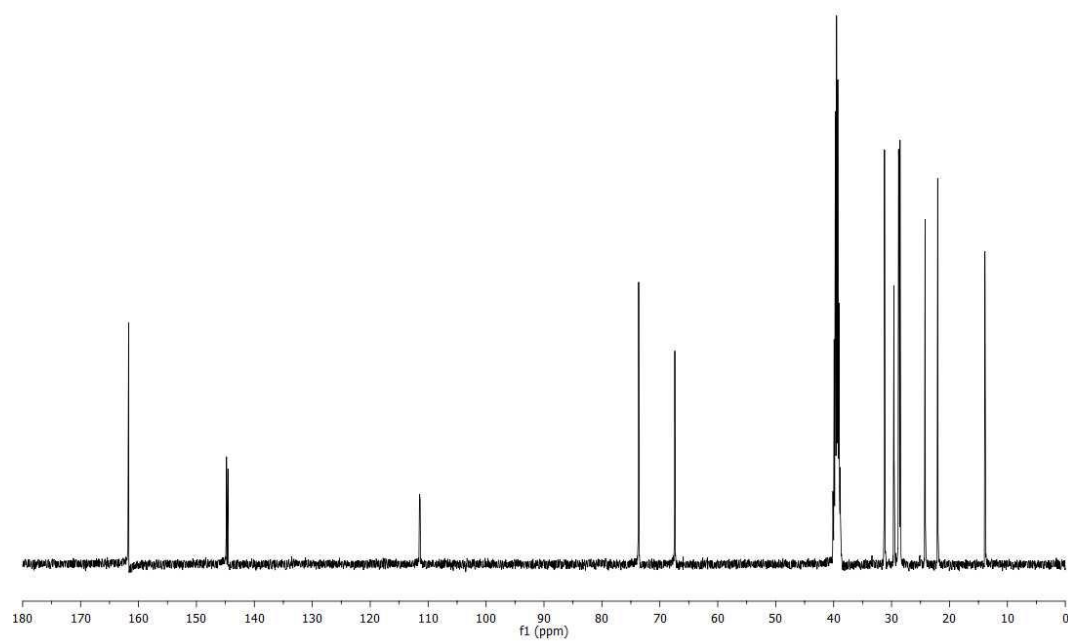


Figure A.11 ^{13}C NMR (DMSO-d_6) spectrum of compound 4

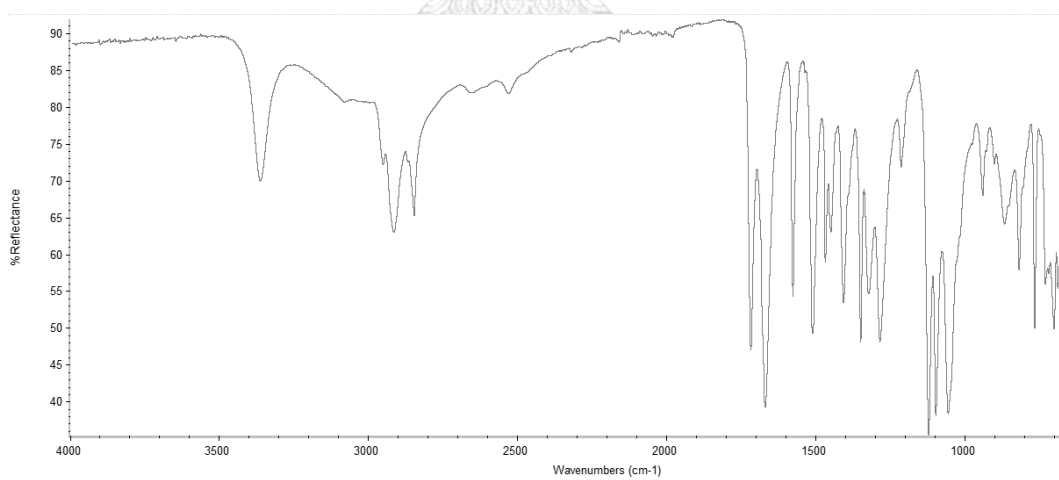


Figure A.12 IR spectrum of compound 4

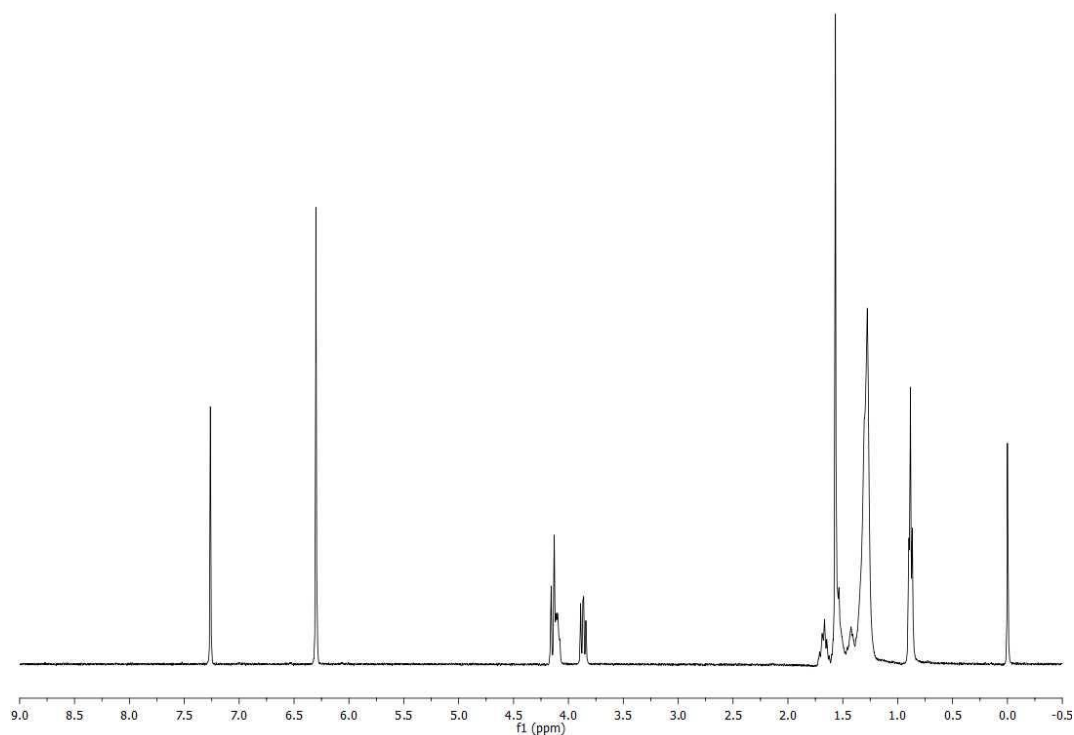


Figure A.13 ^1H NMR (CDCl_3) spectrum of OEDOT

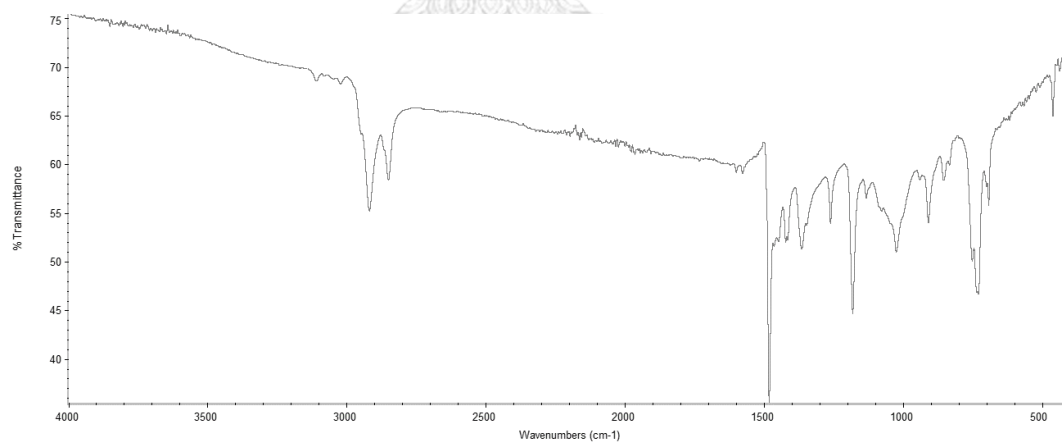


Figure A.14 IR spectrum of OEDOT

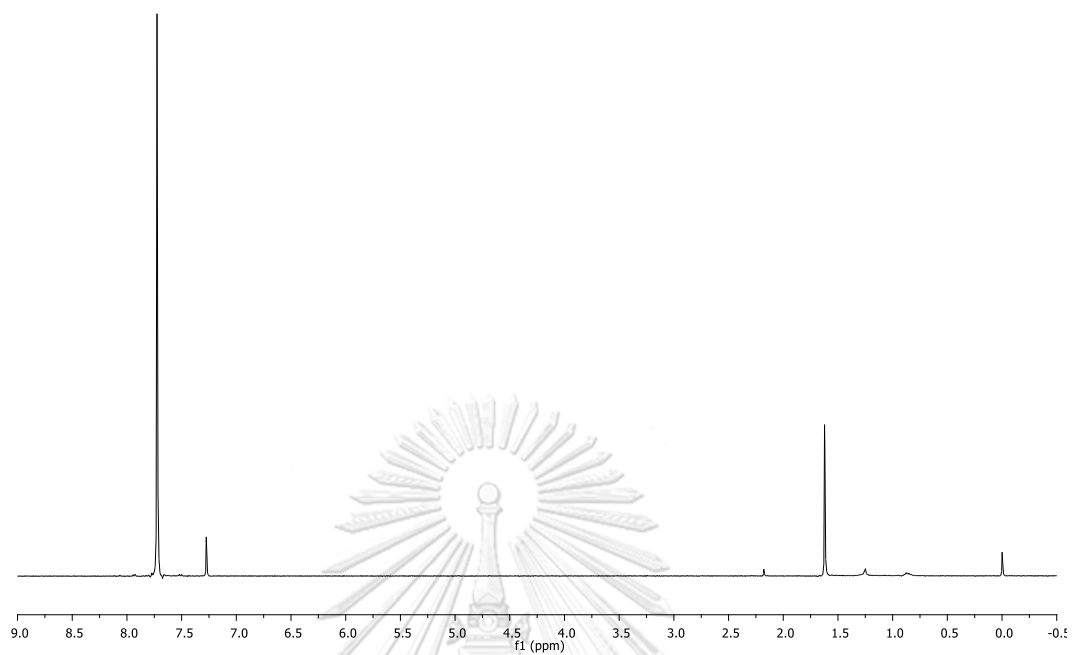


Figure A.15 ^1H NMR (CDCl_3) spectrum of DBBTD

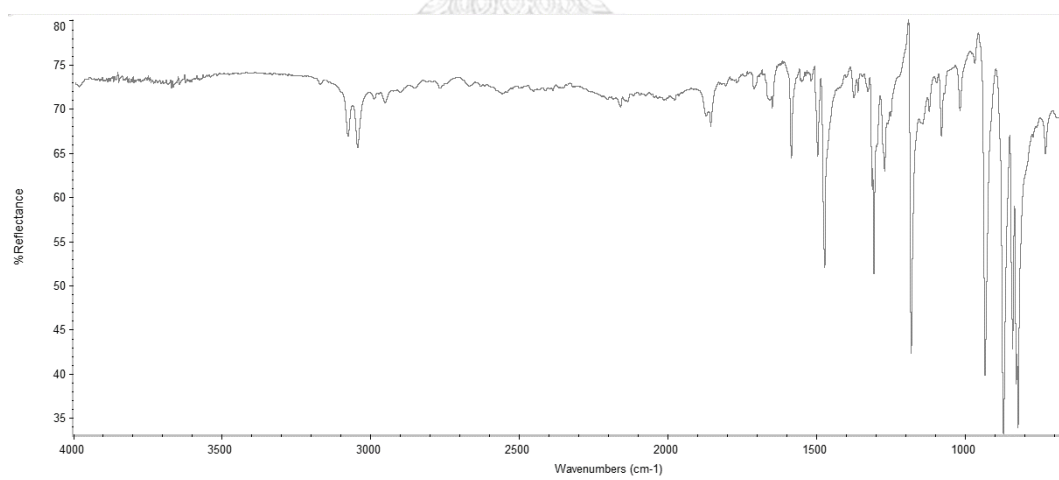


Figure A.16 IR spectrum of DBBTD

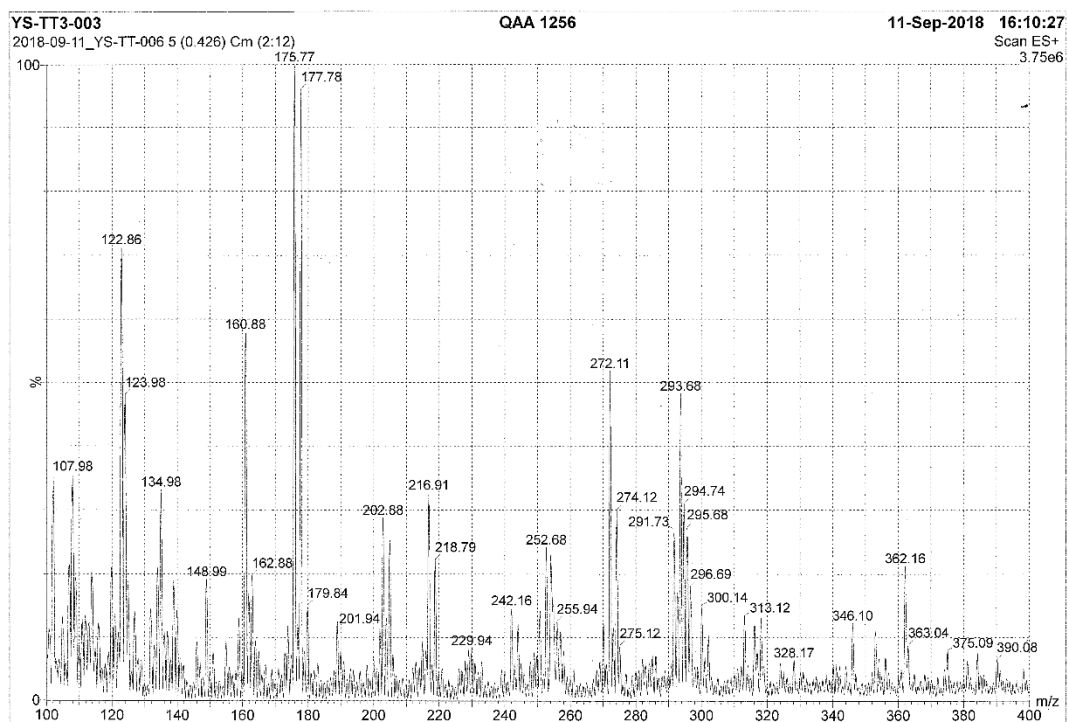
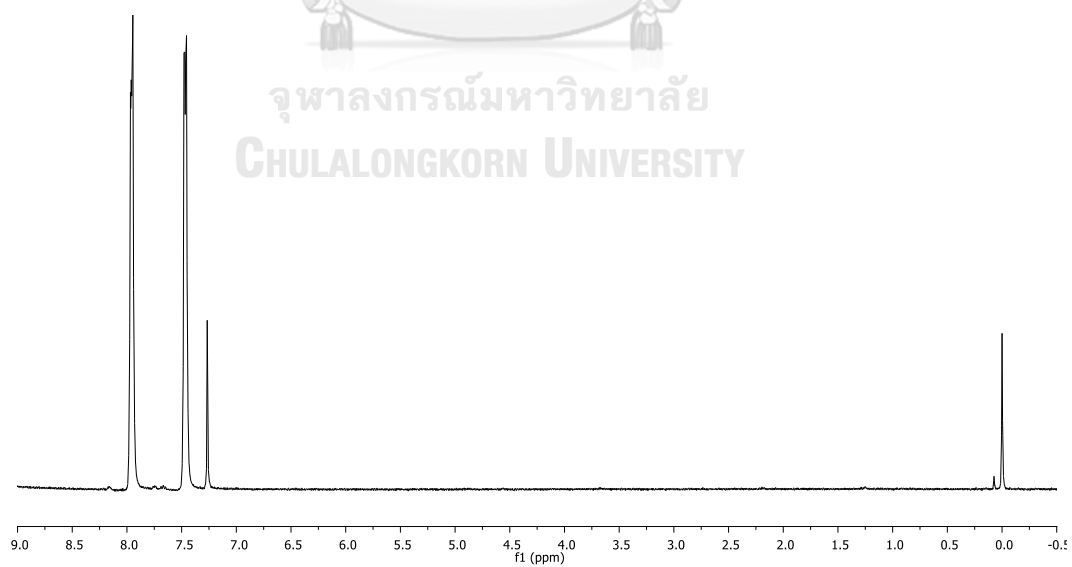


Figure A.17 Mass spectrum of DBBTD

Figure A.18 ^1H NMR (CDCl_3) spectrum of BTZ

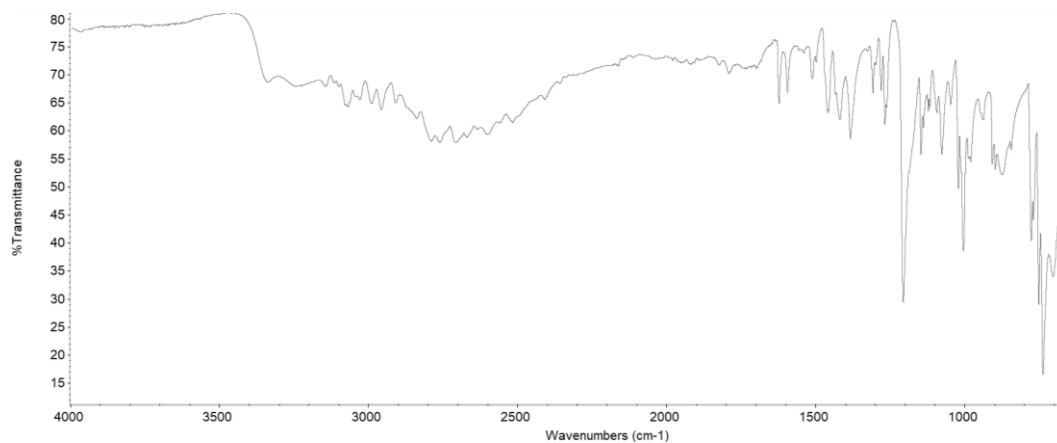


Figure A.19 IR spectrum of BTZ

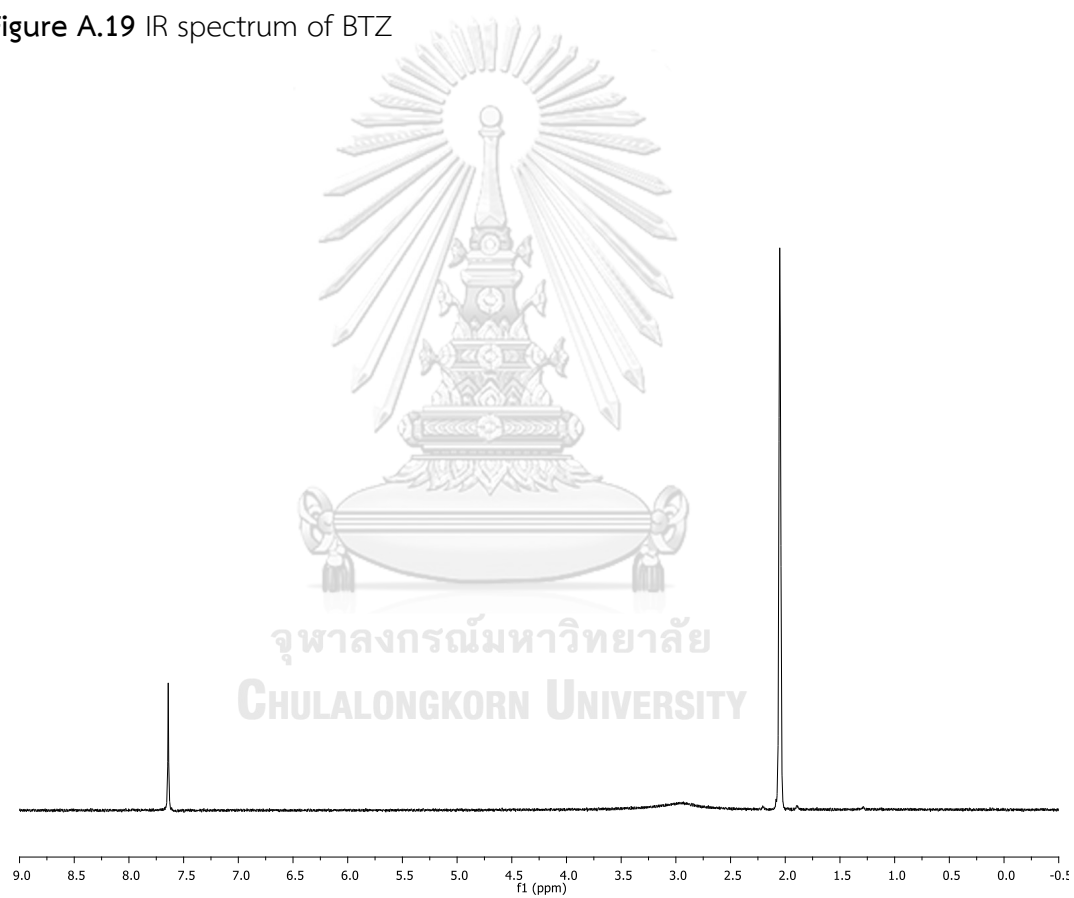


Figure A.20 ^1H NMR (CDCl_3) spectrum of DBBTZ

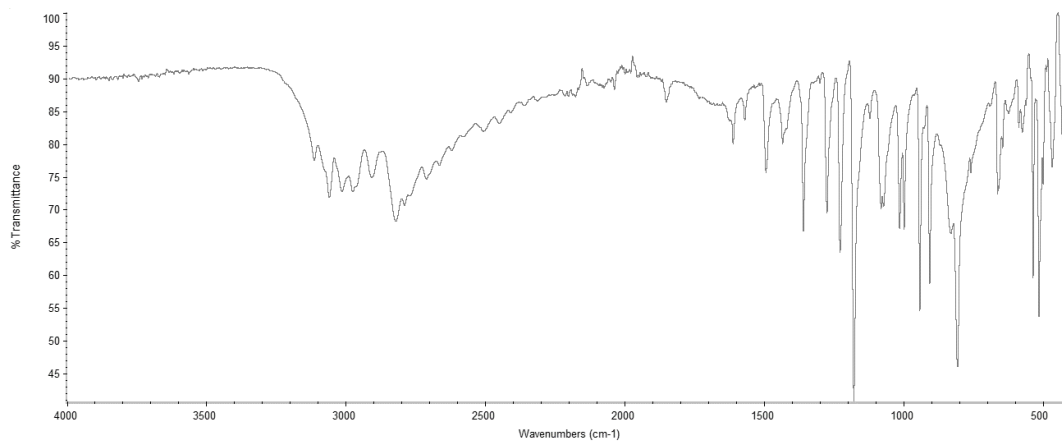


Figure A.21 IR spectrum of DBBTZ

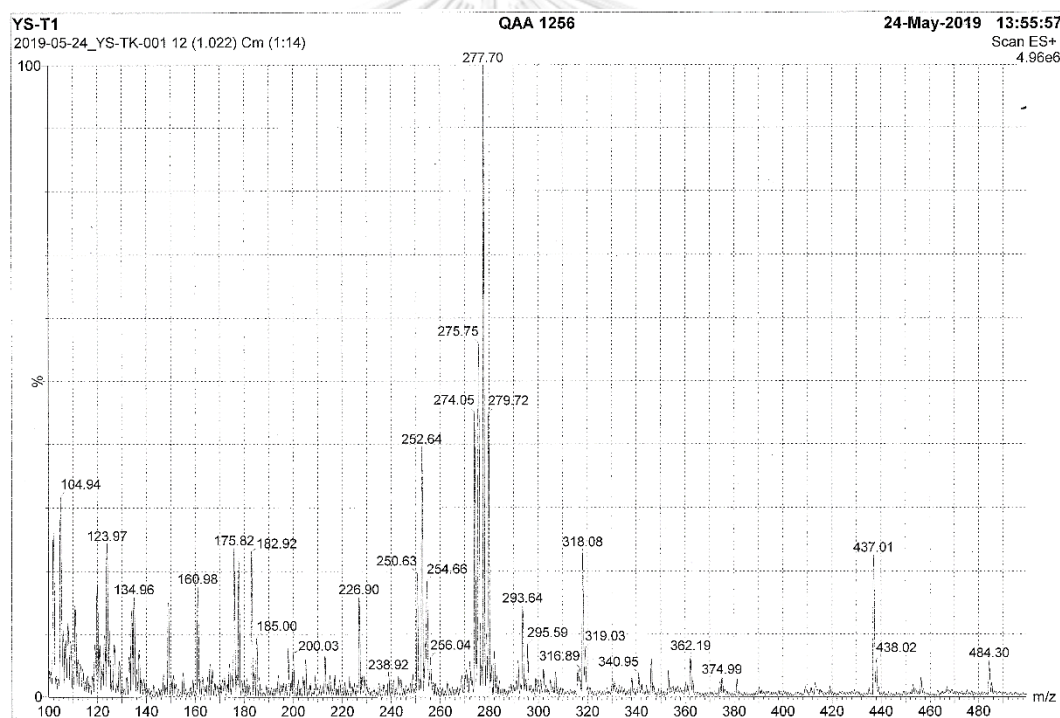


Figure A.22 Mass spectrum of DBBTZ

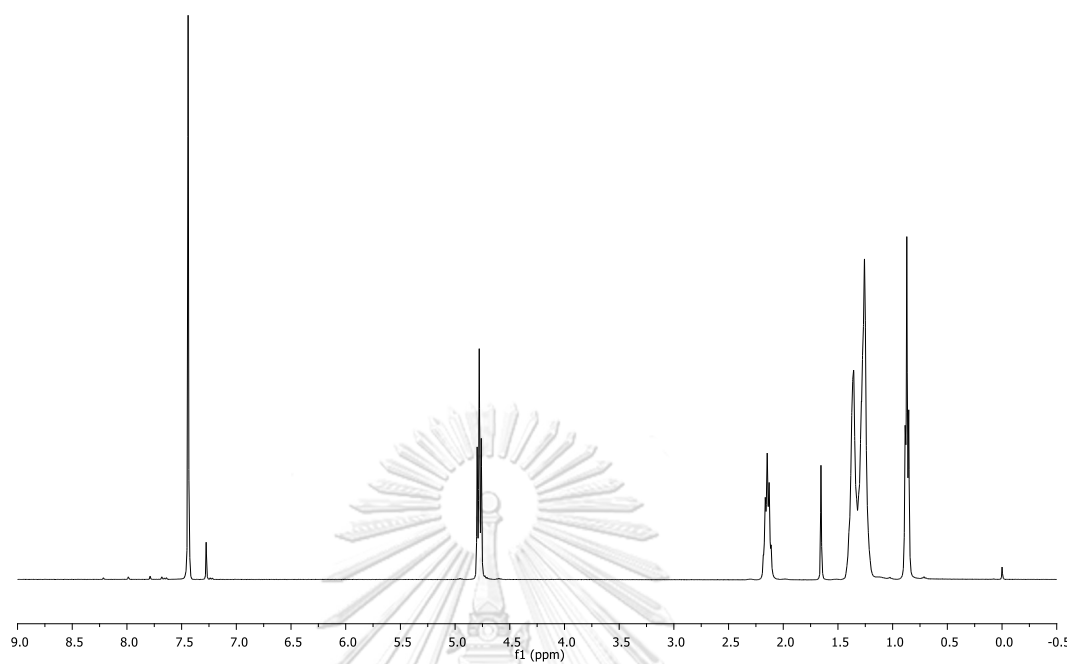


Figure A.23 ^1H NMR (CDCl_3) spectrum of DBOBTZ

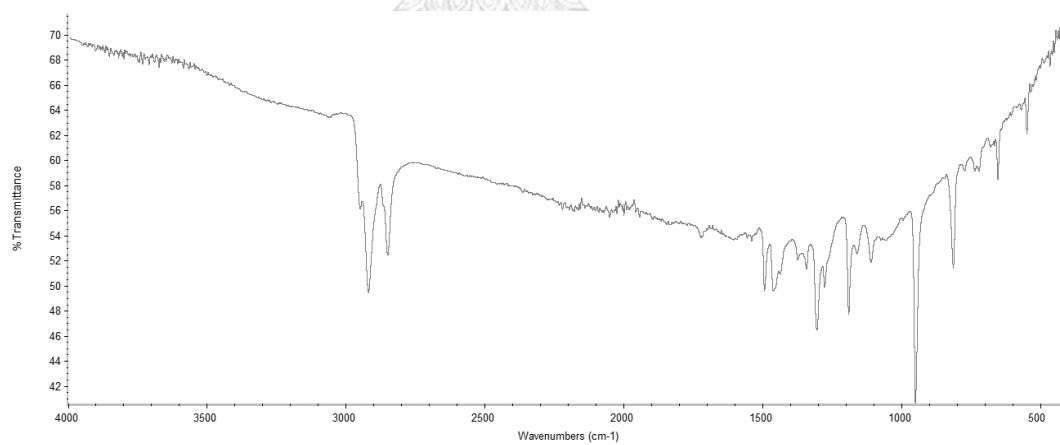


Figure A.24 IR spectrum of DBOBTZ

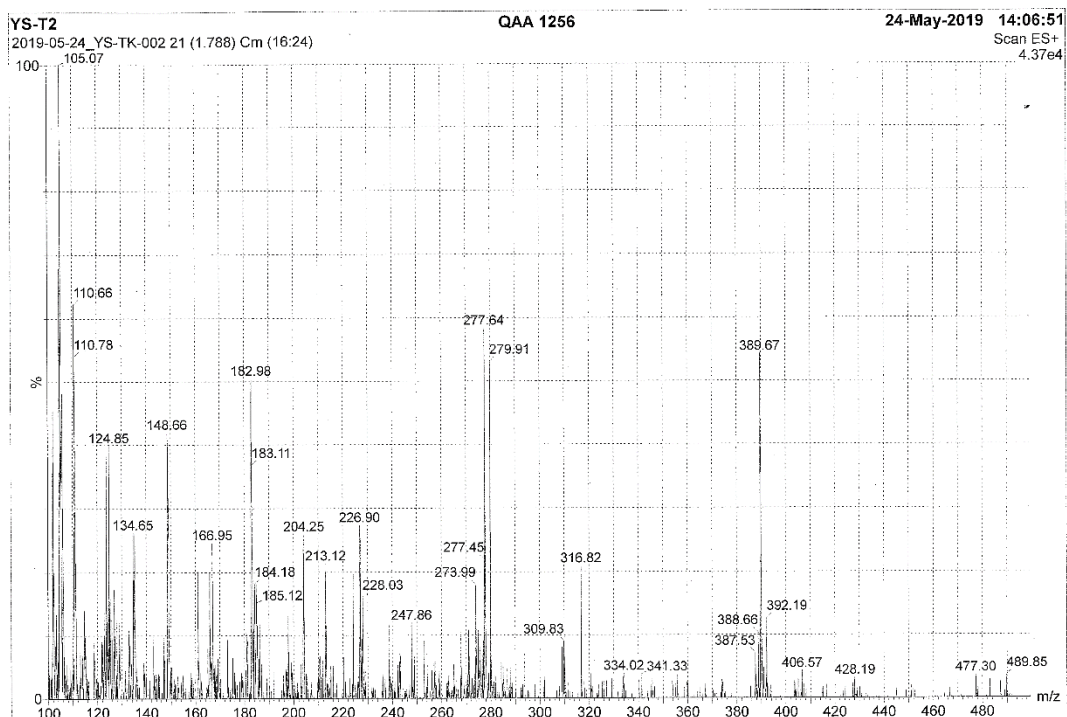


Figure A.25 Mass spectrum of DBOBTZ

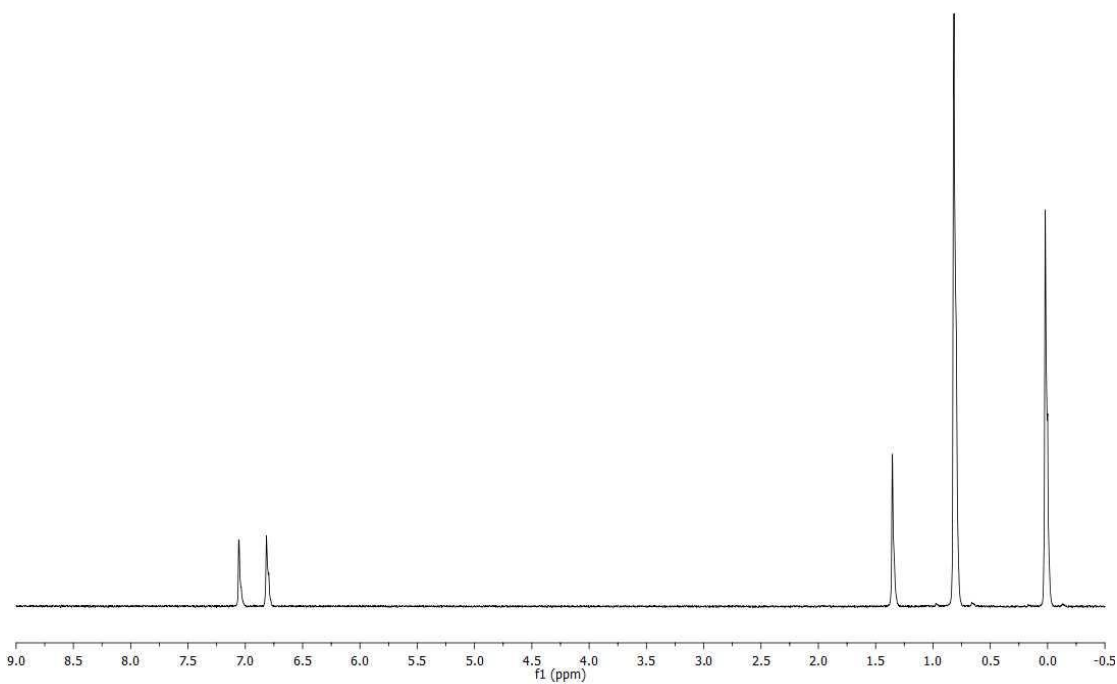


Figure A.26 ^1H NMR (CDCl_3) spectrum of compound 5

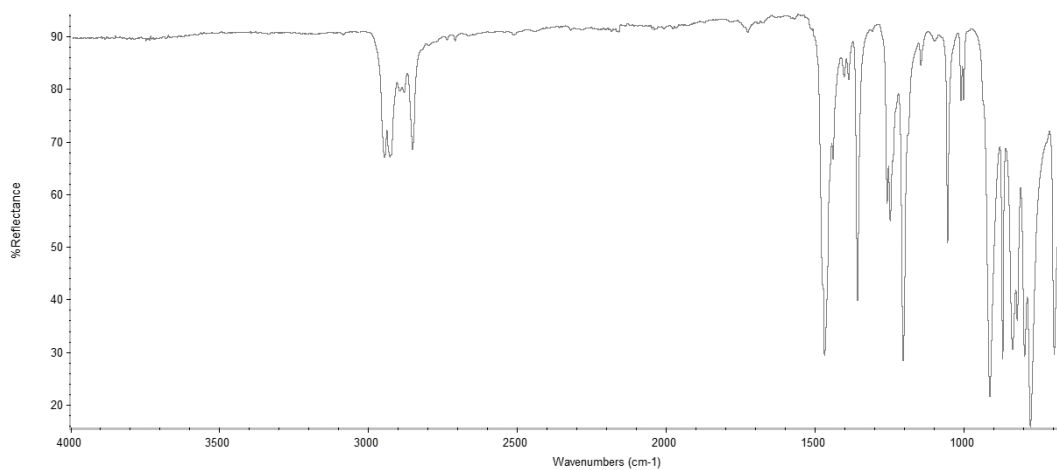


Figure A.27 IR spectrum of compound 5

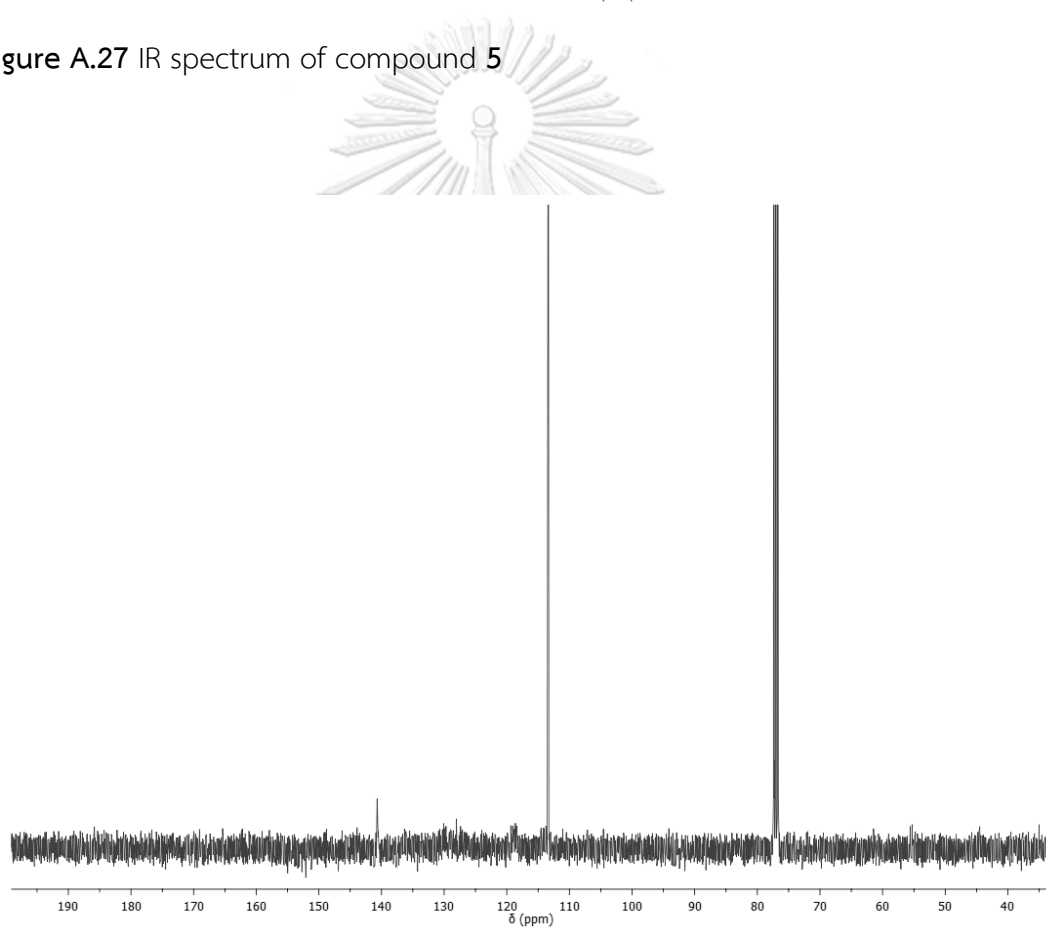


Figure A.28 ¹³C NMR (CDCl₃) spectrum of DBDNT

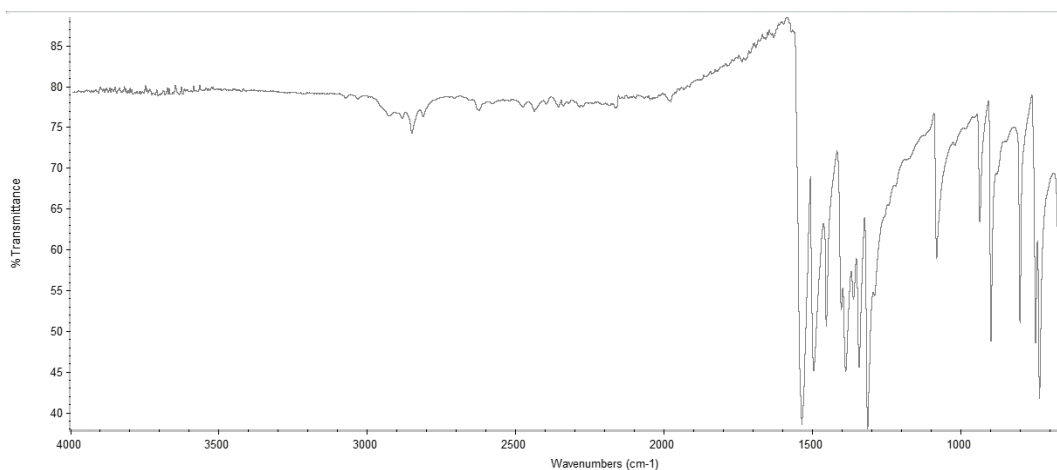


Figure A.29 IR spectrum of DBDNT

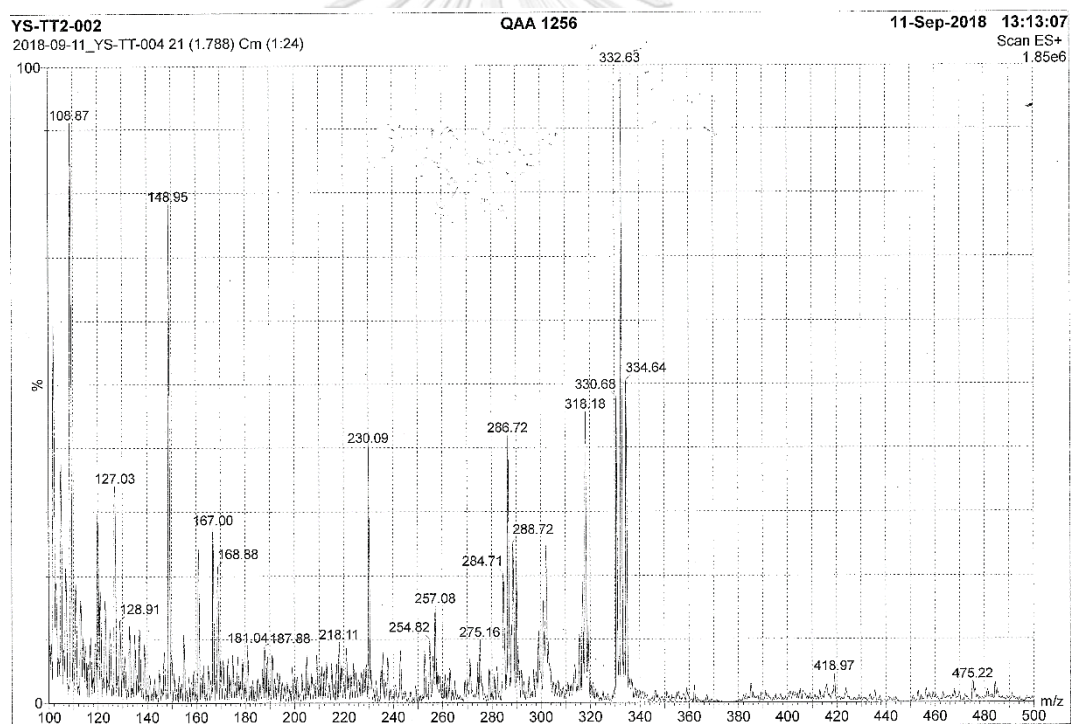


Figure A.30 Mass spectrum of DBDNT

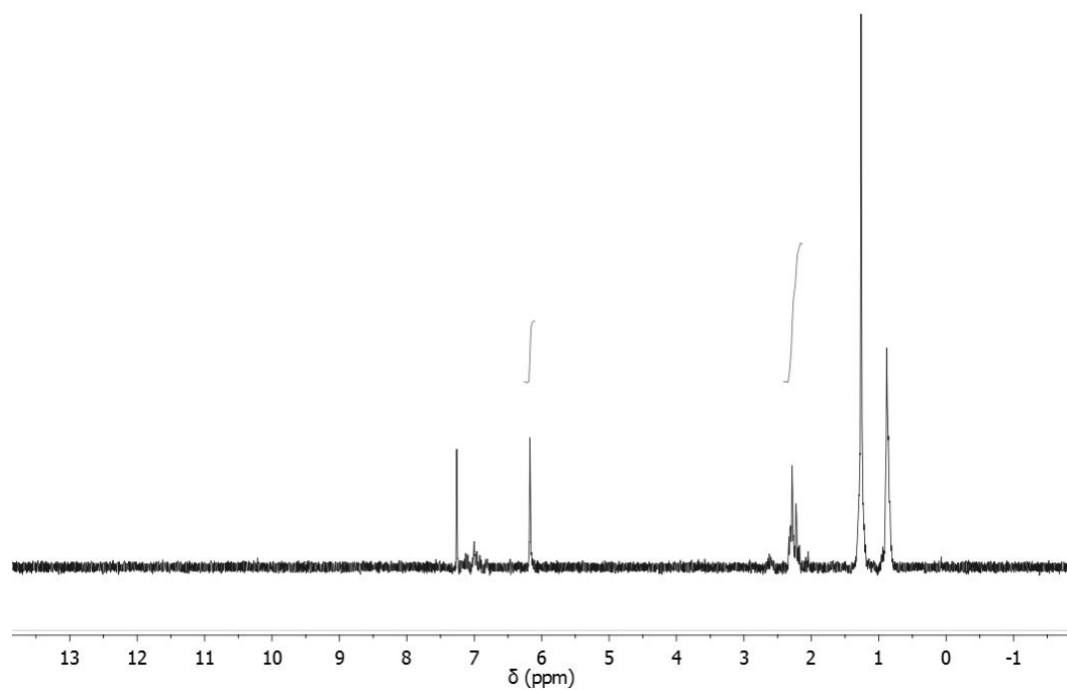


Figure A.31 ^1H NMR (CDCl_3) spectrum of 3,4-diaminothiophene

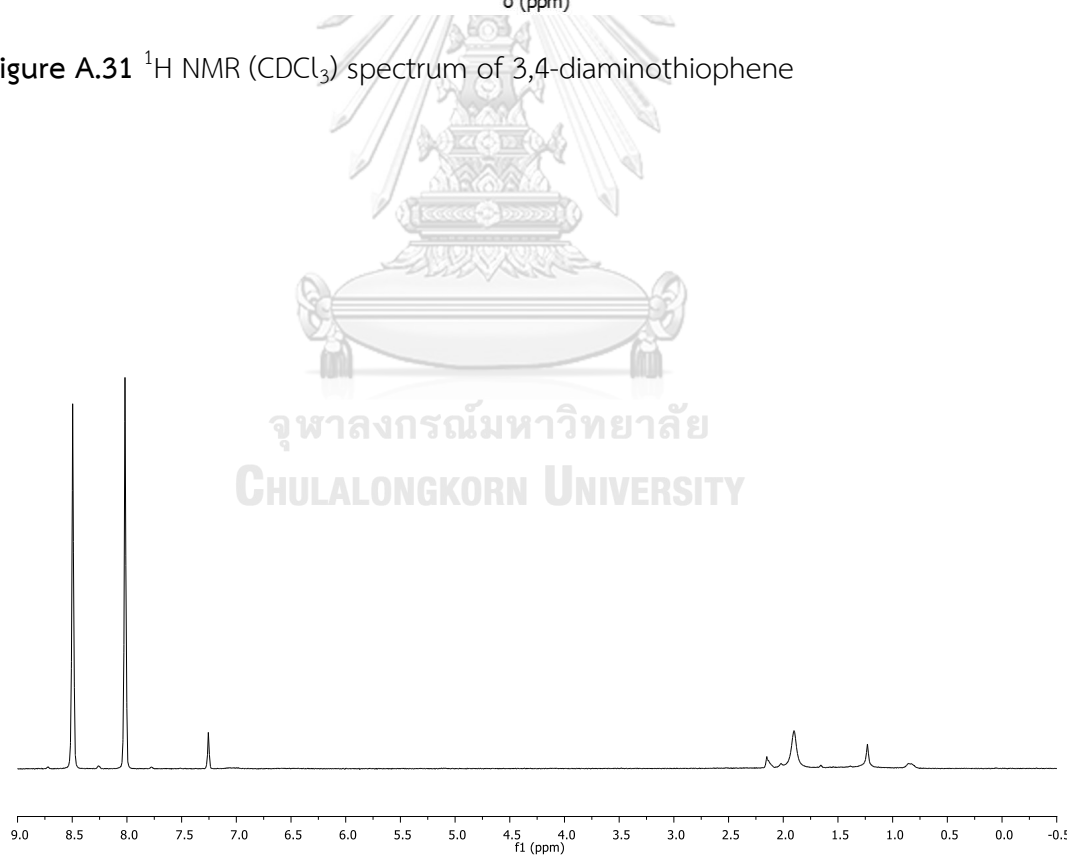


Figure A.32 ^1H NMR (CDCl_3) spectrum of TP

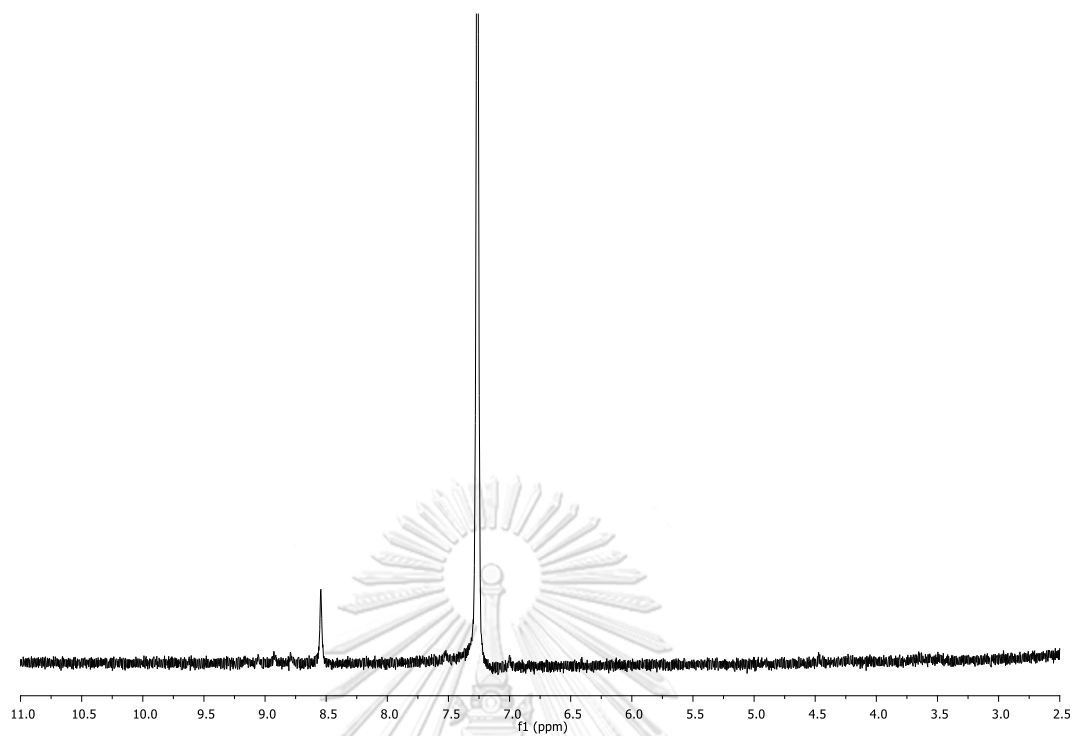
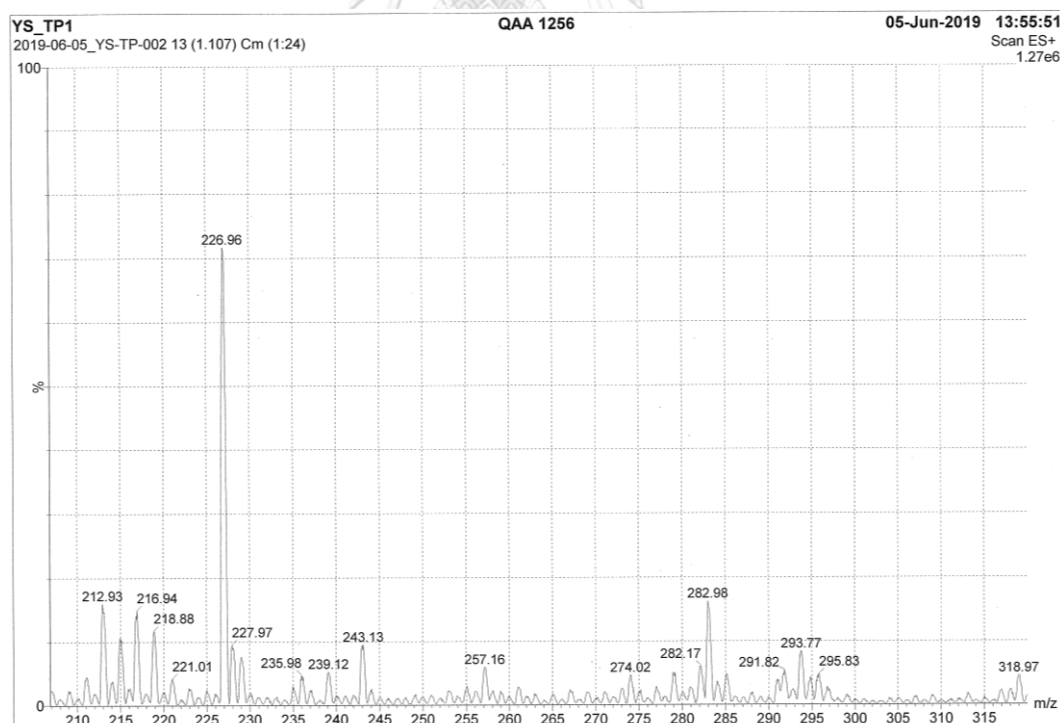
Figure A.33 ^1H NMR (CDCl_3) spectrum of DBTP

Figure A.34 Mass spectrum of DBTP

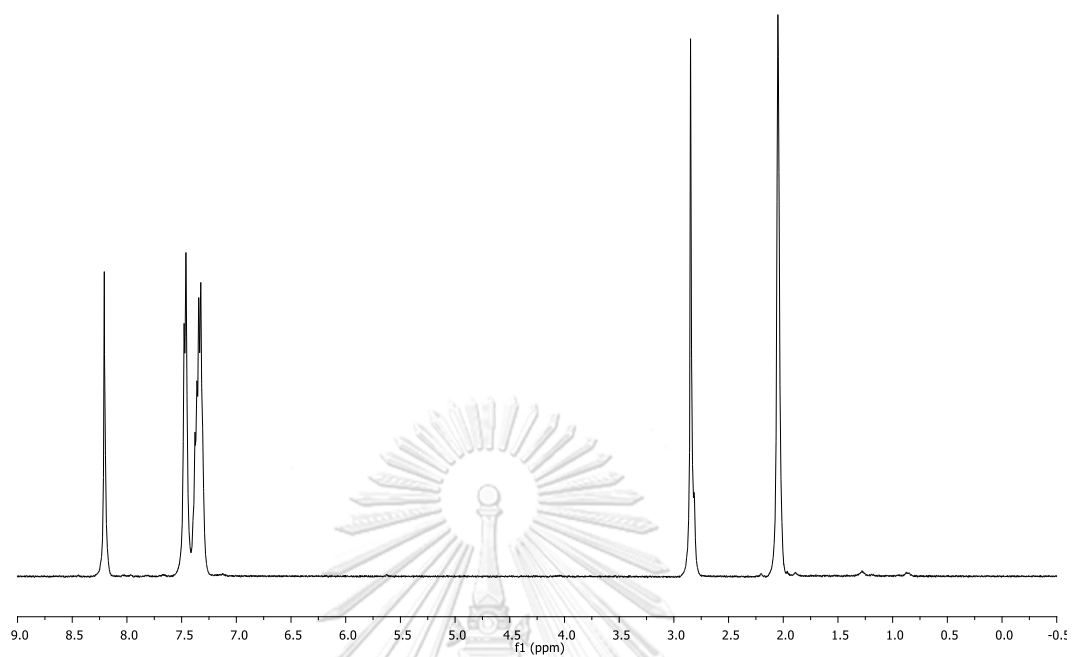


Figure A.35 ^1H NMR (acetone- d_6) spectrum of DPTP

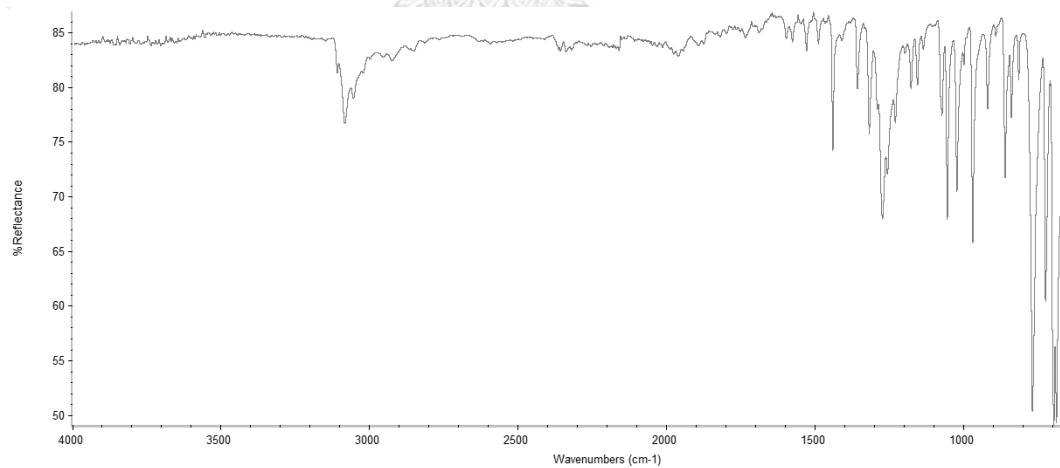


Figure A.36 IR spectrum of DPTP

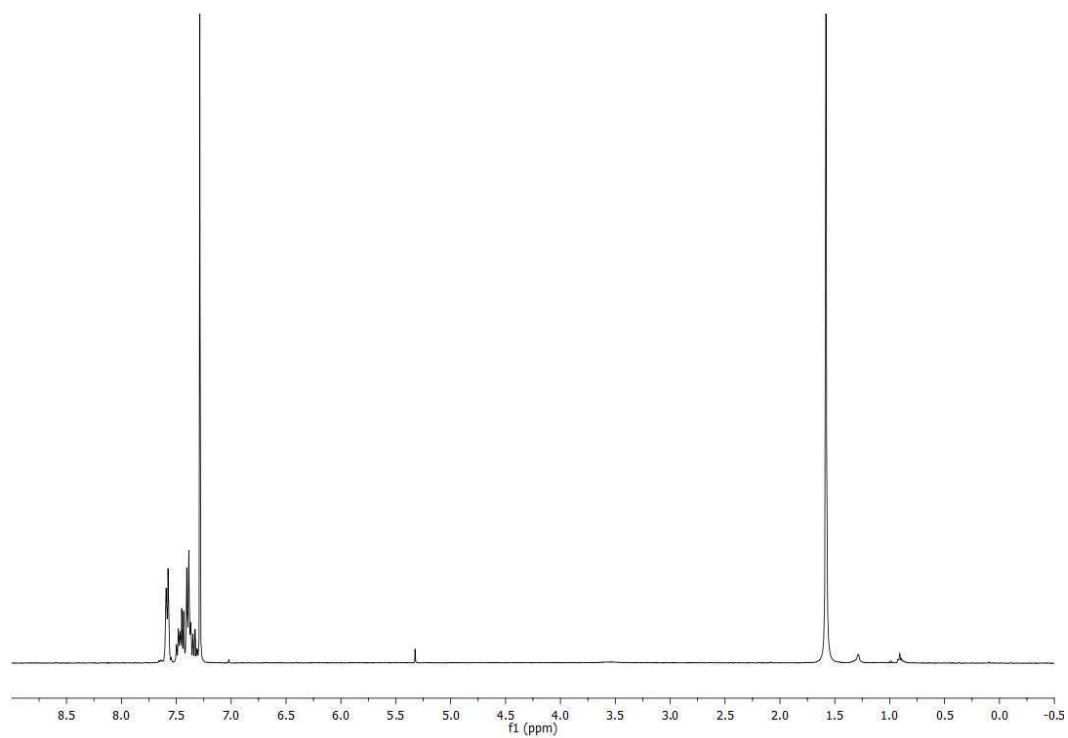


Figure A.37 ^1H NMR (CDCl_3) spectrum of DBDPTP

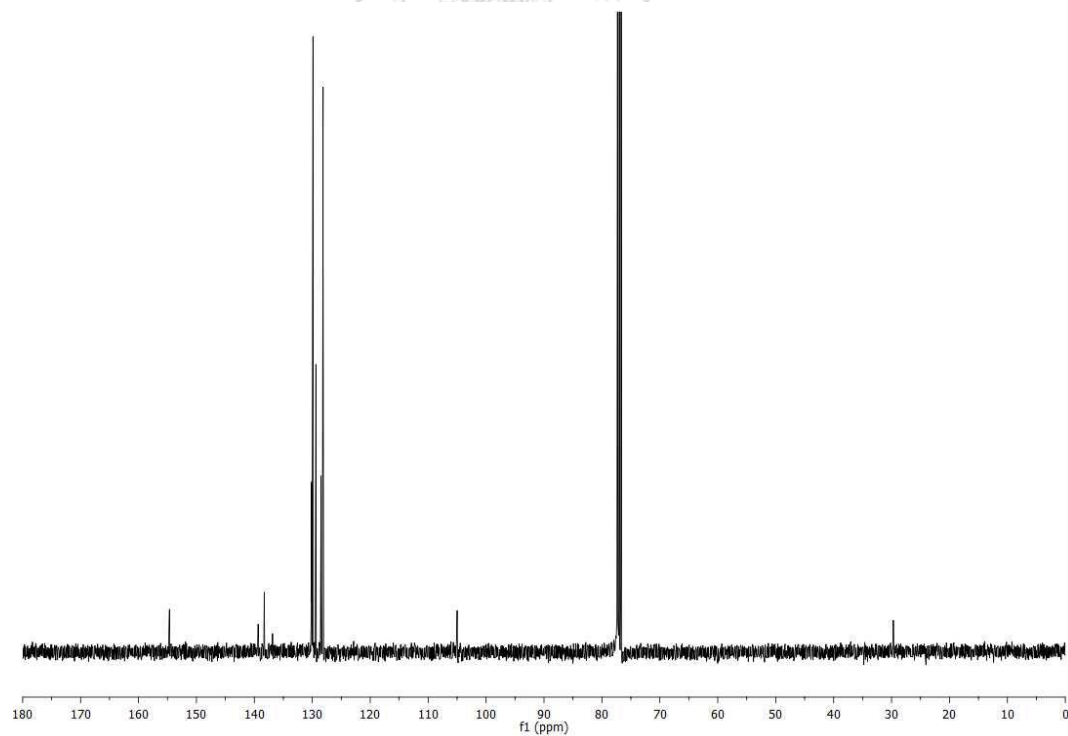


Figure A.38 ^{13}C NMR (CDCl_3) spectrum of DBDPTP

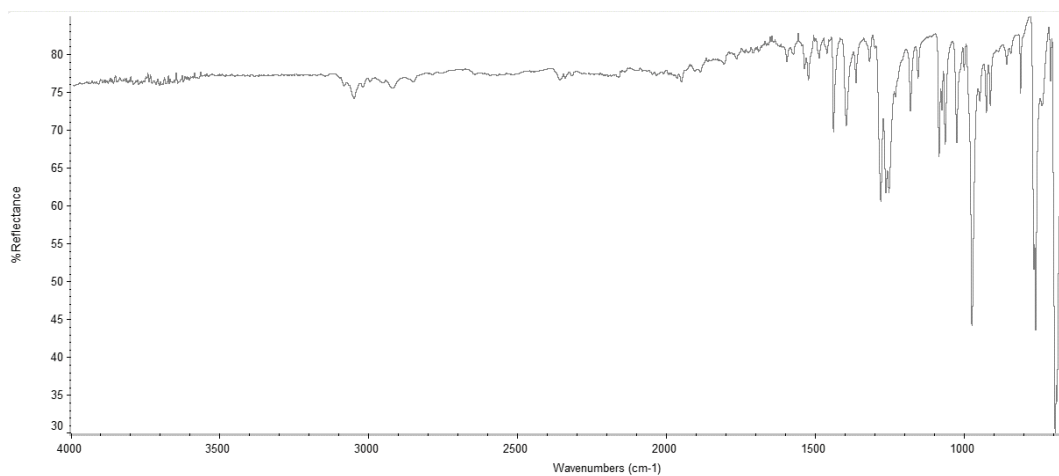


Figure A.39 IR spectrum of DBDPTP

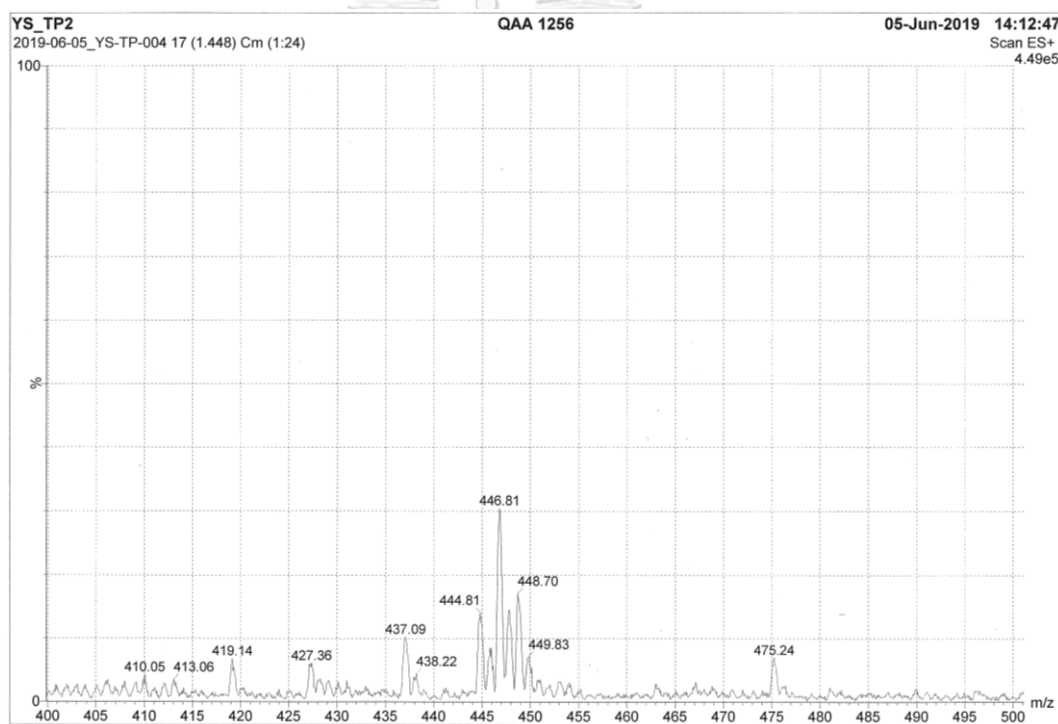


Figure A.40 Mass spectrum of DBDPTP

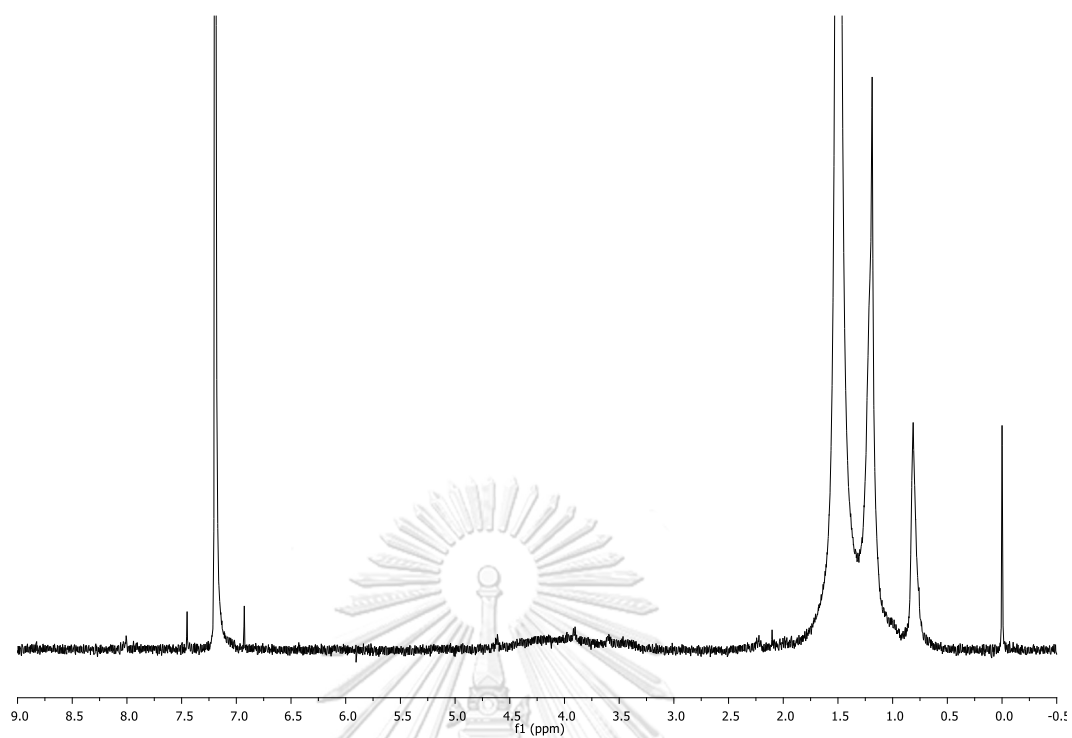


Figure A.41 ^1H NMR (CDCl_3) spectrum of polymer P1



Figure A.42 IR spectrum of polymer P1

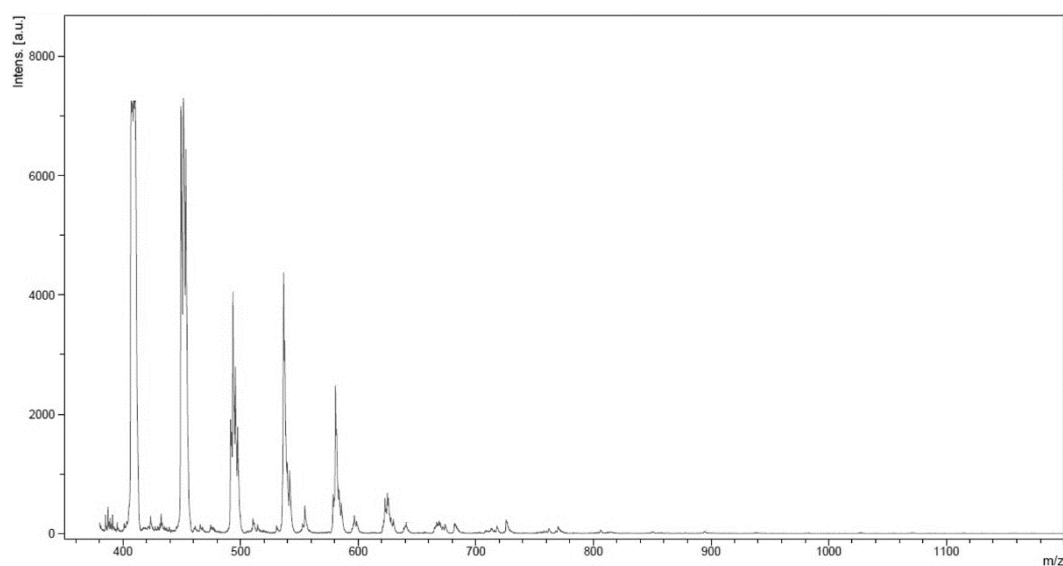


Figure A.43 Mass spectrum of polymer P1

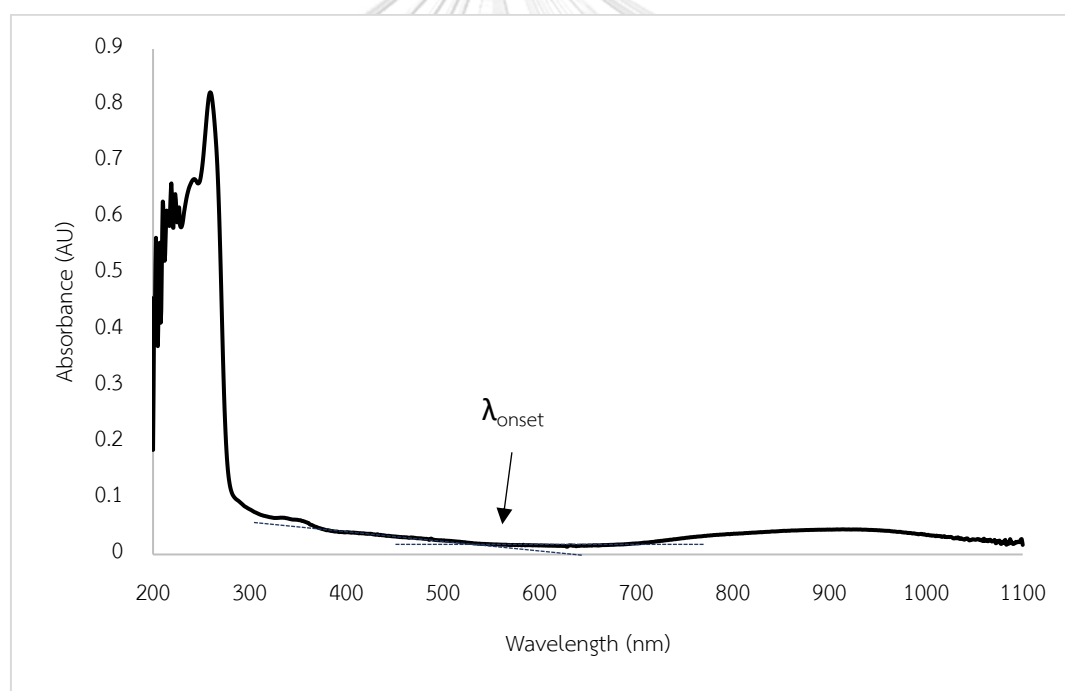


Figure A.44 UV-visible absorption spectrum of polymer P1

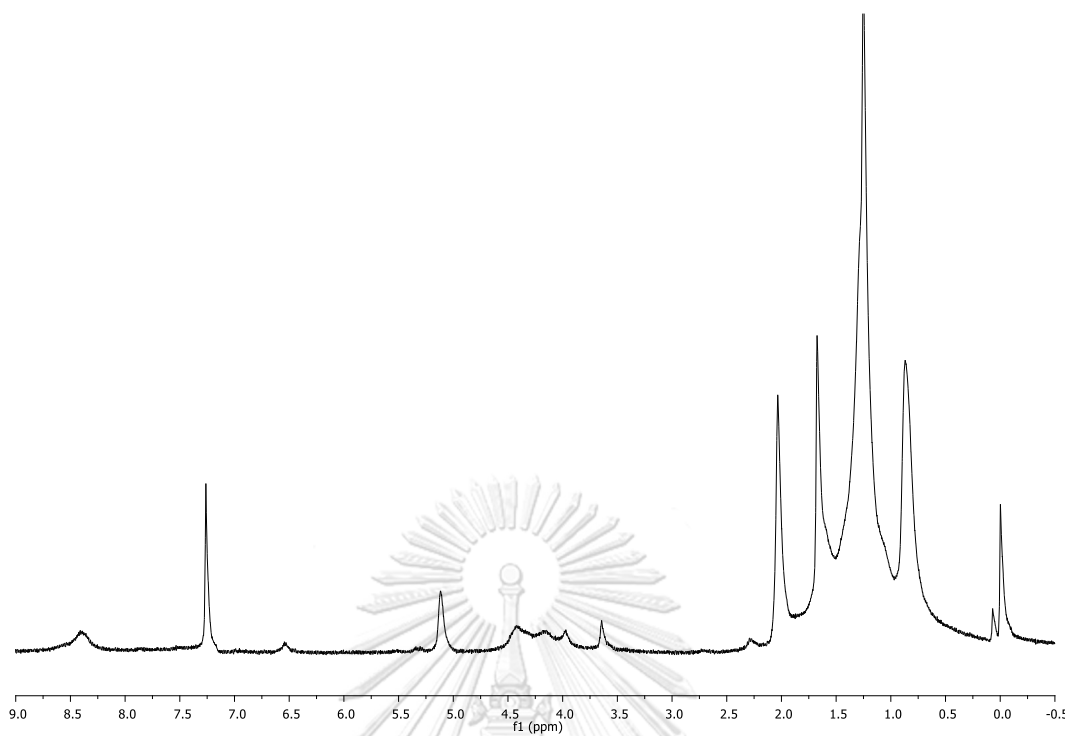


Figure A.45 ^1H NMR (CDCl_3) spectrum of polymer P2

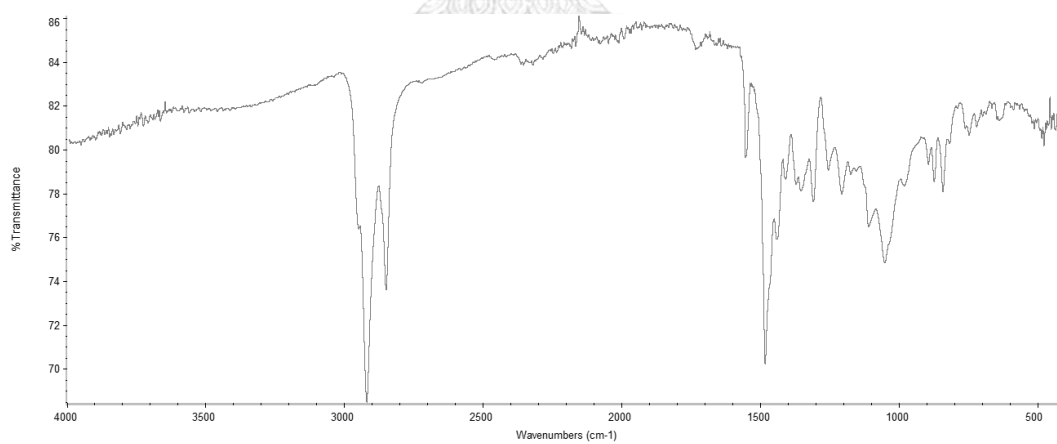


Figure A.46 IR spectrum of polymer P2

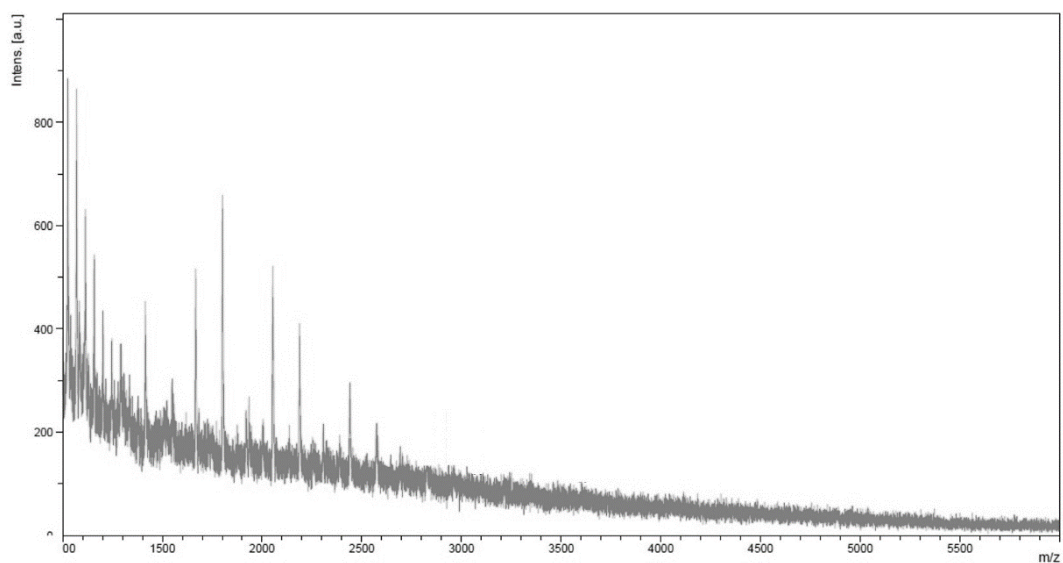


Figure A.47 Mass spectrum of polymer P2

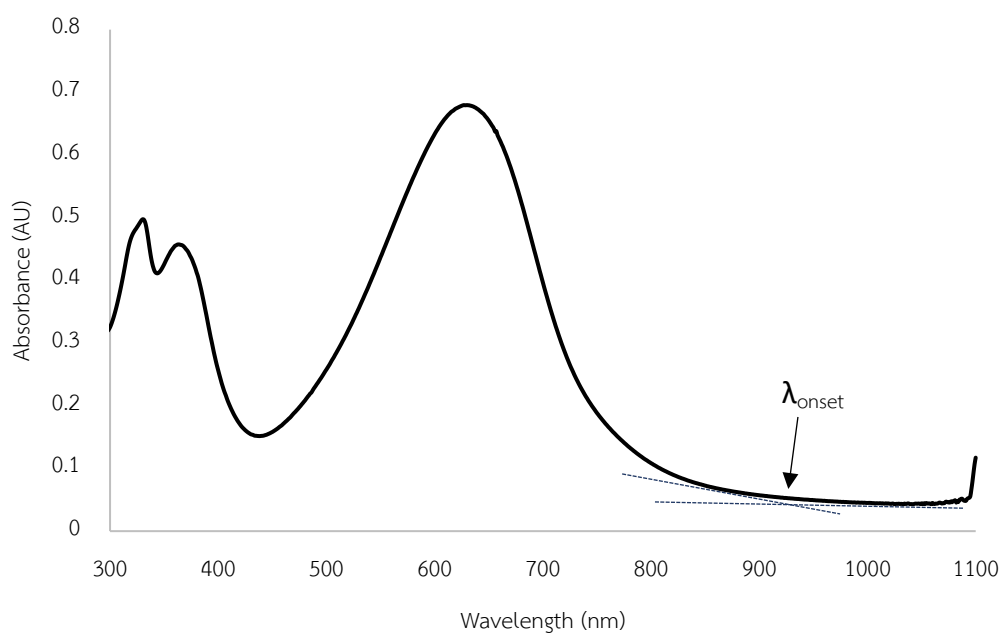


Figure A.48 UV-visible absorption spectrum of polymer P2

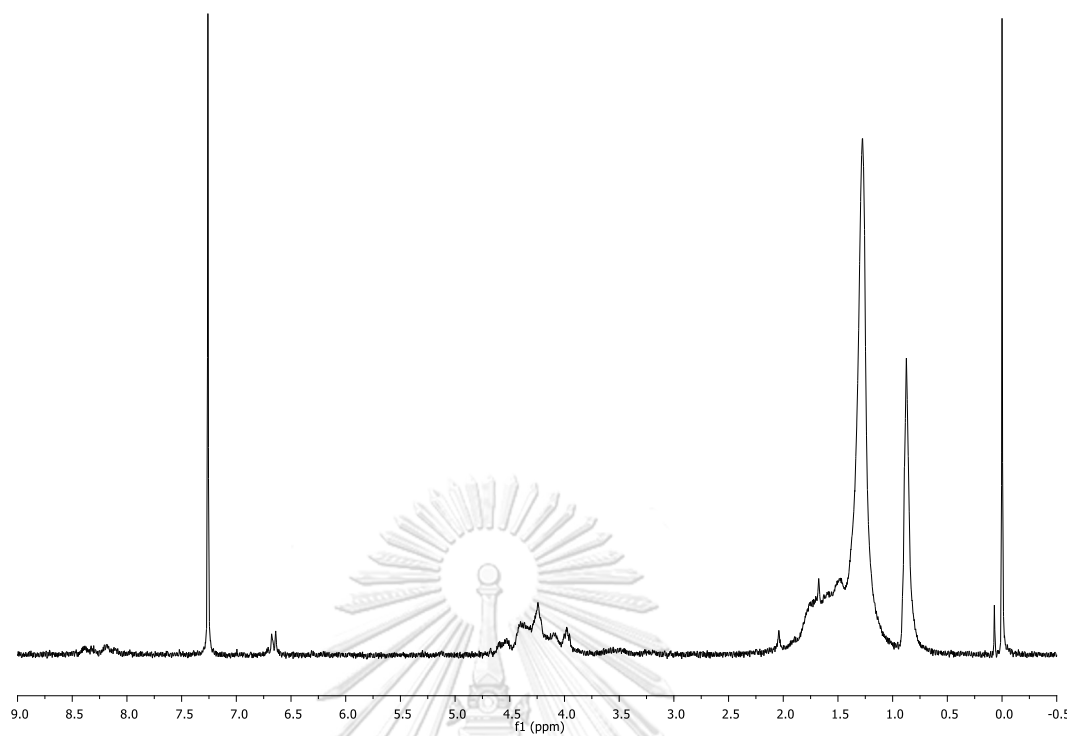


Figure A.49 ^1H NMR (CDCl_3) spectrum of polymer P3

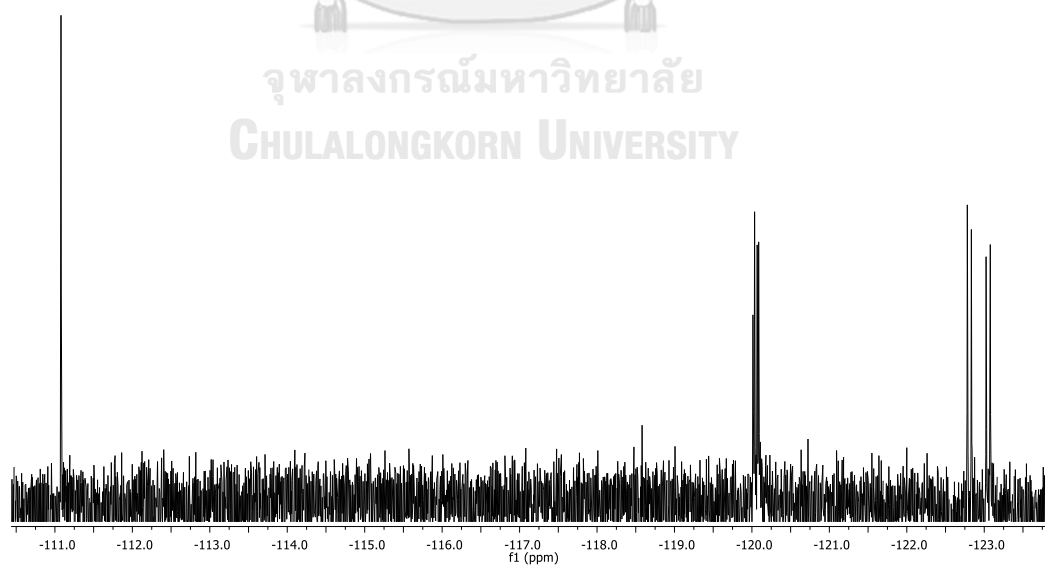


Figure A.50 ^{19}F NMR (CDCl_3) spectrum of polymer P3 (Entry 1)

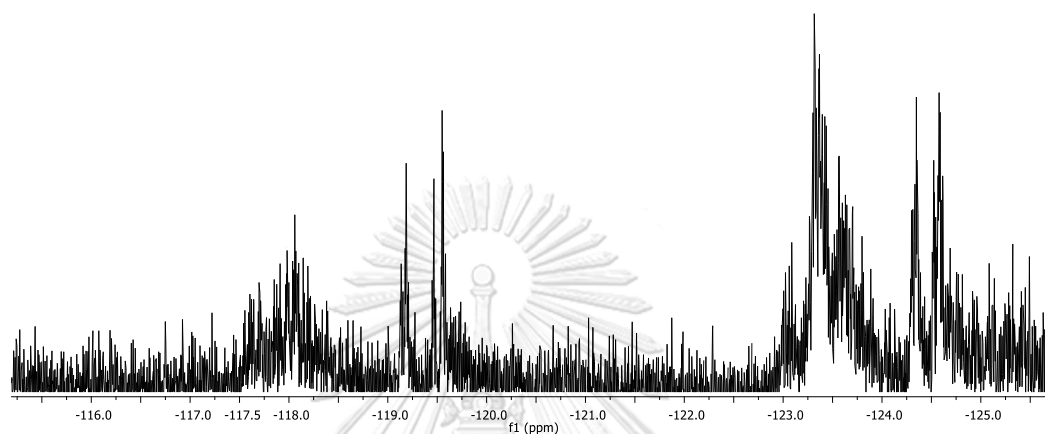


Figure A.51 ^{19}F NMR (CDCl_3) spectrum of polymer P3 (Entry 2)

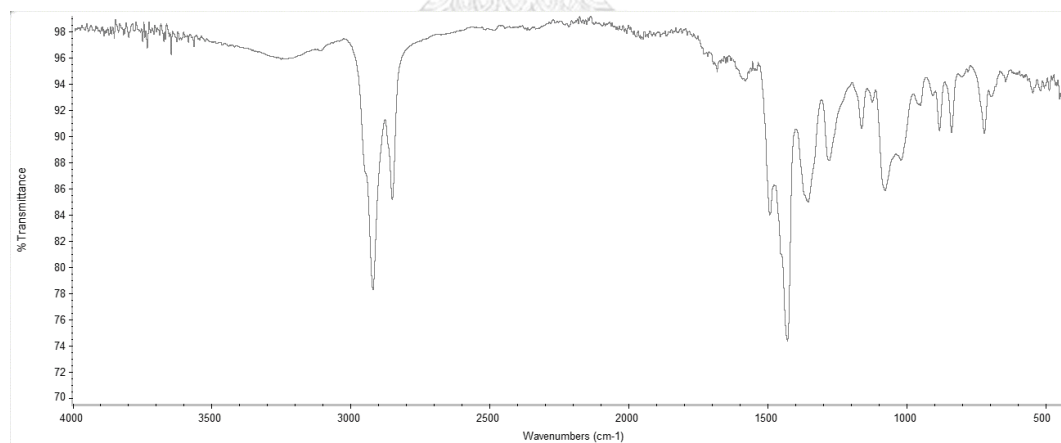


Figure A.52 IR spectrum of polymer P3

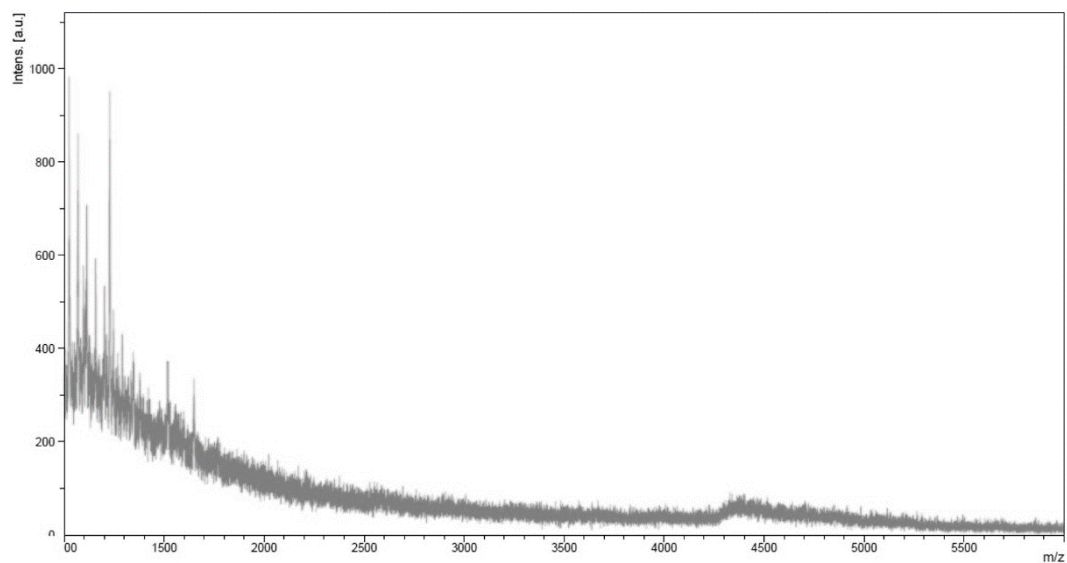


Figure A.53 Mass spectrum of polymer P3

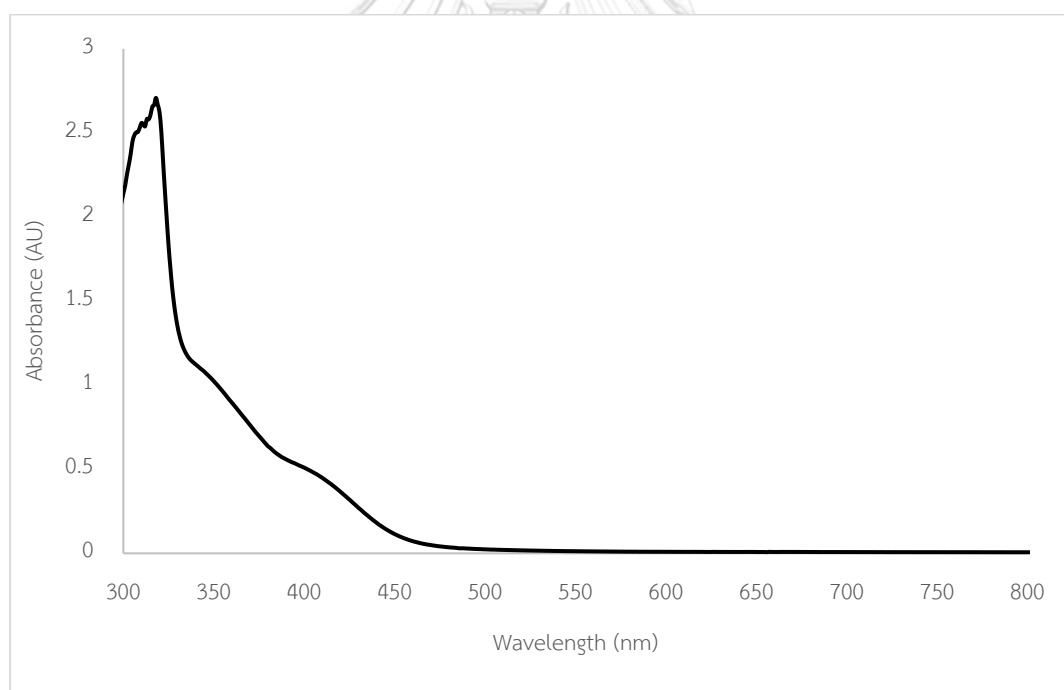


Figure A.54 UV-visible absorption spectrum of polymer P3 (Entry 1)

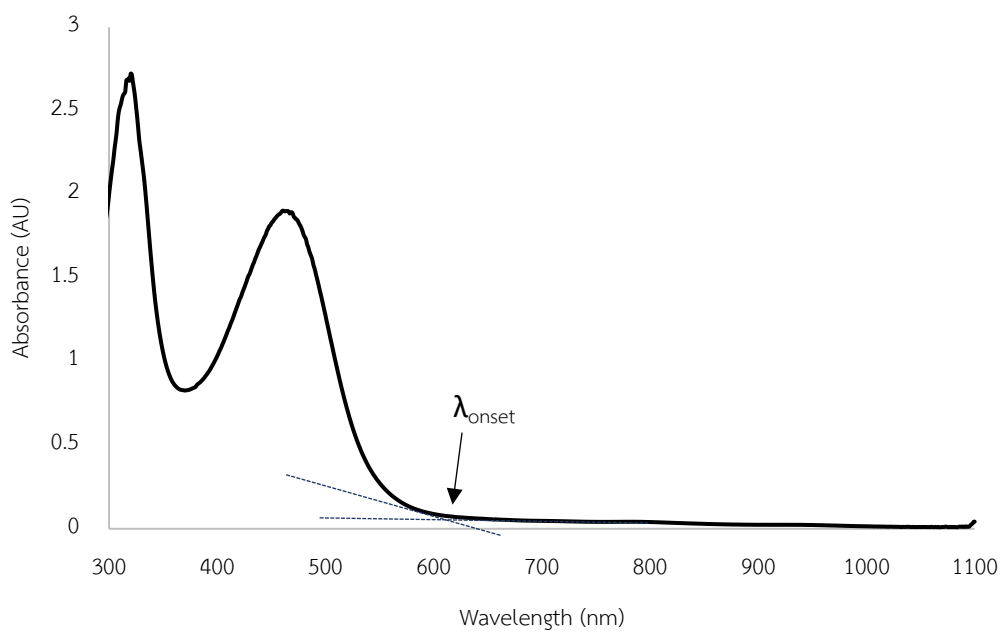


Figure A.55 UV-visible absorption spectrum of polymer P3 (Entry 2)

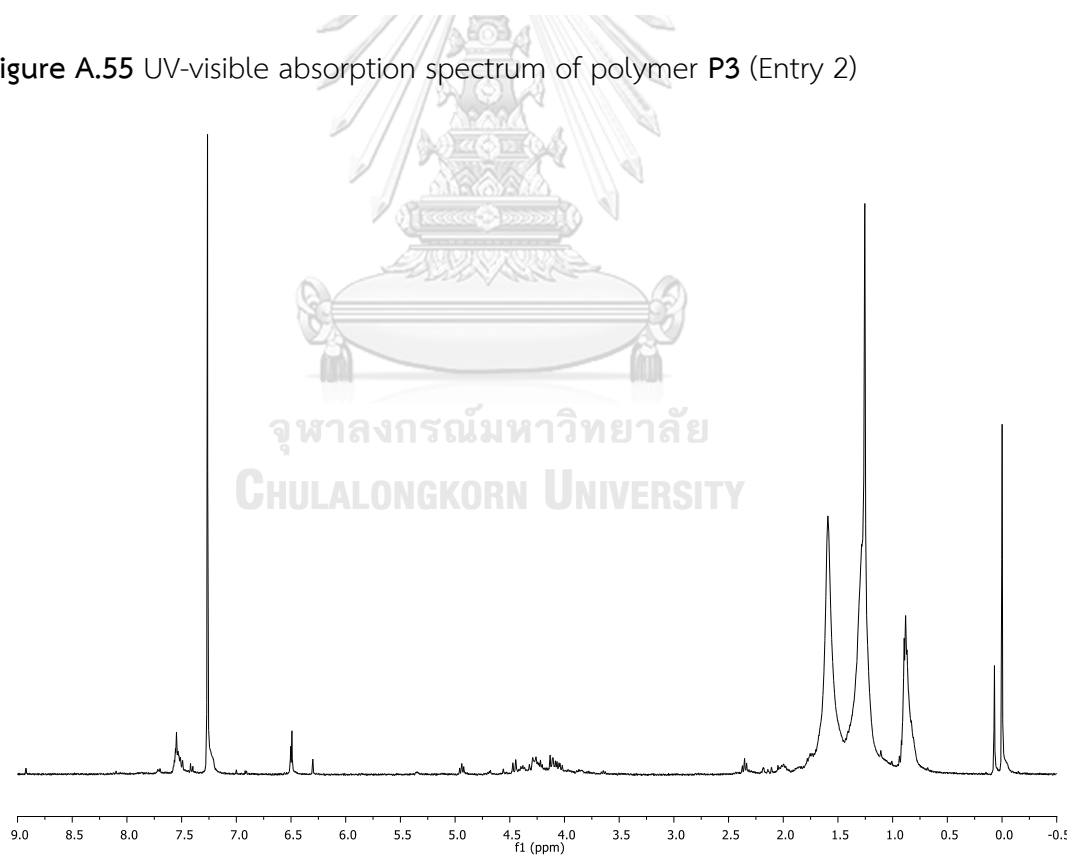


Figure A.56 ^1H NMR (CDCl_3) spectrum of polymer P4

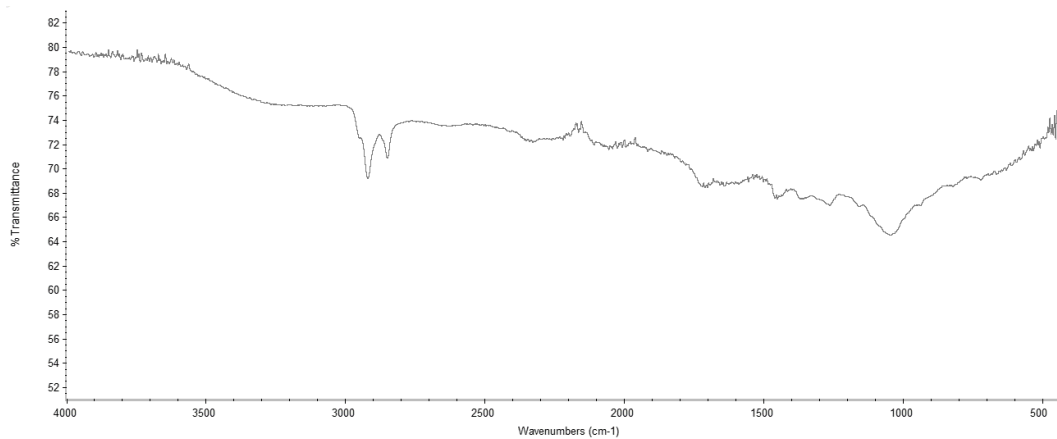


Figure A.57 IR spectrum of polymer P4

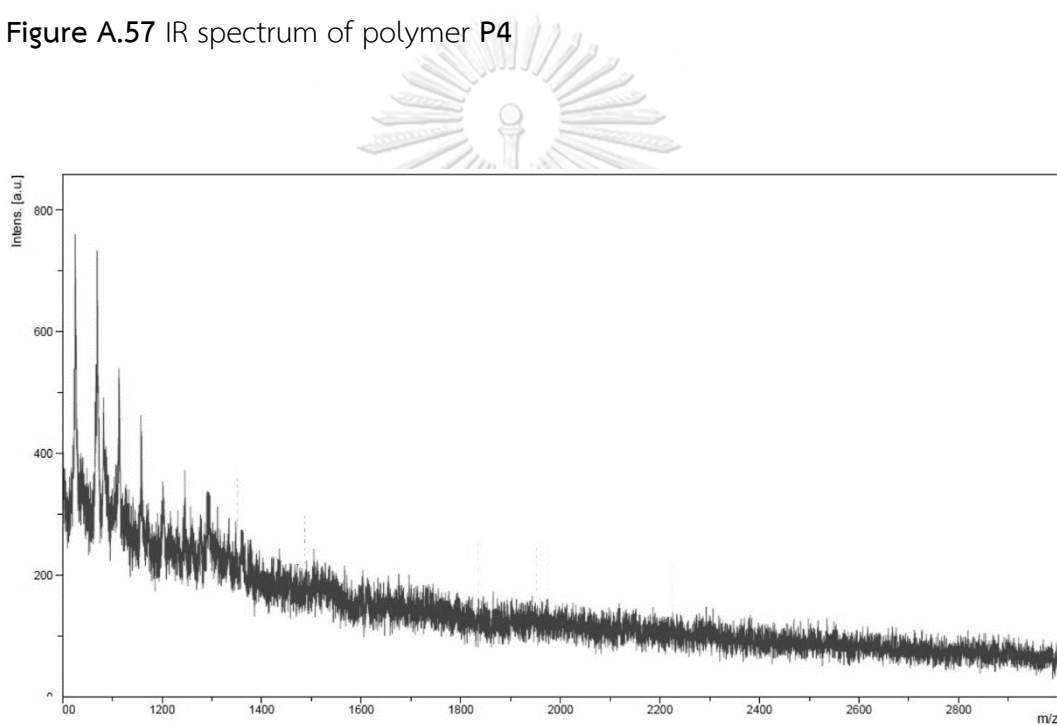


Figure A.58 Mass spectrum of polymer P4

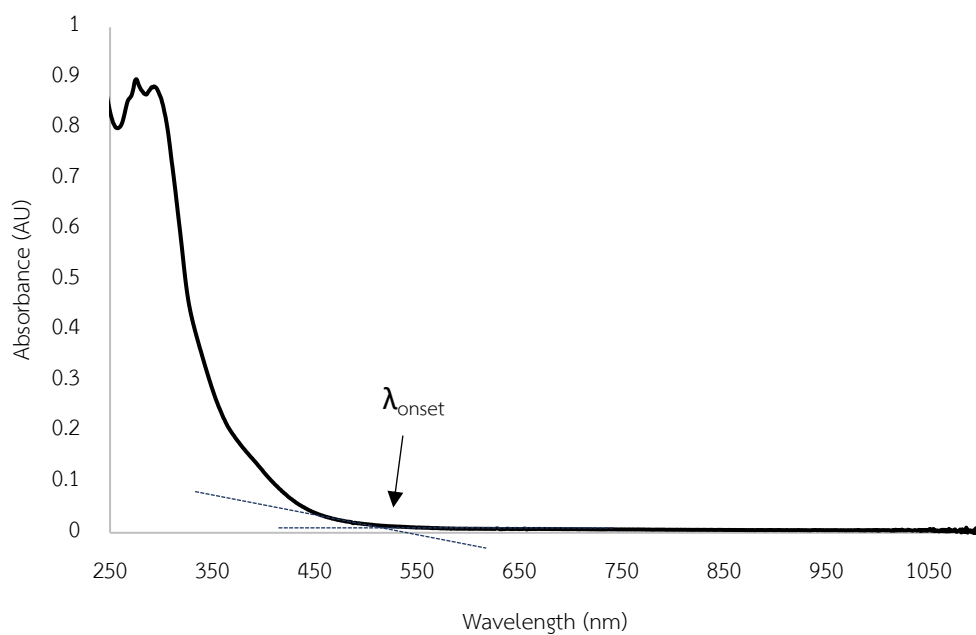


Figure A.59 UV-visible absorption spectrum of polymer P4

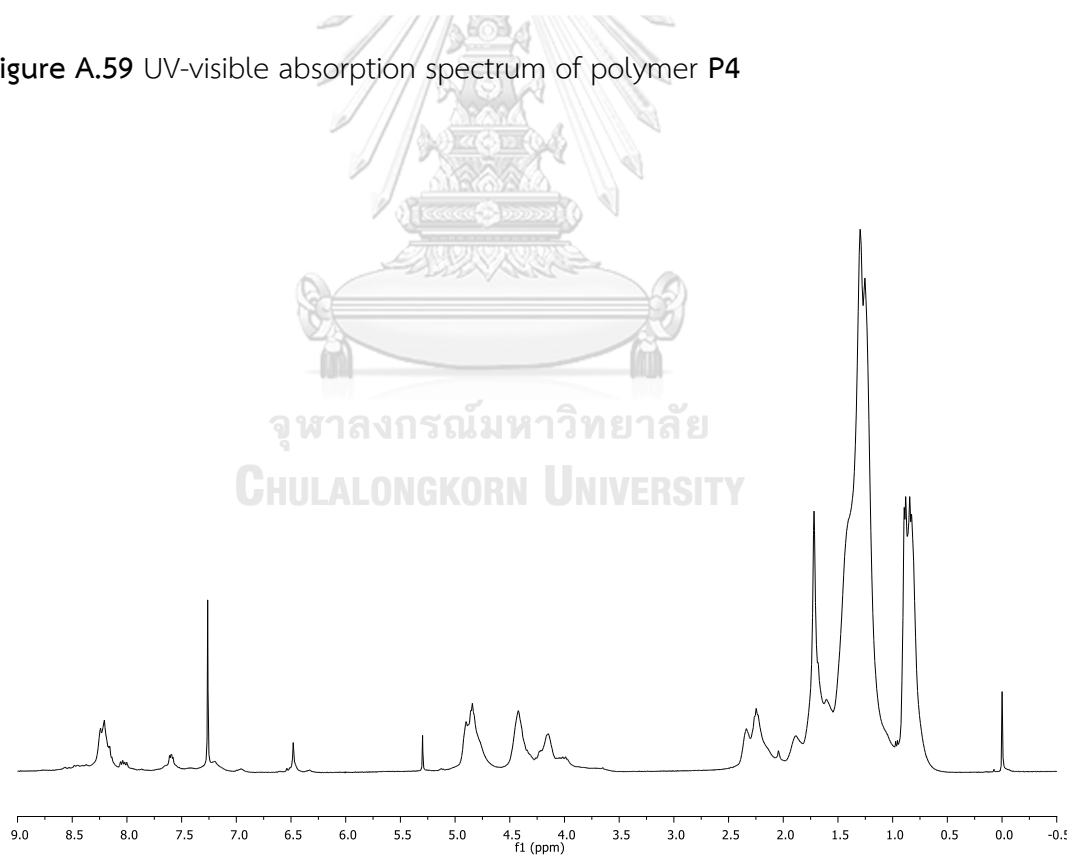


Figure A.60 ^1H NMR (CDCl_3) spectrum of polymer P5

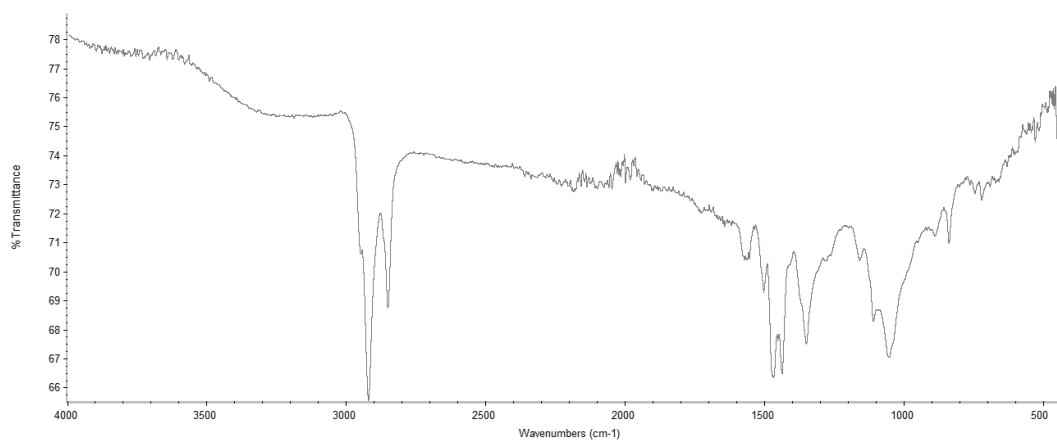


Figure A.61 IR spectrum of polymer P5

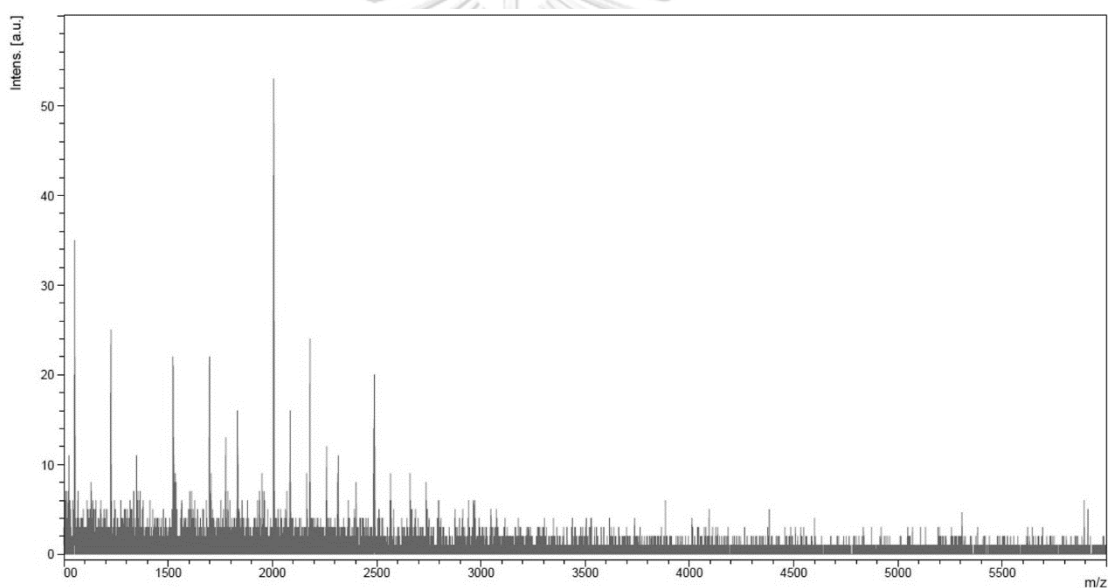


Figure A.62 Mass spectrum of polymer P5

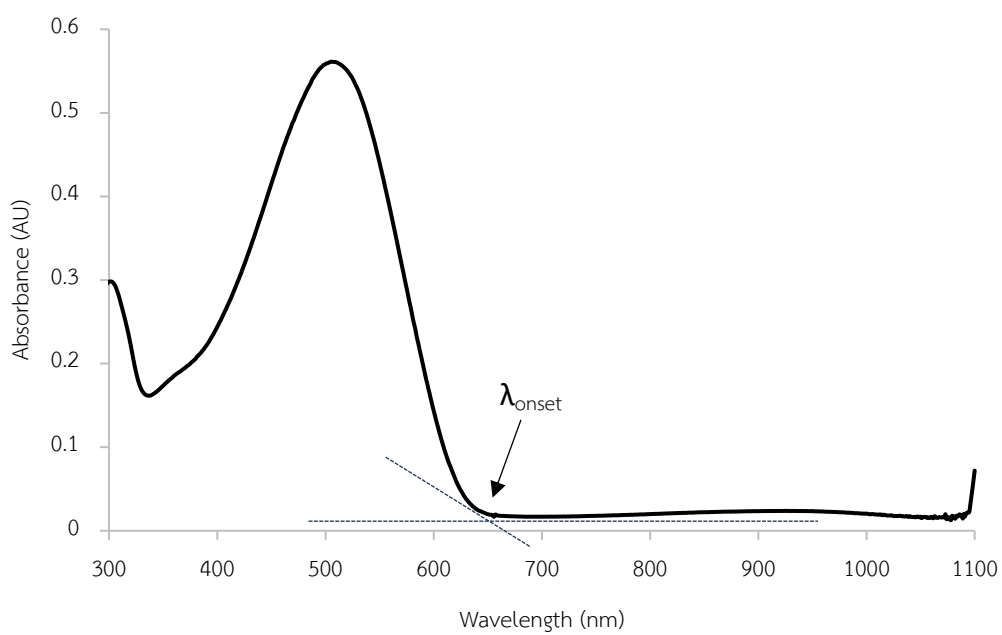


Figure A.63 UV-visible absorption spectrum of polymer P5

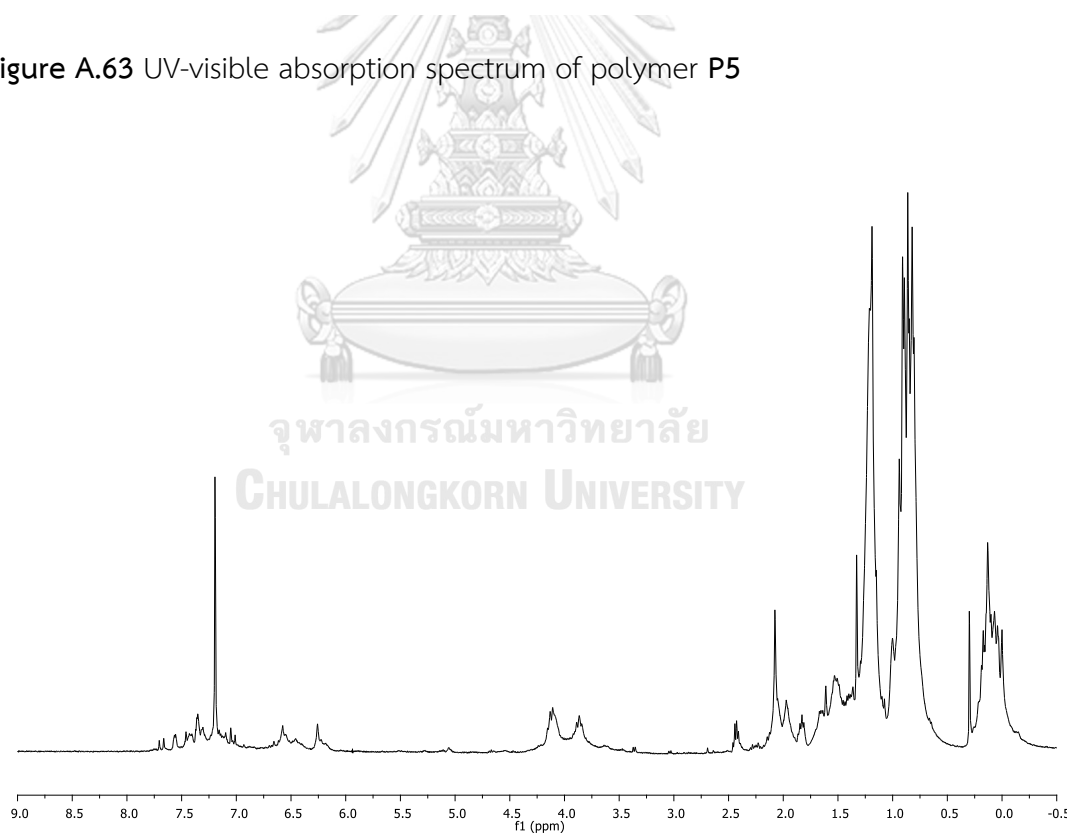


Figure A.64 ^1H NMR (CDCl_3) spectrum of polymer P6

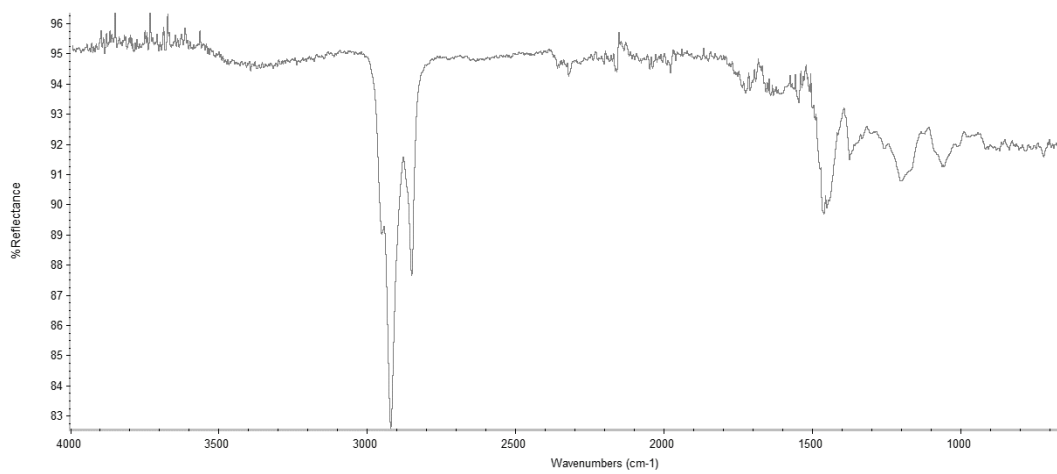


Figure A.65 IR spectrum of polymer P6

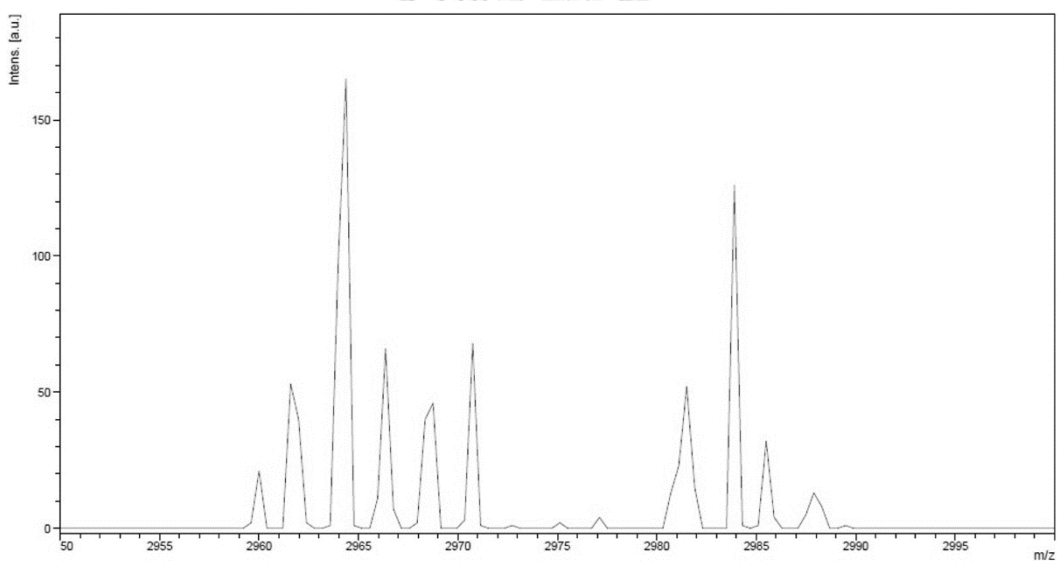


Figure A.66 Mass spectrum of polymer P6

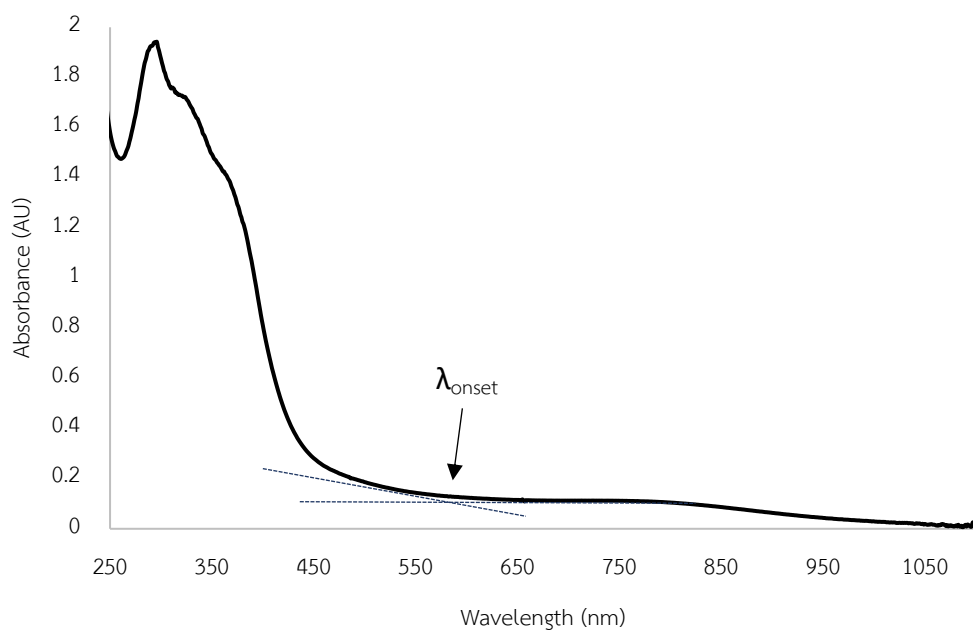


Figure A.67 UV-visible absorption spectrum of polymer P6

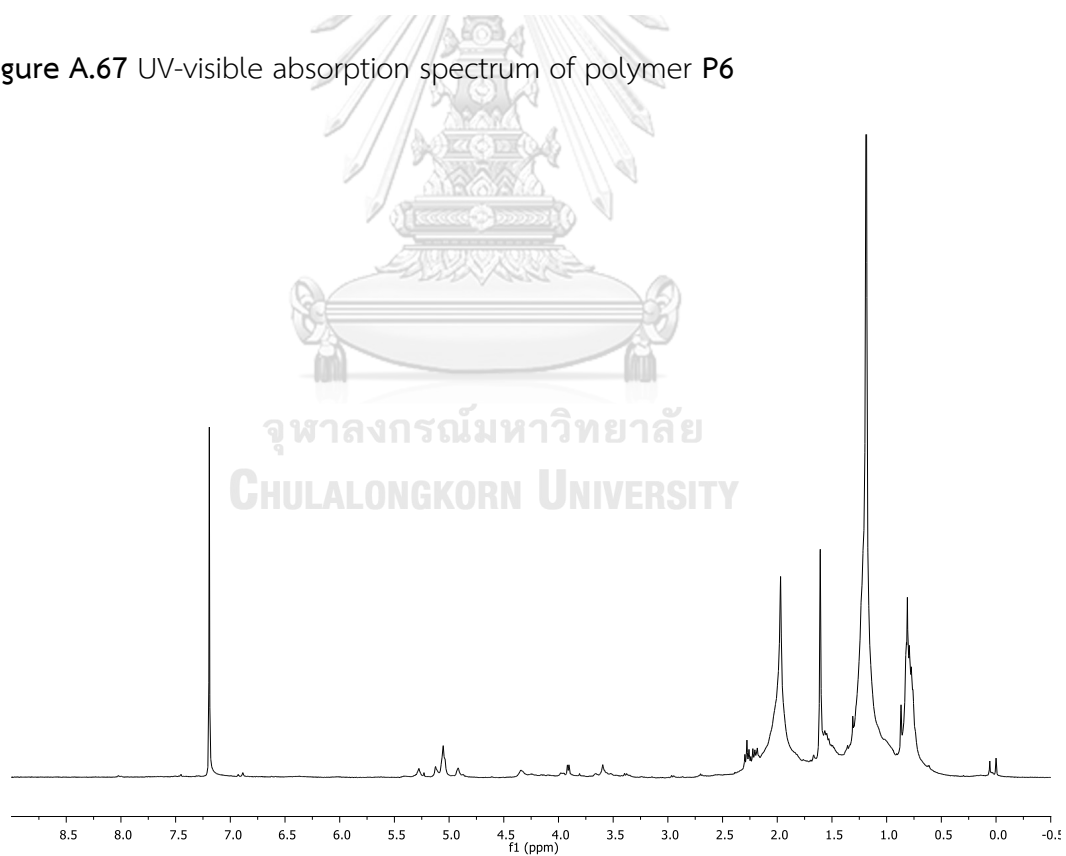


Figure A.68 ^1H NMR (CDCl_3) spectrum of polymer P7

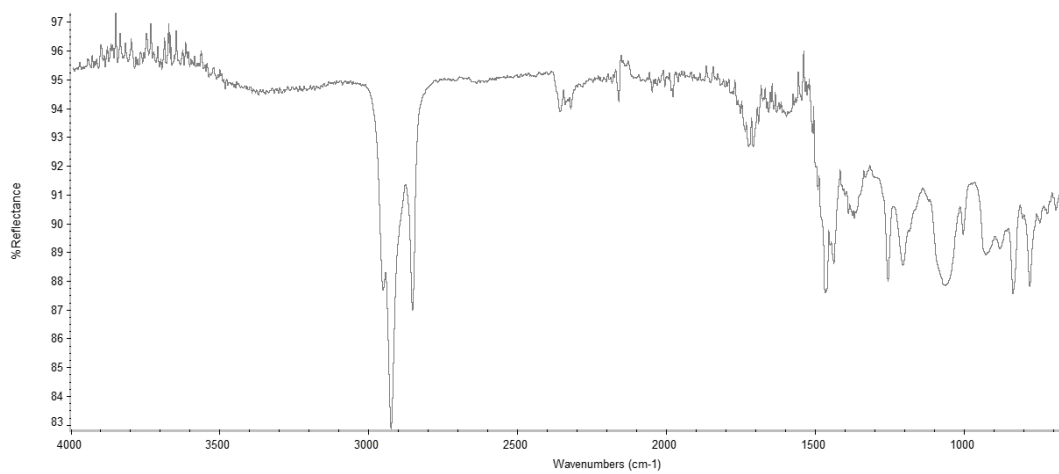


Figure A.69 IR spectrum of polymer P7

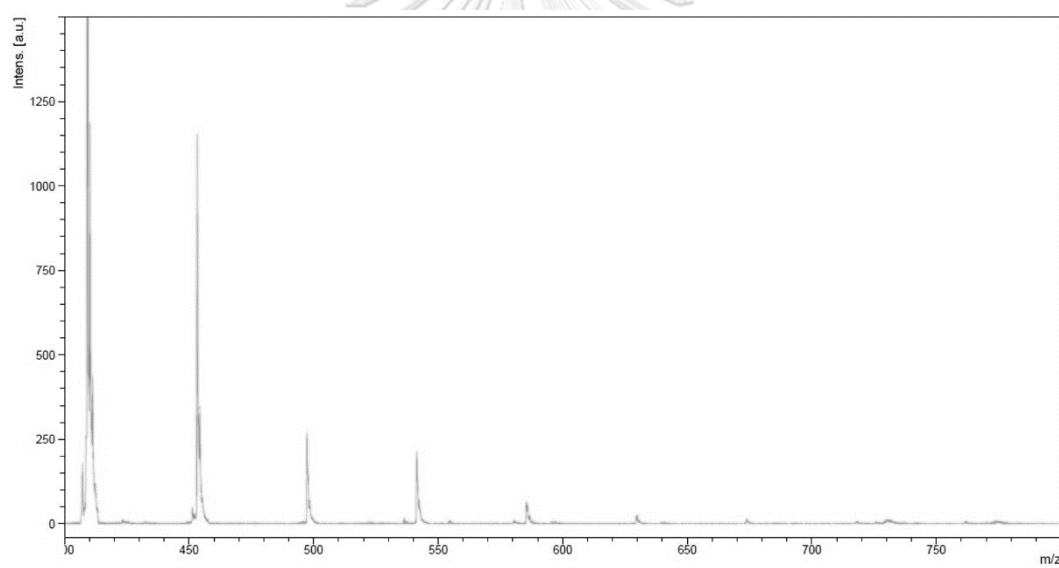


Figure A.70 Mass spectrum of polymer P7

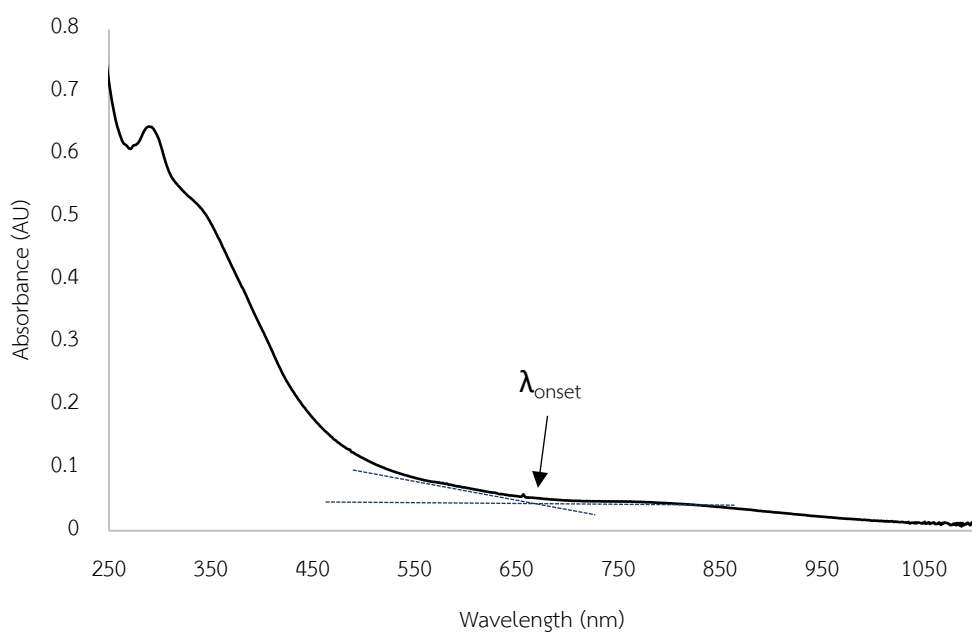


Figure A.71 UV-visible absorption spectrum of polymer P7

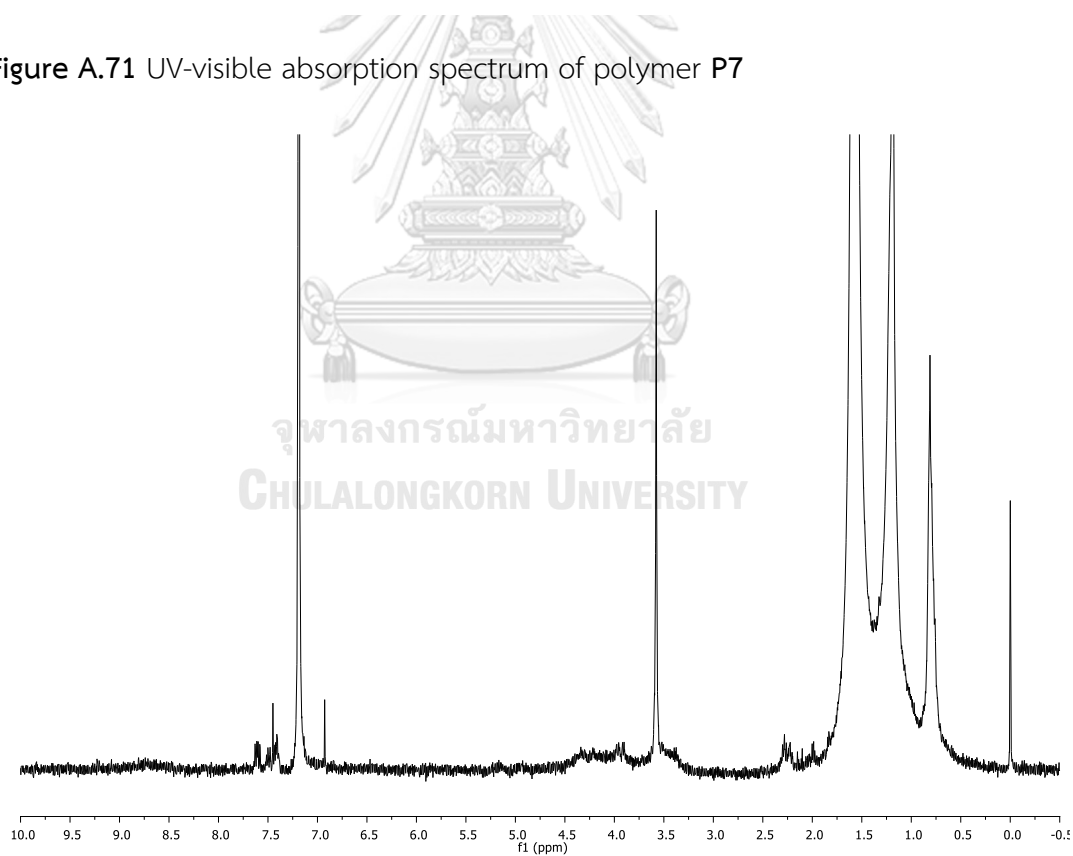


Figure A.72 ^1H NMR (CDCl_3) spectrum of polymer P9

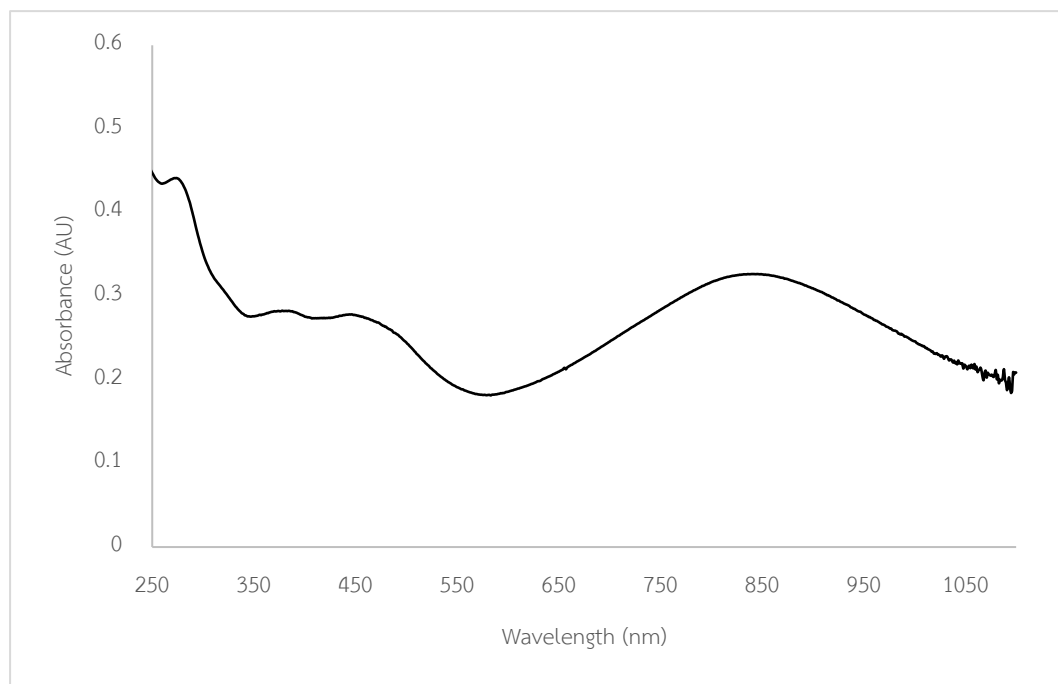


Figure A.73 UV-visible absorption spectrum of polymer P9

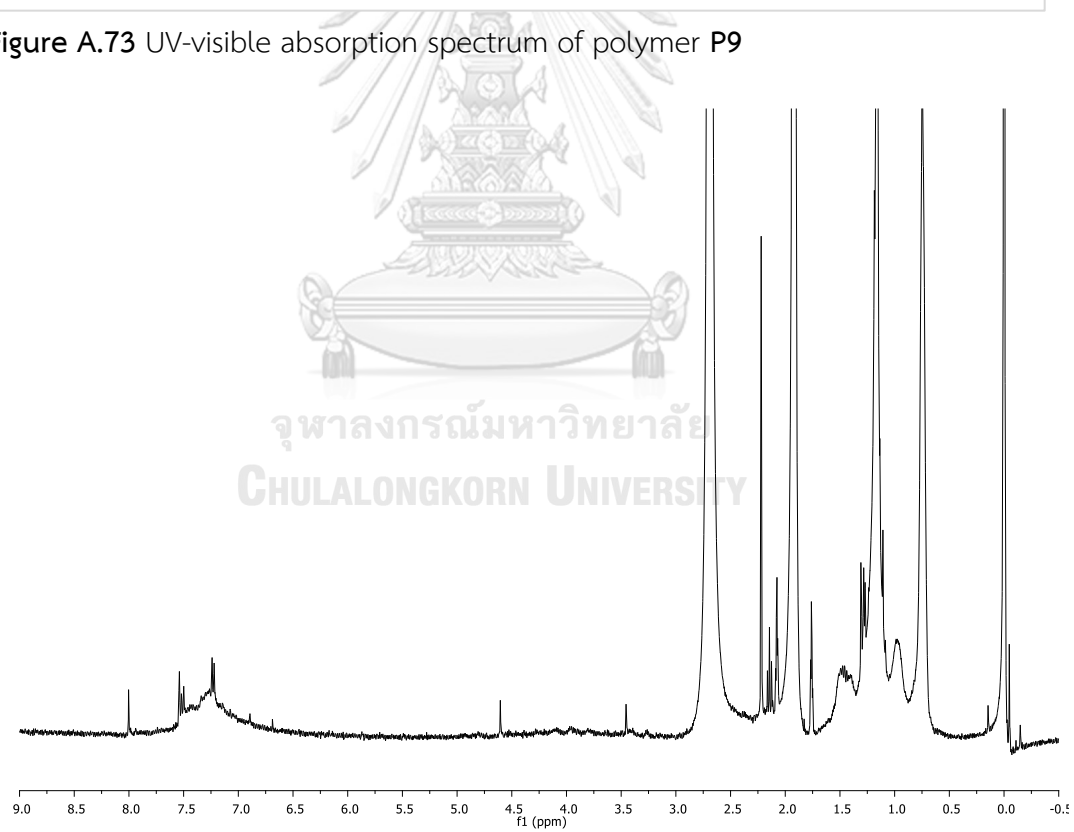


Figure A.74 ¹H NMR (acetone-d₆) spectrum of polymer P10

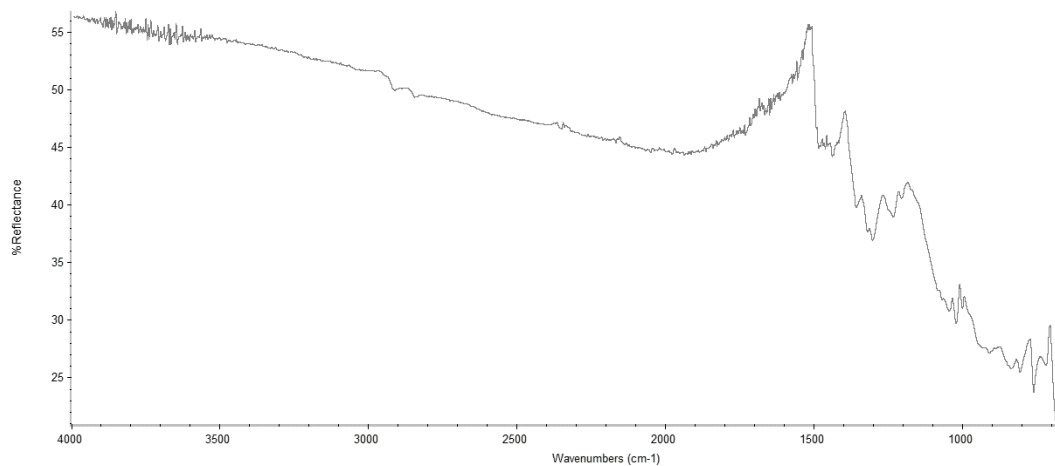


Figure A.75 IR spectrum of polymer P10

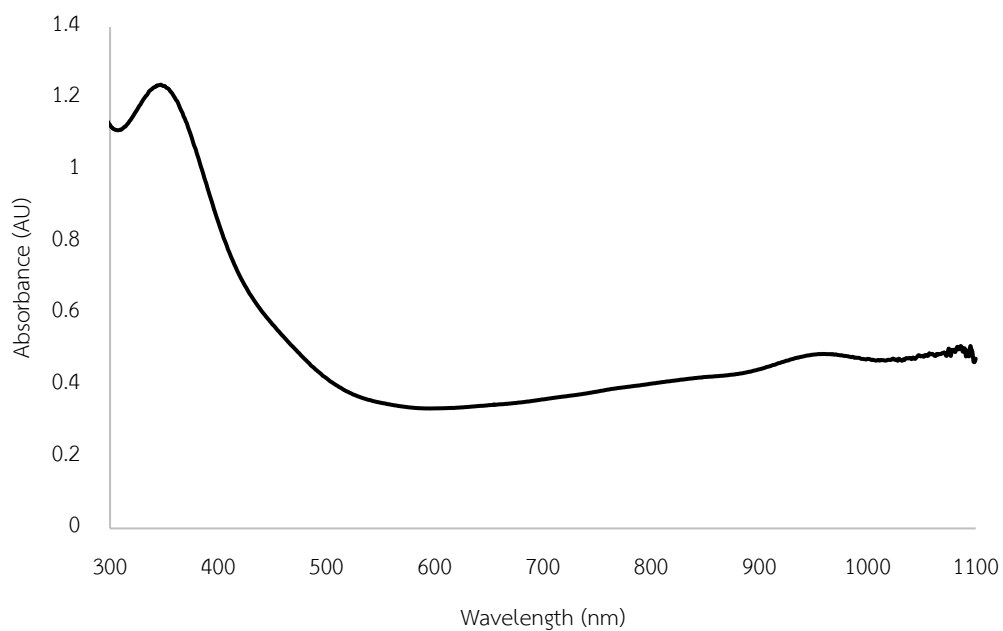


Figure A.76 UV-visible absorption spectrum of polymer P10

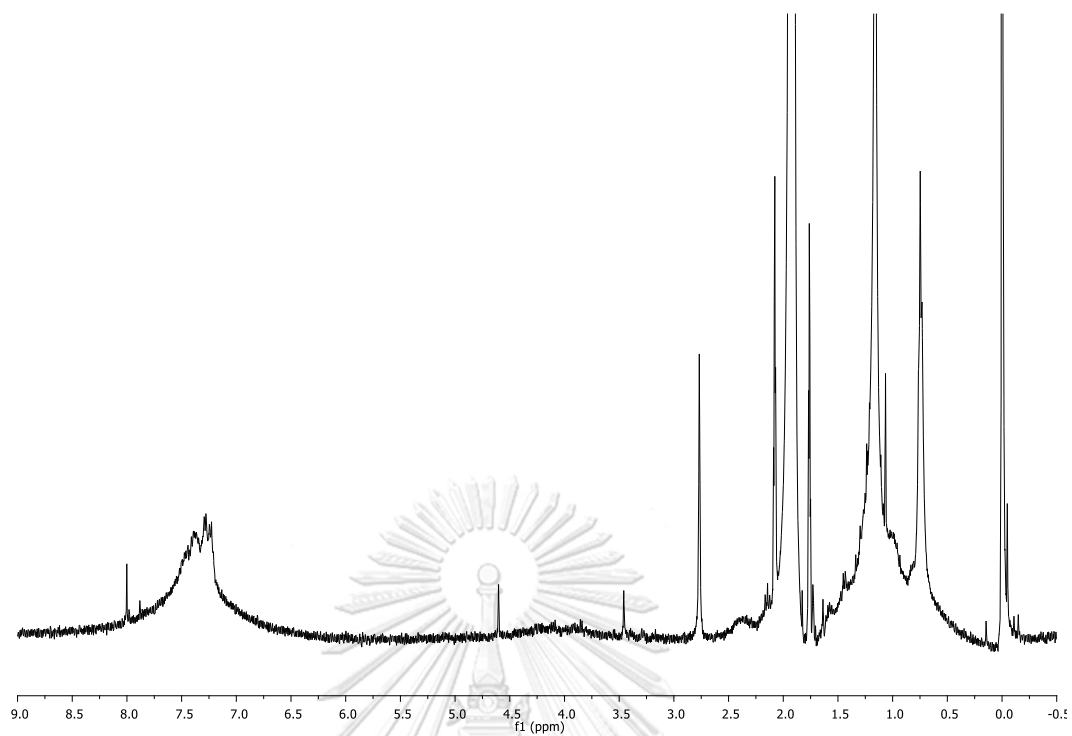


Figure A.77 ^1H NMR (acetone- d_6) spectrum of polymer P10 (Entry 1)

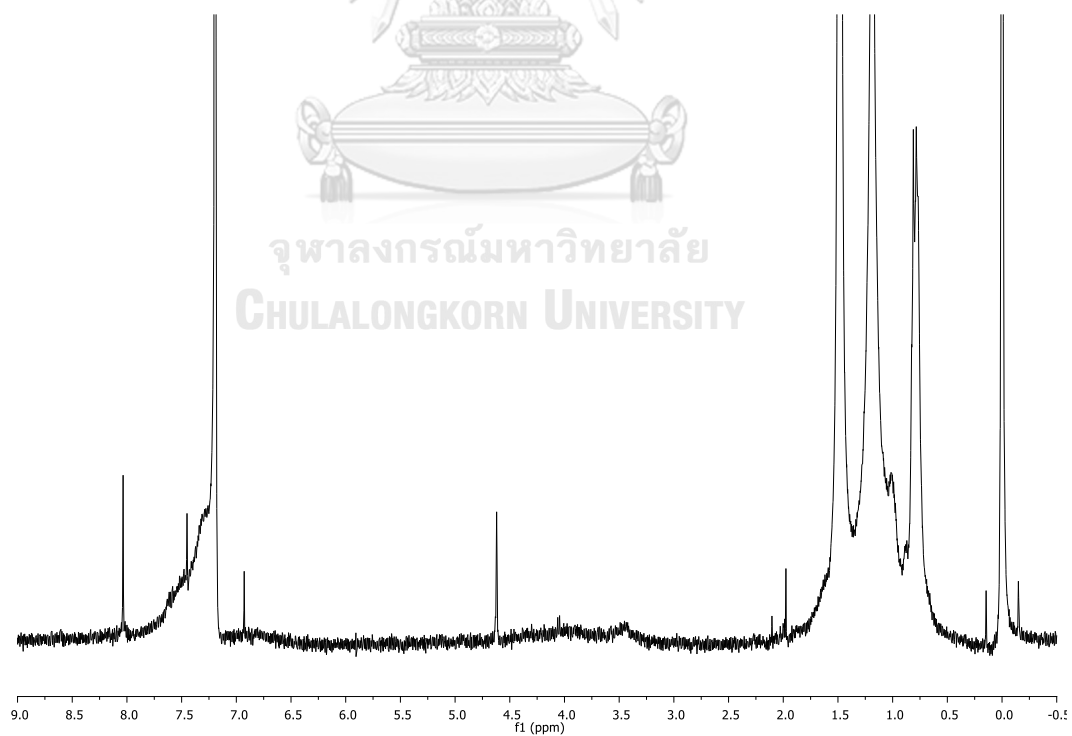


Figure A.78 ^1H NMR (acetone- d_6) spectrum of polymer P10 (Entry 2)

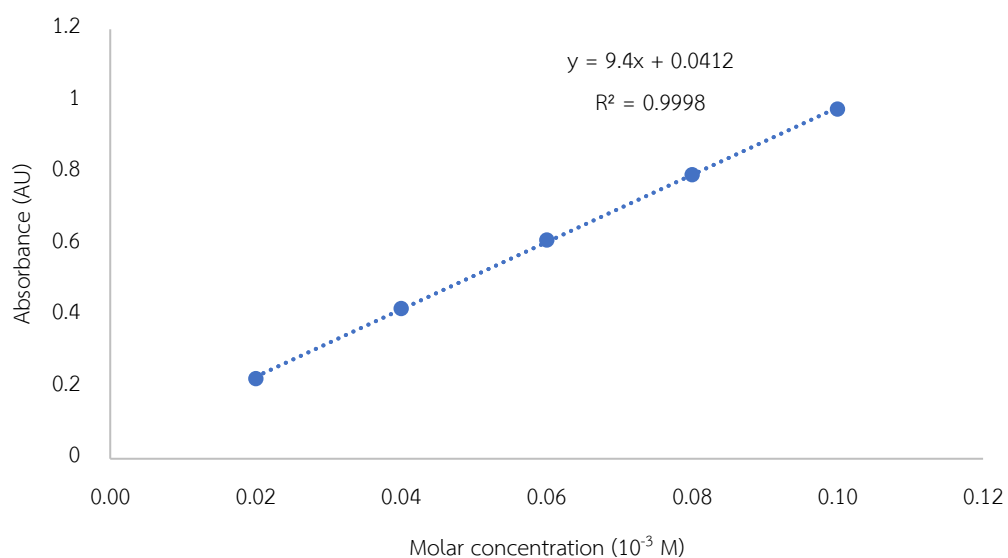


Figure A.79 Determination of molar extinction coefficient (ϵ) for polymer P2 by applying Beer-Lambert law.

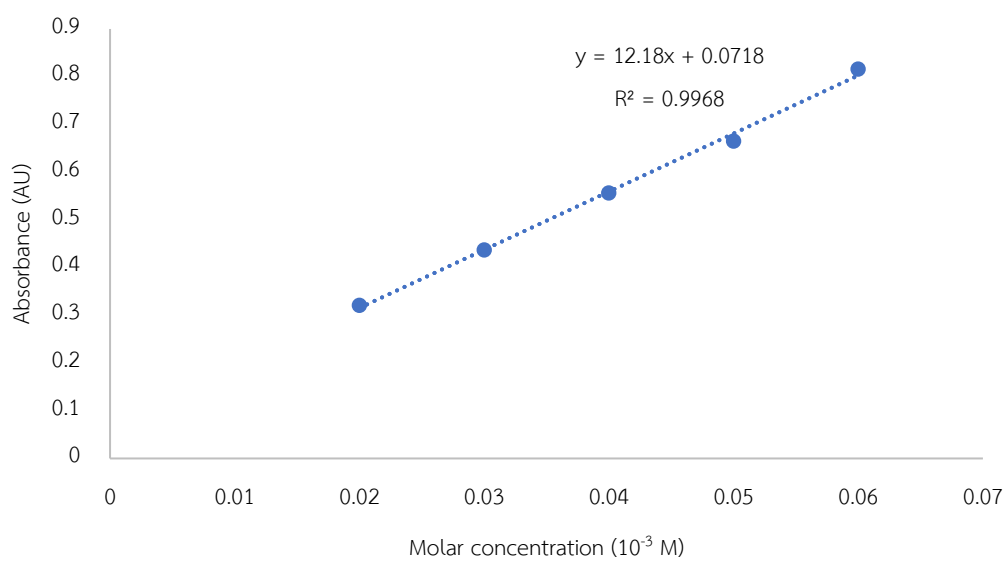


Figure A.80 Determination of molar extinction coefficient (ϵ) for polymer P5 by applying Beer-Lambert law.

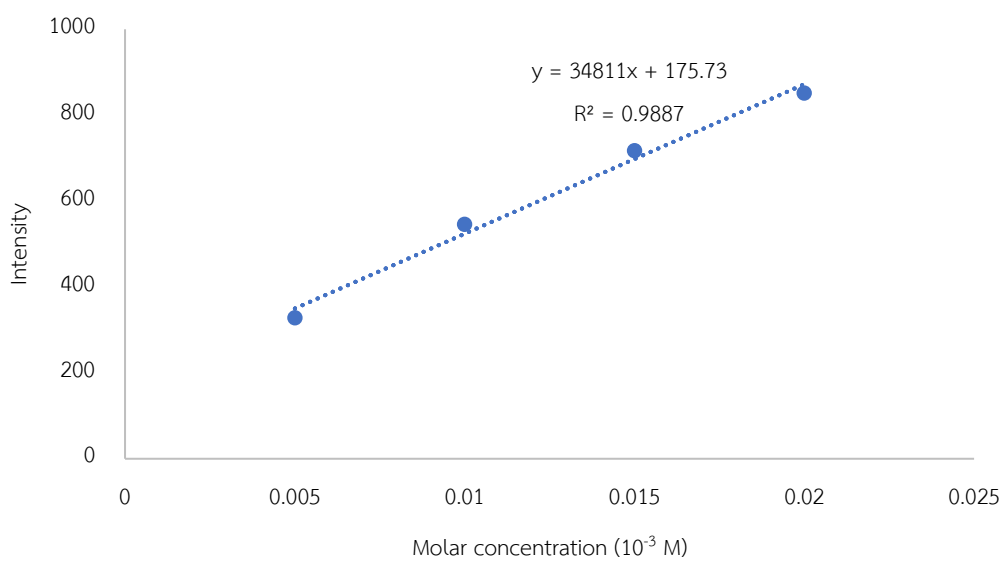
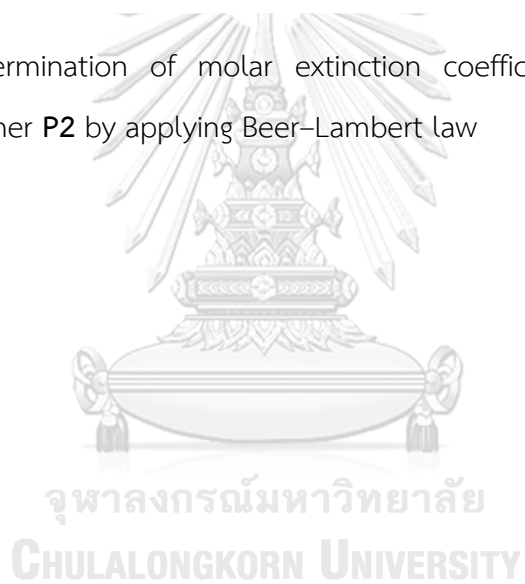


Figure A.81 Determination of molar extinction coefficient (ϵ) of fluorescence emission for polymer **P2** by applying Beer-Lambert law



VITA

NAME Thanat Tiyasakulchai

DATE OF BIRTH 28 November 1994

PLACE OF BIRTH Nonthaburi

INSTITUTIONS ATTENDED Chulalongkorn University

HOME ADDRESS 15 Soi Than Samrit 19/3, Tiwanon Rd., Tha Sai, Mueang
Nonthaburi, Nonthaburi 11000

